

**Instituto Tecnológico de Costa Rica**

**Carrera de Ingeniería Mecatrónica**



**Identification of mechanical faults in wind turbines using parameter estimation**

**Informe de Proyecto de Graduación para optar por el título de Ingeniero en Mecatrónica con el grado académico de Licenciatura**

**Laura Mariana Mora Argüello**

**Cartago, 17 de noviembre de 2016**

**INSTITUTO TECNOLÓGICO DE COSTA RICA**

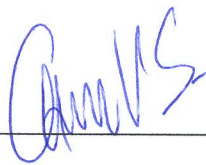
**CARRERA DE INGENIERÍA MECATRÓNICA**

**PROYECTO DE GRADUACIÓN**

**ACTA DE APROBACIÓN**

Proyecto de Graduación defendido ante el presente Tribunal Evaluador como requisito para optar por el título de Ingeniero en Mecatrónica con el grado académico de Licenciatura, del Instituto Tecnológico de Costa Rica.

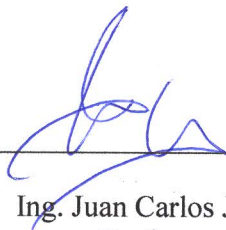
Miembros del Tribunal



Ing. Christopher Vega Sánchez  
Profesor lector



Ing. Carlos Meza Benavides  
Profesor lector



Ing. Juan Carlos Jiménez Robles  
Profesor asesor

Los miembros de este Tribunal dan fe de que el presente trabajo de graduación ha sido aprobado y cumple con las normas establecidas por la Carrera de Ingeniería Mecatrónica

Cartago, 17 de noviembre de 2016

Cartago, 17 de noviembre, 2016

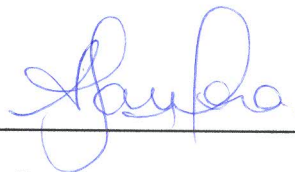
Tecnológico de Costa Rica  
Carrera de Ingeniería Mecatrónica

A quién interese,

Declaro que el presente Proyecto de Graduación ha sido realizado enteramente por mi persona, utilizando y aplicando literatura referente al tema e introduciendo conocimientos propios.

En los casos en que he utilizado bibliografía, he procedido a indicar las fuentes mediante las respectivas citas bibliográficas.

En consecuencia, asumo la responsabilidad total por el trabajo de graduación realizado y por el contenido del correspondiente informe final.



---

**Laura Mariana Mora Argüello**  
Céd. 115490430



Research group  
“Control of Renewable Energy Systems”

Munich School of Engineering  
Technische Universität München  
Dr.-Ing. Christoph Hackl

Laura Mora Arguello

**Bachelor thesis**

Identification of mechanical faults in wind turbines using  
parameter estimation



# Contents

<b>Contents</b>	<b>v</b>
<b>List of Figures</b>	<b>x</b>
<b>List of Tables</b>	<b>xi</b>
<b>Nomenclature</b>	<b>xiii</b>
<b>List of Symbols</b>	<b>xv</b>
<b>Resumen</b>	<b>xvii</b>
<b>Abstract</b>	<b>xix</b>
<b>1 Introduction</b>	<b>1</b>
1.1 Context of the thesis . . . . .	1
1.2 Description of the problem . . . . .	2
1.3 Justification . . . . .	2
1.4 Synthesis of the problem . . . . .	2
1.5 Solution's approach . . . . .	2
<b>2 Goal and objectives</b>	<b>5</b>
2.1 Goal . . . . .	5
2.2 Main objective . . . . .	5
2.3 Specific objectives . . . . .	5
<b>3 Theoretical framework</b>	<b>7</b>
3.1 Modern wind turbines . . . . .	7
3.1.1 Basic components . . . . .	8
3.1.2 Operation principle . . . . .	10
3.1.3 Wind turbine operation regions . . . . .	11
3.2 Modern control systems . . . . .	12
3.2.1 Mechatronic systems . . . . .	14
3.2.2 Mathematical modeling of systems . . . . .	15
3.2.2.1 Differential equations . . . . .	15
3.2.2.2 State variable models . . . . .	17

3.2.2.3	The state differential equation . . . . .	19
3.2.2.4	Feedback control systems . . . . .	20
3.2.2.5	Stability . . . . .	21
3.2.2.6	Observability and controllability . . . . .	22
3.2.2.7	Observer design . . . . .	23
3.2.2.8	Robustness . . . . .	25
3.3	Parameter estimation . . . . .	25
3.3.1	Kalman filtering . . . . .	27
3.3.2	Least squares parameter estimation method . . . . .	28
<b>4</b>	<b>Methodology</b>	<b>31</b>
4.1	Mechanical modeling of wind turbines . . . . .	31
4.1.1	Turbine . . . . .	31
4.1.1.1	Power coefficient . . . . .	32
4.1.1.2	Turbine torque . . . . .	33
4.1.2	Transmission . . . . .	34
4.1.2.1	One-mass system . . . . .	35
4.1.2.2	Two-mass system . . . . .	36
4.2	Speed control for the one-mass system . . . . .	42
4.3	Observer design for the two-mass system . . . . .	44
4.3.1	Augmented system, observability and reachability . . . . .	44
4.3.1.1	Augmented system . . . . .	44
4.3.1.2	Observability and controllability . . . . .	45
4.3.2	Disturbance observer design . . . . .	46
4.3.2.1	Observer design by pole placement . . . . .	48
4.3.2.2	Disturbance observer design by LQR with stability margin . . . . .	50
4.4	Parameter estimation . . . . .	51
4.4.1	Overall nonlinear model . . . . .	52
4.4.2	Discretization . . . . .	52
4.4.3	Extended Kalman Filter . . . . .	54
4.4.3.1	Extended Kalman Filter algorithm . . . . .	55
4.4.4	Recursive Least Squares (RLS) . . . . .	58
4.4.4.1	Principle of the estimation . . . . .	60
<b>5</b>	<b>Analysis and results</b>	<b>63</b>
5.1	Speed control for the one-mass system . . . . .	63
5.1.1	Disturbance observer design for the two-mass system . . . . .	66
5.1.1.1	Disturbance observer design by pole placement . . . . .	67
5.1.1.2	Disturbance observer design by LQR with stability margin . . . . .	74
5.1.1.3	Comparison between disturbance observer design by pole place and by LQR with stability margin . . . . .	80
5.2	Parameter estimation . . . . .	80
5.2.1	Simulation results . . . . .	80

5.3	Detection of mechanical faults . . . . .	84
5.3.1	Changes on the turbine's inertia . . . . .	84
5.3.1.1	Results . . . . .	86
5.3.1.2	Discussion . . . . .	89
5.3.2	Changes on the machine's inertia . . . . .	89
5.3.2.1	Results . . . . .	91
5.3.2.2	Discussion . . . . .	94
5.3.3	Changes on the low-speed shaft's damping . . . . .	94
5.3.3.1	Results . . . . .	96
5.3.3.2	Discussion . . . . .	99
5.4	Changes on the low-speed shaft's stiffness . . . . .	99
5.4.0.1	Results . . . . .	101
5.4.0.2	Discussion . . . . .	104
5.4.1	Summary of the experiment results . . . . .	104
<b>6</b>	<b>Conclutions and recomendations</b>	<b>105</b>
6.1	Conclutions . . . . .	105
6.2	Recomendations . . . . .	105
	<b>Literaturverzeichnis</b>	<b>109</b>
<b>A</b>	<b>Context of the project</b>	<b>111</b>
A.1	TUM.Energy Valley Bavaria . . . . .	111
A.2	Control of Renewable Energy Systems (CRES) . . . . .	112





# List of Figures

3.1	Extraction stream-tube of a wind turbine . . . . .	7
3.2	Axis orientation in a wind turbine . . . . .	8
3.3	Basic components of a wind turbine with horizontal axis . . . . .	9
3.4	Front view of a wind turbine . . . . .	10
3.5	Wind turbine operation areas . . . . .	11
3.6	Process to be controlled . . . . .	12
3.7	Closed-loop feedback control system with feedback . . . . .	13
3.8	Closed-loop feedback system with external disturbances and measurement noise . . . . .	13
3.9	Mechatronics engineering . . . . .	14
3.10	Mechanical rotational system modeling . . . . .	16
3.11	Spring-mass damper system . . . . .	17
3.12	System block diagram . . . . .	20
3.13	Observer with augmented system block diagram . . . . .	24
3.14	Simplified block diagram of the estimation procedure . . . . .	27
3.15	The ongoing discrete Kalman filter cycle . . . . .	28
4.1	Power coefficient for a 2 MW wind turbine . . . . .	33
4.2	Gearbox transmission in a wind turbine . . . . .	35
4.3	Two-mass system in a wind turbine . . . . .	36
4.4	Two mass system block diagram . . . . .	39
4.5	Block diagram for a basic speed control in a wind turbine with a direct drive . . . . .	43
4.6	Augmented system block diagram . . . . .	45
4.7	Observer with augmented system block diagram . . . . .	48
4.8	Sampling principle . . . . .	60
5.1	Wind speed, tip speed ratio, power coefficient, turbine's rotational speed and torques simulation results of a one-mass system . . . . .	65
5.2	Original system and observer with augmented system block diagram . . . . .	67
5.3	Simulation results for the wind speed, tip speed ratio, power coefficient, original and observed rotational speeds and angle displacement in a wind turbine with a two-mass system with a constant wind speed input and an observer designed by pole placement . . . . .	69

5.4	Simulation results for the wind speed, the difference between the original system and the observed system for the rotational speeds and angle displacement, the original turbine's torque and the observed one and the difference between them in a wind turbine with a two-mass system with a constant wind speed input and a observer designed by pole placement . . . . .	70
5.5	Simulation results for the wind speed, tip speed ratio, power coefficient, original and observed rotational speeds and angle displacement in a wind turbine with a two-mass system with a wind profile input and a observer designed by pole placement . . . . .	72
5.6	Simulation results for the wind speed, the difference between the original system and the observed system for the rotational speeds and angle displacement, the original turbine's torque and the observed one and the difference between them in a wind turbine with a two-mass system with a wind profile input and a observer designed by pole placement . . . . .	73
5.7	Simulation results for the wind speed, tip speed ratio, power coefficient, original and observed rotational speeds and angle displacement in a wind turbine with a two-mass system with a constant wind speed input and a observer designed by LQR . . . . .	76
5.8	Simulation results for the wind speed, the difference between the original system and the observed system for the rotational speeds and angle displacement, the original turbine's torque and the observed one and the difference between them in a wind turbine with a two-mass system with a constant wind speed input and a observer designed by LQR . . . . .	77
5.9	Simulation results for the wind speed, tip speed ratio, power coefficient, original and observed rotational speeds and angle displacement in a wind turbine with a two-mass system with a wind profile input and a observer designed by LQR . . . . .	78
5.10	Simulation results for the wind speed, the difference between the original system and the observed system for the rotational speeds and angle displacement, the original turbine's torque and the observed one and the difference between them in a wind turbine with a two-mass system with a wind profile input and a observer designed by LQR . . . . .	79
5.11	Simulation results for the turbine's torque observer designed by pole placement and LQR method with a stability margin, and the difference between them . . . . .	80
5.12	Simulation diagram for the parameter estimation . . . . .	81
5.13	Sinusoidal input for the parameter estimation of the low-speed shaft damping $d_s$ using a sinusoidal input . . . . .	81
5.14	Simulation results of the parameter estimation of the low-speed shaft damping $d_s$ and the low-speed shaft stiffness $c_s$ using a sinusoidal input . . . . .	82

5.15	Simulation results of the parameter estimation of the low-speed shaft damping $d_s$ and the low-speed shaft stiffness $c_s$ using a wind profile as input . . . . .	83
5.16	Simulation results of wind speed, changing turbine's inertia, tip speed ratio, power coefficient, and original system's and observed system's response for the rotational speeds and angle displacement in a wind turbine with a two-mass system . . . . .	86
5.17	Simulation results of wind speed, changing turbine's inertia, difference between the original system's and observed system's response for the rotational speeds and angle displacement, original and observed turbine's torque and the difference between them in a wind turbine with a two-mass system and changing turbine's inertia . . . .	87
5.18	Simulation results of wind speed, changing turbine's inertia and parameter estimation for the low speed shaft's damping and stiffness in a wind turbine with a two-mass system . . . . .	88
5.19	Simulation results of wind speed, changing machine's inertia, tip speed ratio, power coefficient, and original system's and observed system's response for the rotational speeds and angle displacement in a wind turbine with a two-mass system . . . . .	91
5.20	Simulation results of wind speed, changing machine's inertia, difference between the original system's and observed system's response for the rotational speeds and angle displacement, original and observed turbine's torque and the difference between them in a wind turbine with a two-mass system . . . . .	92
5.21	Simulation results of wind speed, changing machine's inertia and parameter estimation for the low speed shaft's damping and stiffness in a wind turbine with a two-mass system . . . . .	93
5.22	Simulation results of wind speed, changing low-speed shaft's damping, tip speed ratio, power coefficient, and original system's and observed system's response for the rotational speeds and angle displacement in a wind turbine with a two-mass system . . . . .	96
5.23	Simulation results of wind speed, changing low-speed shaft's damping, difference between the original system's and observed system's response for the rotational speeds and angle displacement, original and observed turbine's torque and the difference between them in a wind turbine with a two-mass system . . . . .	97
5.24	Simulation results of wind speed, changing low-speed shaft's damping and parameter estimation for the low speed shaft's damping and stiffness in a wind turbine with a two-mass system . . . . .	98
5.25	Simulation results of wind speed, changing low-speed shaft's stiffness, tip speed ratio, power coefficient, and original system's and observed system's response for the rotational speeds and angle displacement in a wind turbine with a two-mass system . . . . .	101

5.26	Simulation results of wind speed, changing low-speed shaft's stiffness, difference between the original system's and observed system's response for the rotational speeds and angle displacement, original and observed turbine's torque and the difference between them in a wind turbine with a two-mass system . . . . .	102
5.27	Simulation results of wind speed, changing low-speed shaft's stiffness and parameter estimation for the low speed shaft's damping and stiffness in a wind turbine with a two-mass system . . . . .	103

# List of Tables

3.1	Through and across variables for a mechanical system . . . . .	16
5.1	Wind turbine and air conditions for simulation . . . . .	63
5.2	Wind turbine and air conditions for two-mass system simulation . . .	66
5.3	Summary of the experiment results for detection of mechanical faults in wind turbines . . . . .	104



# Nomenclature

Notation	Meaning
$\mathbb{N}$	Set of natural numbers
$\mathbb{R}$	Set of real numbers
$x \in \mathbb{R}$	Real scalar
$\mathbf{x} \in \mathbb{R}^n$ (bold)	Real valued vector with $n \in \mathbb{N}$ rows
$\mathbf{x}^\top$	Transpose of $\mathbf{x}$
$\mathbf{0}_n = (0, \dots, 0)^\top$	$n$ -th dimensional zero vector
$\mathbf{X} \in \mathbb{R}^{n \times m}$ (capital bold)	Real valued matrix with $n \in \mathbb{N}$ rows and $m \in \mathbb{N}$ columns
$\mathbf{0} \in \mathbb{R}^{n \times m}$	Zero matrix
$\mathbf{I}_n \in \mathbb{R}^{n \times n}$	Identity matrix
$\mathbf{A} \in \mathbb{R}^{n \times m} =$	Elements of a given matrix
	$\begin{bmatrix} a_{11} & a_{12} & \cdots & a_{1m} \\ a_{21} & a_{22} & \cdots & a_{2m} \\ \vdots & \vdots & \ddots & \vdots \\ a_{n1} & a_{n2} & \cdots & a_{nm} \end{bmatrix}$





# List of Symbols

Variable	Symbol	Units
Tip speed ratio	$\lambda$	1
Optimal tip speed ratio	$\lambda^*$	1
Pitch angle	$\beta$	$^\circ$
Power coefficient	$c_P$	1
Betz factor	$c_{P,Betz}$	1
Gearbox ratio	$g_r$	1
Turbine's radius	$r_T$	m
Turbine's area	$A_T$	$m^2$
Gondola's area	$A_G$	$m^2$
Total inertia	$\Theta$	$kg\ m^2$
Turbine's inertia	$\Theta_T$	$kg\ m^2$
Total machine's inertia	$\Theta_M$	$kg\ m^2$
Related machine's inertia	$\Theta_{M'}$	$kg\ m^2$
Machine's inertia	$\Theta_{M_0}$	$kg\ m^2$
Gearbox' inertia	$\Theta_{GB}$	$kg\ m^2$
Low speed shaft inertia	$\Theta_{LS}$	$kg\ m^2$
High speed shaft inertia	$\Theta_{HS}$	$kg\ m^2$
Turbine's damping	$d_T$	$\frac{N\ m\ s}{rad}$
Machine's damping	$d_M$	$\frac{N\ m\ s}{rad}$
Low speed shaft's damping	$d_s$	$\frac{N\ m\ s}{rad}$
High speed shaft's damping	$d_{HS}$	$\frac{N\ m\ s}{rad}$
Low speed shaft's stiffness	$c_s$	$\frac{N\ m}{rad}$
High speed shaft's stiffness	$c_{HS}$	$\frac{N\ m}{rad}$
Air's density	$\rho$	$kg/m^3$
Wind speed	$v_W$	$\frac{m}{s}$
Nominal wind speed	$v_{W,nom}$	$\frac{m}{s}$
Cut in wind speed	$v_{W_{cut-in}}$	$\frac{m}{s}$
Cut out wind speed	$v_{W_{cut-out}}$	$\frac{m}{s}$
Wind's power	$p_W$	W
Turbine's power	$p_T$	W
Nominal turbine's power	$p_{T,nom}$	W
Minimal turbine's power	$p_{T,min}$	W
Turbine's torque	$m_T$	N m

Variable	Symbol	Units
Nominal turbine's torque	$m_{T,nom}$	N m
Machine's torque	$m_M$	N m
Related machine's torque	$m_{M'}$	N m
Referenced machine's torque	$m_{M,ref}$	N m
Torque produced by the turbine on the machine	$m_{T-M}$	N m
Torque produced by the machine on the turbine	$m_{M-T}$	N m
Torque produced by the turbine on the related machine	$m_{T-M'}$	N m
Torque produced by the related machine on the turbine	$m_{M'-T}$	N m
Turbine's rotational speed	$\omega_T$	$\frac{\text{rad}}{\text{s}}$
Minimal turbine's rotational speed	$\omega_{T,min}$	$\frac{\text{rad}}{\text{s}}$
Nominal turbine's rotational speed	$\omega_{T,nom}$	$\frac{\text{rad}}{\text{s}}$
Machine's rotational speed	$\omega_M$	$\frac{\text{rad}}{\text{s}}$
Related machine's rotational speed	$\omega_{M'}$	$\frac{\text{rad}}{\text{s}}$
Turbine's rotational angle	$\phi_T$	rad
Machine's rotational angle	$\phi_M$	rad
Related machine's rotational angle	$\phi_{M'}$	rad
Angle displacement between turbine and machine	$\Delta\phi_{T-M}$	rad
Angle displacement between turbine and related machine	$\Delta\phi_{T-M'}$	rad
Speed controller gain	$K_p^*$	kg m <sup>2</sup>

# Resumen

La tesis en estudio trata sobre la posible identificación de fallas mecánicas en una turbina eólica mediante la estimación de parámetros de los componentes mecánicos del eje flexible de baja velocidad. No es el propósito de esta tesis establecer la causa de las fallas mecánicas, pero establecer una base para la detección de las fallas. Se analiza el comportamiento global de una turbina eólica hacia diferentes situaciones o experimentos como los incrementos y disminuciones de las principales inercias y los parámetros mecánicos en estudio. La tesis incluye el modelado matemático de una turbina eólica, el diseño de un observador adecuado para el estimador de parámetros, así como el diseño del estimador.

**Palabras claves:** Turbinas eólicas, estimación de parámetros, fallas mecánicas, observador, rls, lqr.



# Abstract

The thesis in subject looks forward the possible identification of mechanical faults in a wind turbine using parameter estimation of the low speed shaft's mechanical components. It is not the purpose of this thesis to establish the reasons of the mechanical faults, but to set up a base for the detection of the faults. It analyzes the overall behavior of a wind turbine towards different situations or experiments such as increments and decreases of the main inertias and mechanical parameters in study. The thesis includes the mathematical modeling of a wind turbine, the design of a suitable observer for the parameter estimator and the design of the parameter estimator.

**Keywords:** Wind turbines, parameter estimation, mechanical faults, observer, rls, lqr.

# Chapter 1

## Introduction

### 1.1 Context of the thesis

Wind energy is the energy produced by the atmospheric air in motion that is commonly known as wind. The wind is generated by several factors, but the more important are due to the rotation of the earth, the changes in ocean temperature, local weather conditions and geography as deserts, mountains, vegetation type, etc. This type of energy has already been used in a limited way for centuries in various parts of the world for shipping, windmills, or to extract groundwater, to mention some [15]. As a combined result of the increasingly worrisome environmental situation, application and development for this specific type of energy has accelerated sharply in the last decades [4]. The progressive reduction of reserves of fossil fuels is one of the most alarming factors [31].

Wind energy is one of the most economic alternative energies and therefore a favorite nowadays [15]. This type of energy has no waste of any kind, requires less exotic or rare-earth materials for power generation and there is no need of water for the production. It does not emit pollutants into the atmosphere and, by now as deeper discussion is taking place, can only be attributed as a slight inconvenience, acoustic noise emission and alteration of the landscape.

Wind turbines are devices that, through their rotation, convert the wind's kinetic energy into mechanical energy. Turbines are usually classified according to the type of aerodynamic force that causes rotation of the rotor, whether these are drag forces or forces of lift; or according to the arrangement of its rotation axis being in horizontal or vertical position.

The reliability of a wind turbine system is a critical factor in the success of a wind energy project. Low reliability directly affects the project revenue stream through increased operation and maintenance costs and lower availability to generate power due to downtime of the turbine [32].

Parameter estimation is the process in which observations for developing dynamic mathematical models that adequately represent system characteristics system are used [23].

The model assumes that the system consists of a finite set of parameters, from

which the value is approximated using estimation techniques. Fundamentally, the approach is based on minimizing the error between the model response and the response of the real system.

With the advent of digital high-speed computers, the most complex and sophisticated techniques such as the method of error filter and other innovative methods based on artificial neural networks have increased their use in parameter estimation problems [23]. The idea behind modeling an engineering system or a process is to improve their performance or design the control system.

Mathematical modeling through parameter estimation is one of the ways leading to a deeper understanding of the characteristics of the system. These parameters often describe the stability of the system. The estimation of these parameters from input-output data (signals) system is thus an important step analysis of the dynamic system. [23]

The thesis is developed in the Technische Universitaet of Muenchen in a research group named "Control of Renewable Energy Systems", focused on the robust control of wind turbines.

## 1.2 Description of the problem

The thesis consists in determining whether it is possible or not to detect mechanical faults in a wind turbine using parameter estimation of the low speed shaft's mechanical constants. For achieving this, understanding the electromechanical system of the turbine is necessary for correctly math model it. As well as the design of a functioning observer and a parameter estimator.

## 1.3 Justification

There is not a proper research in the group about the possibility of detecting mechanical faults in a wind turbine with a two mass system using parameter estimation of the low speed shaft's mechanical constants.

## 1.4 Synthesis of the problem

Identification of mechanical faults in wind turbines before they happen.

## 1.5 Solution's approach

The proposed solution is divided in four main sections: the mathematical modeling of the wind turbine, the control of the wind turbine, the working observer and the parameter estimator.

In the matter of the understanding of the wind turbine's electromechanical system, the mathematical modeling of a one mass system is the initial step based on the

idea of starting with simple working things. To correctly show the behavior of the wind turbine under normal circumstances, the basic modeling should be proposed. After obtaining a working one mass system model, a two mass system model must be implemented based on the one mass system model. Since the two mass system is actually describing the complete electromechanical system of the wind turbine, there are some models that could be obtained. The difference between the models are the state vectors of each, making one more suitable than the other depending of what is desired. In this case, it is chosen a state vector with the turbine and machine's rotational speeds and torques as states. The model should be implemented and simulated in Simulink.

The control of the wind turbine will be done by the usual speed control. The results are going to be checked by the corresponding simulation. The speed control will be applied first to the one mass system model of the wind turbine to move to the two mass system model. If the control works for the one mass system, it should be expected to work on the two mass system model.

For the working observer, a turbine's torque observer is chosen. The turbine's torque is not a measured variable and the observer should work as a sensor for it. Due to the nature of the measurement of the turbine's torque, a trustworthy observer must be implemented. For the design of the observer, it is initially planned to be carried by pole placement. The method is simple and good results are expected. In case this observer does not work as desired, a Linear Quadratic Regulator (LQR) method is stated as a second choice. The results of the section are going to be shown by the proper simulations.

As for the parameter estimator, the estimation is initially decided to be carried on by an Extended Kalman Filter. The EKF has been historically used for online estimations due to the fast convergence and good results obtained from it. As well as the complexity As a second choice, a Recursive Least Squares (RLS) method could be implemented.

With the three main sections completed, the final approach would be the analysis of the data obtained from the simulations and decide whether it is possible or not to detect mechanical faults with this method.





# Chapter 2

## Goal and objectives

### 2.1 Goal

The aim of this thesis is to detect mechanical faults in wind turbines using parameter estimation. This being achieved throughout the analysis and estimation of the low speed shaft's mechanical constants and the design of a reliable turbine's torque observer to check the effect of four main experiments on those.

### 2.2 Main objective

Detection of mechanical faults in a wind turbine using the estimation of the low speed flexible shaft's mechanical constants.

### 2.3 Specific objectives

- Attain a mathematical model of a wind turbine with a low speed flexible shaft.
- Design of an observer for the turbine's torque.
- Implement a parameter estimator for the mechanical constants of the low speed shaft.
- Analyze the estimated parameters and their effect on the overall turbine's behavior.



# Chapter 3

## Theoretical framework

### 3.1 Modern wind turbines

Wind turbines are devices that through their rotation, convert the wind's kinetic energy into mechanical energy. Modern wind turbines have switched, almost exclusively, to produce electricity. In the past, wind turbine concepts were applied to other different activities. Throughout the world, wind farms have become very popular in the last decades as such wind turbines can be built on land or offshore in large bodies of water like oceans and lakes [16].

The aerodynamical functioning of the wind turbine can be explained as shown in Fig. 3.1. By removing some of its kinetic energy the wind must slow down, but only that mass of air which passes through the rotor disc is affected. Assuming that the affected mass of air remains separate from the air which does not pass through the rotor disc and does not slow down, a boundary surface can be drawn. No air flows across the boundary and so the mass flow rate of the air flowing along the stream-tube will be the same for all stream-wise positions along the stream-tube. Because the air within the stream-tube slows down, but does not become compressed, the cross-sectional area of the stream-tube must expand to accommodate the slower moving air [8].

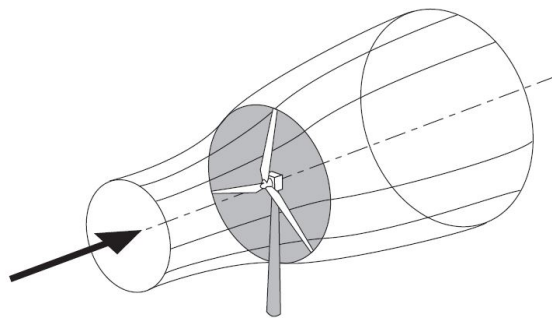


Figure 3.1: *Extraction stream-tube of a wind turbine*[8, p.40]

Modern wind turbines can be divided into two basic groups: the horizontal-axis (HAWT) variety and the vertical-axis (VAWT) design, as can be identified in the

Fig. 3.2. Horizontal-axis wind turbines usually have three blades operating "upwind", which means facing into the wind. Vertical-axis wind turbines are always aligned with the wind, so there is no need of adjustment in case of wind direction changes.

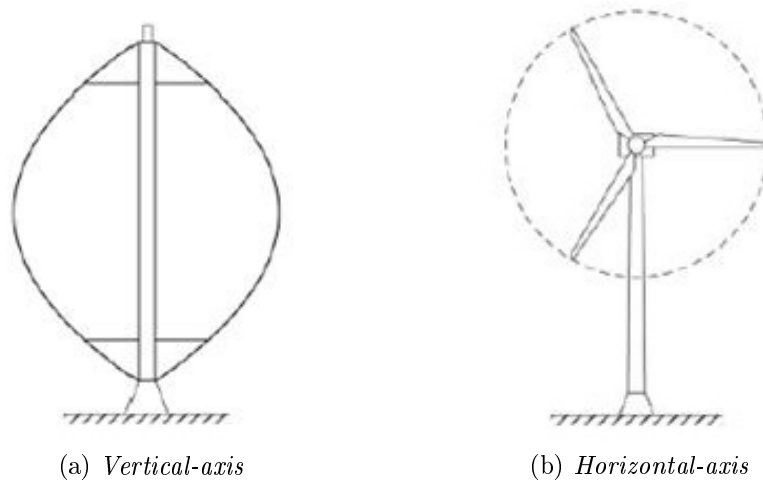


Figure 3.2: *Axis orientation in a wind turbine* [5]

In a vertical-axis wind turbine, the shaft is mounted vertically, perpendicular to the ground. VAWTs need a boost from the electrical system to start moving because it can not begin all by itself. Instead of a tower, it typically uses guy wires for support, so the rotor elevation is lower. Lower elevation means slower wind due to ground interference, so VAWTs are generally less efficient than HAWT. On the upside, all equipment is at ground level for easy installation and servicing; but that means a larger footprint for the turbine, which is a big disadvantage in wind farming areas. [24]

As the name refers to it in a HAWT, the shaft is mounted horizontally, parallel to the ground. As HAWTs are facing "upwind", there is the need to constantly align the blades with the wind using a yaw-adjustment mechanism. The yaw system typically consists of electric motors and gearboxes that move the entire rotor left or right in small increments. The turbine's electronic controller reads the position of the wind and adjusts the position of the rotor to capture the most wind energy available. HAWTs use a tower to lift the turbine components to an optimum elevation for wind speed and take up very little ground space since almost all of the components are up to 80 meters in the air. [24]

### 3.1.1 Basic components

A wind turbine is a complex mechatronical system and in modern wind turbines of more than 1 MW there are a some basic components that can be identified. Some of them have been mentioned before and are shown in Fig. 3.3. Section based on [1].

### 3.1. MODERN WIND TURBINES

---

Components:

- Turbine on a horizontal axis with three pitch-regulated rotor blades
- Gearbox
- Electric machine or generator
- Back-to-Back Converter
- Line reactor or filter
- Transformer
- Grid with fixed frequency, in this case,  $f=50$  Hz

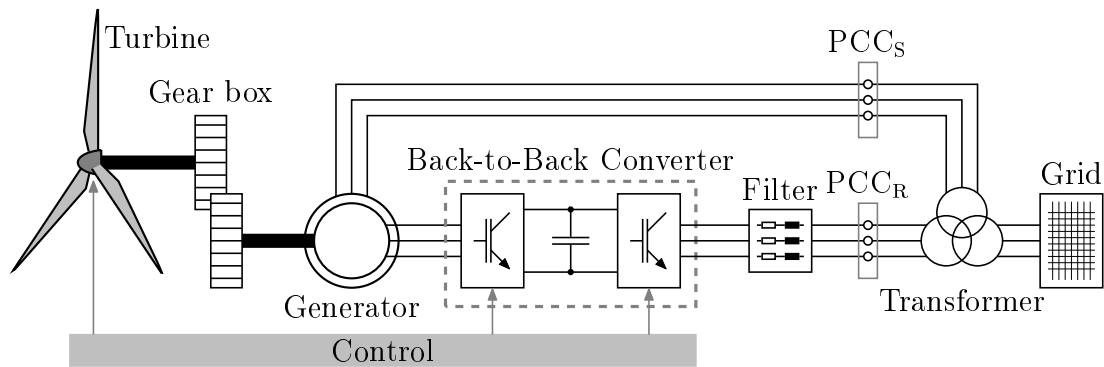


Figure 3.3: *Basic components of a wind turbine with horizontal axis [12].*

The overall components are divided in different categories, for example, in one horizontal axis wind turbine you will find the following:

1. Foundation
2. Tower
3. Turbine and turbine's blades
4. Nacelle with drive train
5. Electronic equipment
6. Others

### 3.1.2 Operation principle

Wind turbines operate on a very simple principle. The process, from start to finish, of generating electricity from wind begins with the rotor blades transforming the wind's speed,  $v_w$  [ $\frac{m}{s}$ ], into a rotational movement described by the rotational speed of the turbine  $\omega_T$  [ $\frac{rad}{s}$ ]. The rotational movement of the turbine is then transferred to a generator. Where the rotation of the turbine is transformed into electricity.

The turbine usually includes three blades, and the turbine radius,  $r_T$  [m] and turbine area  $A_T$  [ $m^2$ ] are given by the blade dimensions. Each blade has a pitch system that can set a pitch angle  $\beta$  [ $^\circ$ ], for the turbine to obtain the nominal power from wind. The most important variables needed to understand how a wind turbine works are shown in Fig. 3.4.

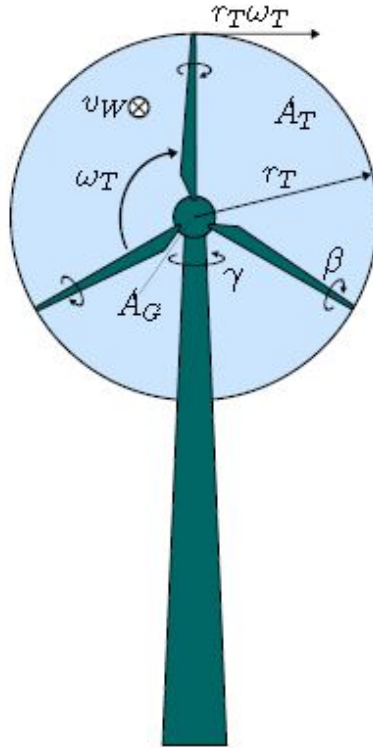


Figure 3.4: *Front view of a wind turbine [13, p.9]*

The nacelle, as mentioned before, includes the gearbox, electronic control, yaw controller and breaks. The gearbox increases the speed of the shaft between the rotor and the generator. The generator uses the rotational energy of the shaft to generate electricity using electromagnetism.

The electronic control unit is the monitoring system that controls the yaw mechanism and shuts down the turbine in case of malfunction. The yaw controller moves the rotor certain degrees,  $\gamma$  [ $^\circ$ ], to align it with the direction of the wind. The brakes stop the rotation of the shaft in case of a power overload or a system failure.

The tower is the one that supports the rotor and nacelle and lifts entire setup to a higher elevation where blades can safely be.

Finally, there is the electrical equipment which carries electricity from generator down through tower and controls many safety elements of turbine. In this part of the wind turbine the convertor, transformer and filter can be found.

### 3.1.3 Wind turbine operation regions

Depending on the wind speed,  $v_W$ , a wind turbine can be functioning in 4 different regions as displayed in Fig. 3.5.

- Region I: Zone in which the wind speed is lower than the necessary,  $v_{W,cut-in}$  [ $\frac{m}{s}$ ], to produce the minimal power,  $p_{T,min}$  [W]. The wind turbine is not even connected to the network.
- Region II: In this region the wind speed is capable to achieve the minimal power,  $p_{T,min}$ , necessary to start functioning. The wind turbine is connected to the network but working at a variable speed until the nominal power,  $p_{T,nom}$  [W], is achieved. The wind speed begins at  $v_{W,cut-in}$ , which is the minimum to start, and stops increasing when nominal wind speed,  $v_{W,nom}$ , is reached.
- Region III: The wind turbine is working at nominal wind speed,  $v_{W,nom}$ , to achieve the nominal power,  $p_{T,nom}$ , for as long as it is possible. The operation region ends when it is necessary to shut down the wind turbine.
- Region IV: Region in which the wind turbine needs to be shut down because of  $v_W > v_{W,cut-out}$  [ $\frac{m}{s}$ ]. It should be a progressive shut down.

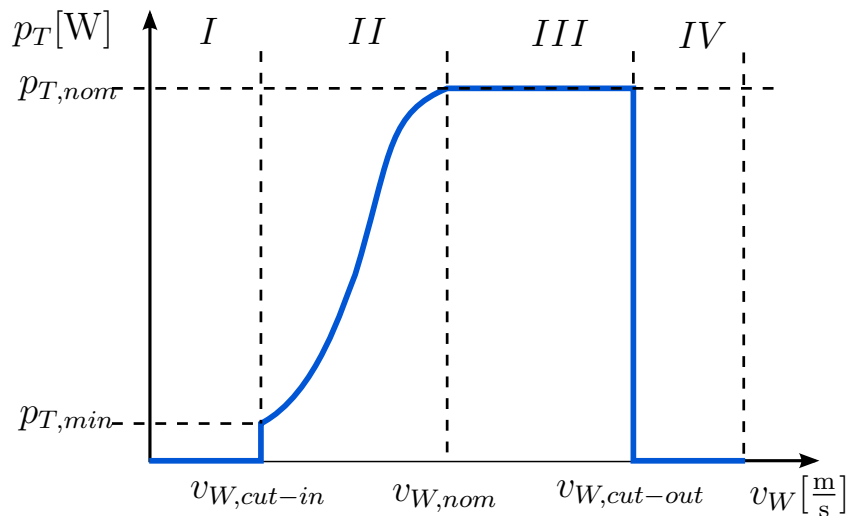


Figure 3.5: *Wind turbine operation areas [13, p.18]*



## 3.2 Modern control systems

This section is based on [14]. The basis of engineering come from the understanding and controlling of our environment for the benefit of humankind and applying it to small segments of our daily life, usually called systems. These systems are the used for the creation of useful devices or products. Part of the effective control of these systems require the individual understanding and modeling of each system.

In between the new challenges of control engineers are the modeling and control of modern, complex, interrelated systems such as traffic control systems, chemical processes, and robotic systems. Nevertheless, the opportunity to control machines and industrial and economic processes for the benefit of society is, perhaps, the most characteristic quality of control engineering [14].

Control engineering is based on feedback theory and linear system analysis, and integrating concepts of network communication theory. Therefore control engineering can not be limited to engineering disciplined, but it must be equally applicable to any other aspect of life. In addition to it, as the understanding of the dynamics of business, social, and political systems increases, the ability to control them also increase.

A control system is an interconnection of components forming a system configuration that will provide a desired system response [14]. The basis for the system's analysis is the linear system theory and the assumptions of cause-effect relationships for the components in the system. In this way, processes can be represented by blocks, such as shown in Fig. 3.6. The cause-and-effect relationship of the process is represented by the input-output relationship, which represents as well a processing of the input signal to provide an output signal variable, often with a power amplification [14].

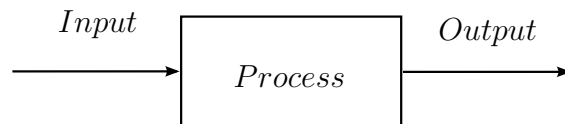


Figure 3.6: *Process to be controlled* [14]

One of the ways to differentiate control systems is by the feedback signal in it. A feedback signal means there is an additional measure of the actual output to compare the actual output with the desired output response. An open-loop control system uses a controller and an actuator to obtain the desired response, and an open-loop system is a system without feedback. Different from it, a closed-loop control system uses the feedback signal.

A feedback control system is a control system that tends to maintain a prescribed relationship of one system variable to another by comparing functions of these variables and using the difference as a means of control. With an accurate sensor, the measured output is a good approximation of the actual output of the system [14]. Usually, a feedback control system uses the relationship between the output and the input as a function to control the process. In these cases, the difference between the

output of the process that is under control and the input of is amplified and used to control the process, and by way reduce the difference.

This difference between the output that is desired and the actual output of the system is known to be the error of the process, which in a feedback system, as mentioned before is adjusted by the controller to modify the response of the system. The output of the controller causes the actuator to modulate the process in order to reduce the error. Feedback control systems tend to be negative, the output of the system is usually subtracted from the input, the difference signal is now the input signal for the controller. The feedback concept has been the foundation for control system analysis and design [14] and it is shown in Fig. 3.7.

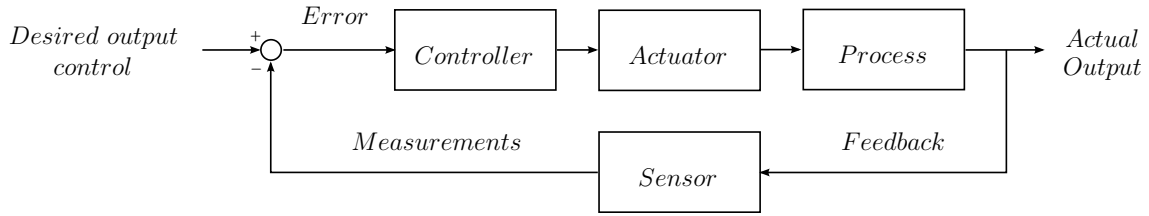


Figure 3.7: Closed-loop feedback control system with feedback [14]

Closed-loop control has many advantages over open-loop control including the ability to reject external disturbances and improve measurement noise attenuation. A system with disturbances and measurement noise is shown in Fig. 3.8. External disturbances and measurement noise are inevitable in real-world applications and must be addressed in practical control system designs [14]. One characteristic of feedback control systems is that they might contain one or more feedback loops.

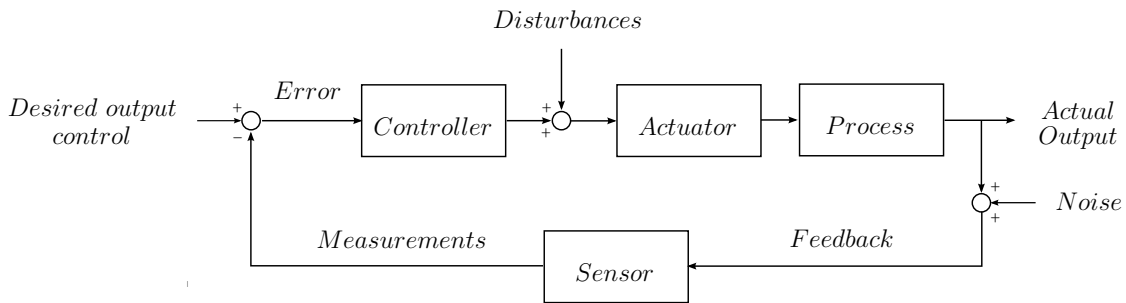


Figure 3.8: Closed-loop feedback system with external disturbances and measurement noise [14]

Due to the increasing complexity of the system under control and the interest in achieving optimum performance, the importance of control system engineering has grown in the past decade. Furthermore, as the systems become more complex, the interrelationship of many controlled variables must be considered in the control scheme.

### 3.2.1 Mechatronic systems

Mechatronics comes in to modern engineering as a natural stage in the evolutionary process. The term "mechatronics" was first mentioned in Japan in the 1970s [14] and talks about the synergistic integration of mechanical, electrical, and computer systems. It has evolved over the past 30 years leading the development of a new type of intelligent products and systems.

The key elements of mechatronics are physical systems modeling, sensors and actuators, signals and systems, computers and logic systems, and software and data acquisition [14]. Feedback control encompasses aspects of all five key elements of mechatronics, transforming feedback control is an integral aspect of modern mechatronic systems even though it primarily is associated with signals and system elements.

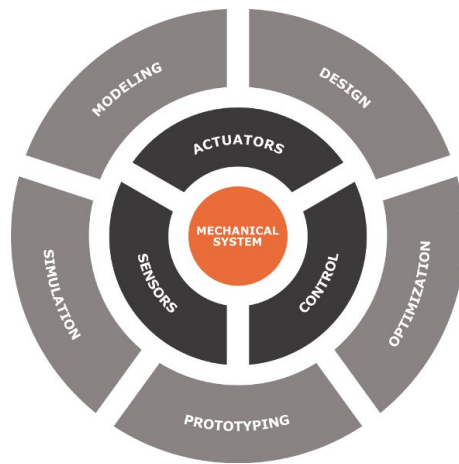


Figure 3.9: *Mechatronics engineering* [30]

A revolutionized engineering design started with the advances in computer hardware and software technology mixed with the desire to increase the performance-to-cost ratio of the products. As days go by, new products are being developed at the intersection of traditional disciplines of engineering, computer science, and the natural sciences.

The continued advances in traditional disciplines facilitated an exponential growth of mechatronic systems by providing "enabling technologies" [14]. For example, microprocessors are known to be an enabling technology because of its deep and important effect on the design and development of new products. In between the category of "enabling categories", the following are found: microprocessors and microcontrollers, novel sensors and actuators enabled by advancements in applications of microelectromechanical systems (MEMS), advanced control methodologies and real-time programming methods, networking and wireless technologies, and mature computer-aided engineering (CAE) technologies for advanced system modeling, virtual prototyping, and testing [14]. It is only a matter of time for the development smart products of new different areas.

An exciting area of future mechatronic system development in which control systems will play a significant role is the area of alternative energy production and consumption. Hybrid fuel automobiles and efficient wind power generation are two examples of systems that can benefit from mechatronic design methods [14].

In fact, the mechatronic design philosophy can be illustrated in a very clear way by analyzing the example of the evolution of the modern cars or automobiles. Before the 1960s, the radio was the only significant electronic device in an automobile. Nowadays cars have 30-60 microcontrollers, up to 100 electric motors, about 200 pounds of wiring, a multitude of sensors, and thousands of lines of software code [14]. So it can be assumed that a modern cars isn't just a mechanical machine, it transformed itself into a mechatronic system. As it is the topic of this thesis, modern wind power generation systems are as well, mechatronic examples.

### 3.2.2 Mathematical modeling of systems

The understanding and controlling of complex physical systems is made through quantitative mathematical models in order to carry on the design and analysis of control systems. It is necessary then to analyze the existing relationships between the system's variables and obtain a mathematical model. Because the systems that are being considered are dynamic in nature, the descriptive equations are usually differential equations. Since most physical systems are nonlinear, but these equations can be linearized to simplify the method of solution.

In practice, the complexity of systems and our ignorance of all the relevant factors will then require the introduction of assumptions about the system's operation. Initially it is useful to consider the physical system, express the necessary assumptions if they exist, and try to linearize the system and obtain the differential equations. Finally, a solution is obtained describing the operation of the system.

The approach to dynamic system modeling can be enumerated as:

1. Define the system and its components.
2. Formulate the mathematical model and fundamental necessary assumptions based on basic principles.
3. Obtain the differential equations representing the mathematical model.
4. Solve the equations for the desired output variables.
5. Examine the solutions and the assumptions.
6. If necessary, reanalyze or redesign the system.

#### 3.2.2.1 Differential equations

The differential equations describing the dynamic performance of a physical system, equally applied to mechanical, electrical, fluid, and thermodynamic system, are obtained by utilizing the physical laws of the process [14].

While describing a system, two types of variables can exist: through variables that are measured with a gauge connected in series to an element and across variables that are measured with a gauge connected in parallel to an element [28].

A mechanical system could be translational, rotational or both. In those cases the through and across variables for each one are:

Table 3.1: *Through and across variables for a mechanical system*

System	Variable through element	Integrated through variable	Variable across element	Integrated across variable
Mechanical translational	Force	Translational momentum	Velocity difference	Displacement difference
Mechanical rotational	Torque	Angular momentum	Angular velocity difference	Angular displacement difference

The basic mechanical modeling that is going to be further used is explained in Fig. 3.10 where  $J$  corresponds to a rotational inertia,  $k$  to a rotational spring,  $b$  to a rotational damper,  $\phi(t)$  to the angular displacement,  $\omega(t)$  to the rotational speed and  $m(t)$  to the torque applied.

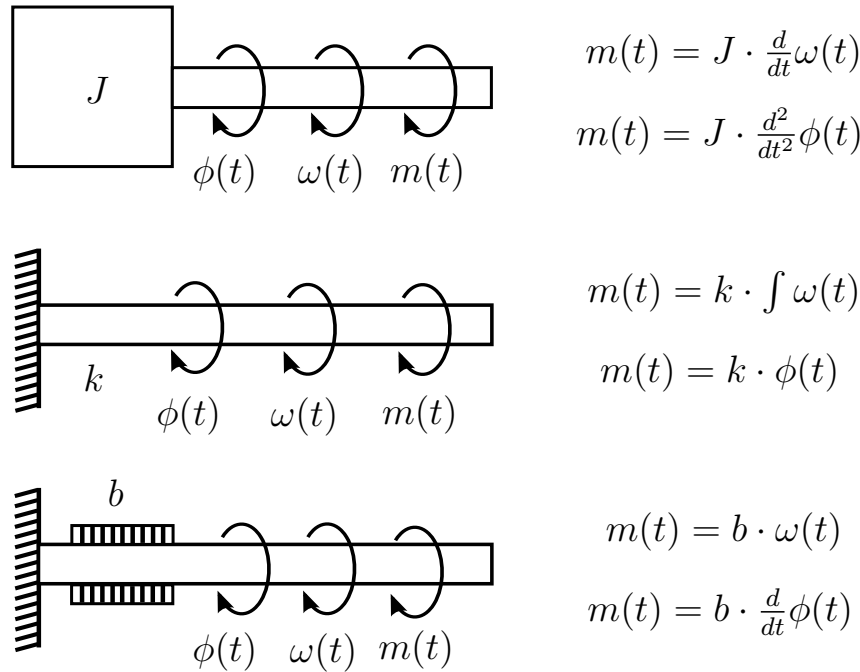


Figure 3.10: *Mechanical rotational system modeling [9]*

The basic modeling of a mechanical system can be explained through a spring-mass-damper example [14] as shown in Fig. 3.11.

The model includes the wall friction as a viscous damper, which means that the friction force is linearly proportional to the velocity of the mass. Friction in reality

is much more complicated, but for more about friction and its modeling, see [20, pp.17-28]. For a well-lubricated, sliding surface, the viscous friction is appropriate. Summing the forces acting on  $M$  and utilizing Newton's second law, the system can be modeled. To describe a mechanical system, the Newton's laws are used and for the description of an electrical system, Kirchhoff's voltage and current laws are used.

$$M \frac{d^2}{dt^2} y(t) + b \frac{d}{dt} y(t) + ky(t) = u(t) \quad (3.1)$$

where  $k$  is the spring constant of the ideal spring and  $b$  is the friction constant.

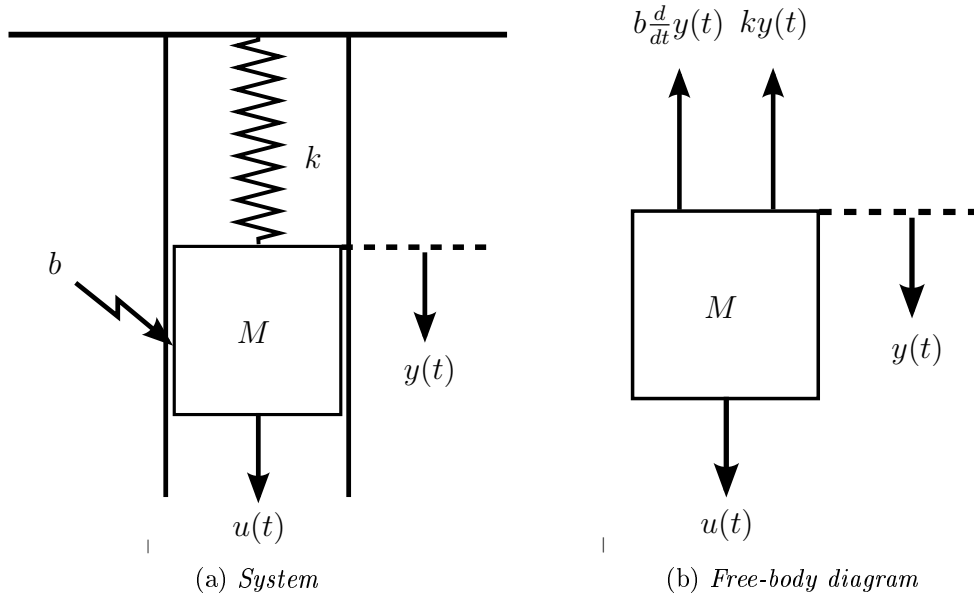


Figure 3.11: *Spring-mass damper system [14]*

Equation (3.1) is a second-order linear constant-coefficient differential equation. Which can be transformed into

$$M \frac{d}{dt} v(t) + bv(t) + k \int_0^t v(t) dt = u(t) \quad (3.2)$$

by  $v(t) = \frac{d}{dt} y(t)$ .

### 3.2.2.2 State variable models

The state of a system is a set of variables whose values, together with the input signals and the equations describing the dynamics, will provide the future state and output of the system. To describe a model as a state variable model, it is necessary to consider the time domain formulation of the equations. The time-domain techniques can be used for nonlinear, time-varying, and multivariable systems and itself, a time-

varying control system is defined as a system in which one or more of the parameters of the system may vary as a function of time [14].

The time-domain description of a dynamic system is represented by the system's differential equations. The time domain is the mathematical domain that incorporates the response and description of a system in terms of time,  $t$  [14]. As it is, the representation of control systems in time-domain has become an essential basis for modern control theory and system optimization.

For a dynamic system, the state of a system is described in terms of a set of state variables  $(x_1(t), x_2(t), \dots, x_n(t))^T$ . The state variables are those variables that determine the future behavior of a system when the present state of the system and the excitation signals are known [14]. The state variables describe the present configuration of a system and can be used to determine the future response, given the excitation inputs and the equations describing the dynamics.

The concept of a set of state variables that represent a dynamic system can be illustrated in terms of the spring-mass-damper system shown in Fig. 3.11 and equation (3.1). The number of state variables chosen to represent a system should be as small as possible in order to avoid redundant state variables [14]. In this case, state variables for the position and velocity of the mass are sufficient to describe the system. The state variables are defined as  $(x_1, x_2)^T$ , where

$$x_1(t) = y(t) \quad \text{and} \quad x_2 = \frac{d}{dt}y(t) \quad (3.3)$$

Transforming, in this case, equation (3.1) into

$$M \frac{d}{dt}x_2(t) + bx_2(t) + kx_1(t) = u(t) \quad (3.4)$$

the behavior of the spring-mass damper system can now be described as the set of two first-order differential equations in terms of the rate of change of each state variable.

$$\frac{d}{dt}x_1(t) = x_2(t) \quad (3.5)$$

$$\frac{d}{dt}x_2(t) = \frac{1}{M} \left( u(t) - bx_2(t) - kx_1(t) \right) \quad (3.6)$$

The state variables that describe a system are not a unique set, and several alternative sets of state variables can be chosen depending on what is desired to control and the adequately way to describe the dynamics of the system. It is usual to choose a set of state variables that can be readily measured [14].

The concept of system state is not limited to the analysis of physical systems and is particularly useful in analyzing biological, social, and economic systems. For these systems, the concept of state is extended beyond the concept of the current configuration of a physical system to the broader viewpoint of variables that will be capable of describing the future behavior of the system.

**3.2.2.3 The state differential equation**

As explained, the response of a system is described by a set of first-order differential equations written in terms of the state variables  $(x_1(t), x_2(t), \dots, x_n(t))^T$  and the inputs  $(u_1(t), u_2(t), \dots, u_m(t))^T$ . Describing a system with  $n$ -state variables and  $m$ -inputs.

These first-order differential equations can be written in general form as

$$\begin{aligned} \frac{d}{dt}x_1 &= a_{11}x_1 + a_{12}x_2 + \dots + a_{1n}x_n + b_{11}u_1 + \dots + b_{1m}u_m \\ \frac{d}{dt}x_2 &= a_{21}x_1 + a_{22}x_2 + \dots + a_{2n}x_n + b_{21}u_1 + \dots + b_{2m}u_m \\ &\vdots \\ \frac{d}{dt}x_n &= a_{n1}x_1 + a_{n2}x_2 + \dots + a_{nn}x_n + b_{n1}u_1 + \dots + b_{nm}u_m \end{aligned} \quad (3.7)$$

Whom can be simultaneously written in matrix form as:

$$\begin{bmatrix} \frac{d}{dt}x_1(t) \\ \frac{d}{dt}x_2(t) \\ \vdots \\ \frac{d}{dt}x_n(t) \end{bmatrix} = \begin{bmatrix} a_{11} & a_{12} & \dots & a_{1n} \\ a_{21} & a_{22} & \dots & a_{2n} \\ \vdots & \dots & \dots & \vdots \\ a_{n1} & a_{n2} & \dots & a_{nm} \end{bmatrix} \begin{bmatrix} x_1(t) \\ x_2(t) \\ \vdots \\ x_n(t) \end{bmatrix} + \begin{bmatrix} b_{11} & \dots & b_{1m} \\ \vdots & \dots & \vdots \\ b_{n1} & \dots & b_{nm} \end{bmatrix} \begin{bmatrix} u_1(t) \\ u_2(t) \\ \vdots \\ u_m(t) \end{bmatrix} \quad (3.8)$$

The matrix representation gives us the, from now on, "state vector" and it is written as

$$\mathbf{x}(t) = \begin{bmatrix} x_1(t) \\ x_2(t) \\ \vdots \\ x_n(t) \end{bmatrix} \quad (3.9)$$

and also referenced as  $(x_1(t), x_2(t), \dots, x_n(t))^T$ . In the same way, the input vector is defined as  $\mathbf{u}$ .

$$\mathbf{u}(t) = \begin{bmatrix} u_1(t) \\ u_2(t) \\ \vdots \\ u_m(t) \end{bmatrix} \quad (3.10)$$

Then the system can be represented by the compact or reduced notation of the state differential equation as

$$\frac{d}{dt}\mathbf{x}(t) = \mathbf{A}\mathbf{x}(t) + \mathbf{B}\mathbf{u}(t) \quad (3.11)$$

which is commonly references as the state equation. In here,  $\mathbf{A}$  is a square matrix as in  $\mathbf{A} \in \mathbb{R}^{n \times n}$ ,  $\mathbf{B}$  is a matrix as  $\mathbf{B} \in \mathbb{R}^{n \times m}$ .

The state differential equation relates the rate of change of the state of the system to the state of the system and the input signals. The outputs of the system are also related to the state variables and the input signals by the defined as "output



equation"

$$\mathbf{y}(t) = \mathbf{C}\mathbf{x}(t) + \mathbf{D}\mathbf{u}(t) \quad (3.12)$$

In here,  $\mathbf{C}$  is a matrix defined as  $\mathbf{C} \in \mathbb{R}^{n \times m}$ ,  $\mathbf{D}$  is a matrix as  $\mathbf{D} \in \mathbb{R}^{n \times m}$ . The  $\mathbf{D}$  matrix is usually zero due to the system's physics, so it is commonly neglected.

The block diagram is shown in Fig. 3.12

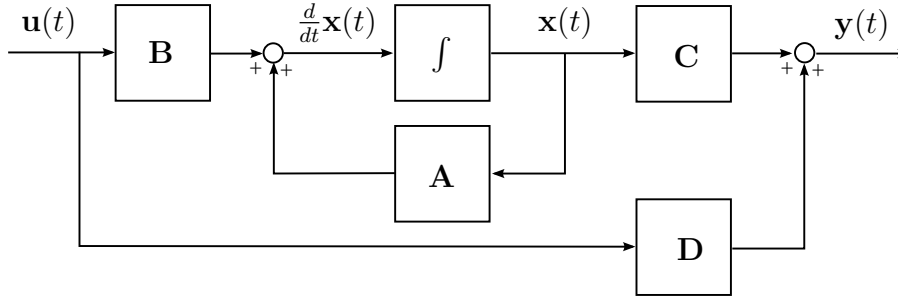


Figure 3.12: *System block diagram*

If the system is defined in the matrix form, the characteristic equation of the system is given by

$$\det(p\mathbf{I} - \mathbf{A}) = 0 \quad (3.13)$$

where  $\mathbf{I}$  corresponds to an identity matrix of size  $n \times n$  and  $p$  represents the roots of the characteristic equation commonly referred as the poles of the system

### 3.2.2.4 Feedback control systems

A control system is defined as an interconnection of components forming a system that will provide a desired system response [14]. As explained by Dorf and Bishop, a feedback system is a system that uses a signal proportional to the error between the desired and the actual response of the system to control it. Feedbacks often appear to the need of improving the control system. Interesting enough, feedback appears also in nature, being the human heart an example of a feedback control system.

As mentioned before, a system without feedback is often called an open-loop system. In these cases, disturbances directly influence the output of the system, becoming highly sensitive to disturbances and to changes in parameters. An open-loop system operates without feedback and directly generates the output in response to an input signal [14].

Different from it, a closed-loop system uses a measurement of the output signal and a comparison with the desired output to generate an error signal that is used by the controller to adjust the actuator, adding the following advantages:

- Less sensitivity of the system to variations in the parameters of the process.
- Better rejection of the disturbances.
- Better measurement noise attenuation.

- Improved reduction of the steady-state error of the system.
- Easy control and adjustment of the transient response of the system.

**Error signal** From a closed-loop feedback control system, the tracking error is defined as the difference between the actual response  $y(t)$  and the desired one  $y_{ref}(t)$

$$\varepsilon(t) = y_{ref}(t) - y(t) \quad (3.14)$$

### 3.2.2.5 Stability

When considering the design and analysis of feedback control systems, stability is of the utmost importance [14]. From a practical point of view, both closed-loop and open-loop systems might be unstable, and some are even designed to be unstable. Active control is introduced by engineers to stabilize the unstable systems to address other considerations, such as transient performance. A feedback, we can stabilize unstable systems and then, by choosing the correct parameters in the controller design, adjust the transient performance. For open-loop stable systems, feedback is still used to meet the design specifications.

Closed-loop feedback systems can either be stable or unstable, referencing to absolute stability. There could also exist "relative stability".

**Definition 1** (Absolute stability). A control system that is completely stable.

**Definition 2** (Relative stability). A control system with a certain degree of stability.

For more information about absolute and relative stability, please check [14].

A system is absolutely stable by analyzing the characteristic polynomial of transfer function of the system. For the system to be stable, all of its poles need to be lying in the left-half imaginary plane, or equivalently, have all the eigenvalues of the system matrix  $\mathbf{A}$  lie in the left-half imaginary plane in case of continuous time or inside the unitary circle for discrete time. Relative stability can be analyzed by examining the relative locations of the poles (or eigenvalues) [14].

A stable system is defined as a system with a bounded system response. That means that if the system is subjected to a bounded input or disturbance and the response is bounded in magnitude, the system is said to be stable [14]. A stable system is a dynamic system with a bounded response to a bounded input. The response to a displacement, or initial condition, is going to result in either a decreasing, neutral, or increasing response.

The location in the imaginary-plane of the poles of a system indicates the resulting transient response. The poles in the left-hand portion of the imaginary-axis result in a decreasing response and the right-hand portion of the imaginary-axis result in a neutral or an increasing response, respectively, for a disturbance input. Clearly, the poles of desirable dynamic systems must lie in the left-hand portion of the imaginary-plane [14].

### 3.2.2.6 Observability and controllability

While designing or just analyzing a system, a key question that shows up is whether or not all the poles of the closed-loop system can be arbitrarily placed or are placed in the complex plane. If a system is controllable and observable, then its poles can be placed in desired locations to meet the performance specifications for the design. Usually, pole-placement techniques are used for the design of the systems, but it is important to note that a system must be completely controllable and completely observable to allow the flexibility to place all the closed-loop system poles arbitrarily [14].

The concepts of controllability and observability were introduced by Kalman in the 1960s. Rudolph Kalman was a hugely important person in the development of mathematical systems theory. He is well known for his role in the development of the "Kalman filter", which was instrumental in the successful Apollo moon landings [14]. As defined by Richard Dorf and Robert Bishop in their book,

**Definition 3.** A system is completely controllable if there exists an unconstrained control  $u(t)$  that can transfer any initial state  $x(0)$  to any other desired location  $x(t)$  in a finite time,  $t_0 \leq t \leq T$ .

Assuming the system

$$\frac{d}{dt}\mathbf{x}(t) = \mathbf{A}\mathbf{x}(t) + \mathbf{B}\mathbf{u}(t) \quad (3.15)$$

$$\mathbf{y}(t) = \mathbf{C}\mathbf{x}(t) + \mathbf{D}\mathbf{u}(t) \quad (3.16)$$

It can be determined whether the system is controllable by examining the following condition

$$\mathbf{M} = \begin{bmatrix} \mathbf{B} & \mathbf{A}\mathbf{B} & \mathbf{A}^2\mathbf{B} & \dots & \mathbf{A}^{n-1}\mathbf{B} \end{bmatrix} \quad (3.17)$$

In here,  $\mathbf{A}$  is defined as  $\mathbf{A} \in \mathbb{R}^{n \times n}$  and  $\mathbf{B}$  as  $\mathbf{B} \in \mathbb{R}^{n \times 1}$ . For a single-input, single-output system, the controllability matrix  $\mathbf{M}$  is described in terms of  $\mathbf{A}$  and  $\mathbf{B}$  as a matrix with dimensions  $n \times n$ . In this case, if the determinant of  $\mathbf{M}$  is nonzero or if the rank of the matrix  $\mathbf{M}$  is  $n$ , the system is controllable. [14].

In advanced state variable design techniques, some situations where the system is not completely controllable can be handled, but the states that cannot be controlled are inherently stable. Those types of systems are considered stabilizable and even if the system is completely controllable, it is also considered stabilizable. For those cases, the Kalman state-space decomposition provides a mechanism for partitioning the state-space so that it becomes apparent which states (or state combinations) are controllable and which are not [14].

Defined as well by Dorf and Bishop, observability refers to the ability to estimate a state variable.

**Definition 4.** A system is completely observable if and only if there exists a finite time  $T$  such that the initial state  $x(0)$  can be determined from the observation history  $\mathbf{y}(t)$  given the control  $\mathbf{u}(t)$ ,  $t_0 \leq t \leq T$ .

It can be determined whether the system is observable by examining the following condition

$$\mathbf{S} = \begin{bmatrix} \mathbf{C} \\ \mathbf{CA} \\ \mathbf{CA}^2 \\ \vdots \\ \mathbf{CA}^{n-1} \end{bmatrix} \quad (3.18)$$

Considering a single-input, single-output system where  $\mathbf{C}$  is a  $1 \times n$  row vector, and  $\mathbf{x}$  is a  $n \times 1$  column vector. This system is completely observable when the determinant of the observability matrix  $\mathbf{S}$  is nonzero or if the rank of the matrix  $\mathbf{S}$  is  $n$ . In this case,  $\mathbf{S}$  is a  $n \times n$  matrix.

The same that happens with systems that are not completely controllable happens with systems that are completely observable, but where the states that cannot be observed are inherently stable. These type of systems are classified as detectable and even if the system is completely observable, it is also detectable. As well as in the controllability, the Kalman state-space decomposition is able to provide a mechanism for partitioning the state-space so that it becomes apparent which states (or state combinations) are observable and which are not [14].

### 3.2.2.7 Observer design

Even though it is hoped that all systems are completely controllable and observable, generally speaking, only a subset of the states are readily measurable and available. Most of the time having all the states available implies that these states are measured with a sensor or sensor combinations which increases the cost and complexity of the control system. So, even in situations where extra sensors are available, it may not be cost effective to employ if the control can accomplish the needs. If the system is observable with a given set of outputs, then it is possible to estimate the states that are not directly measured or observed.

According to Luenberger [14], a full-state observer for a system defined as

$$\frac{d}{dt}\mathbf{x}(t) = \mathbf{A}\mathbf{x}(t) + \mathbf{B}\mathbf{u}(t) \quad (3.19)$$

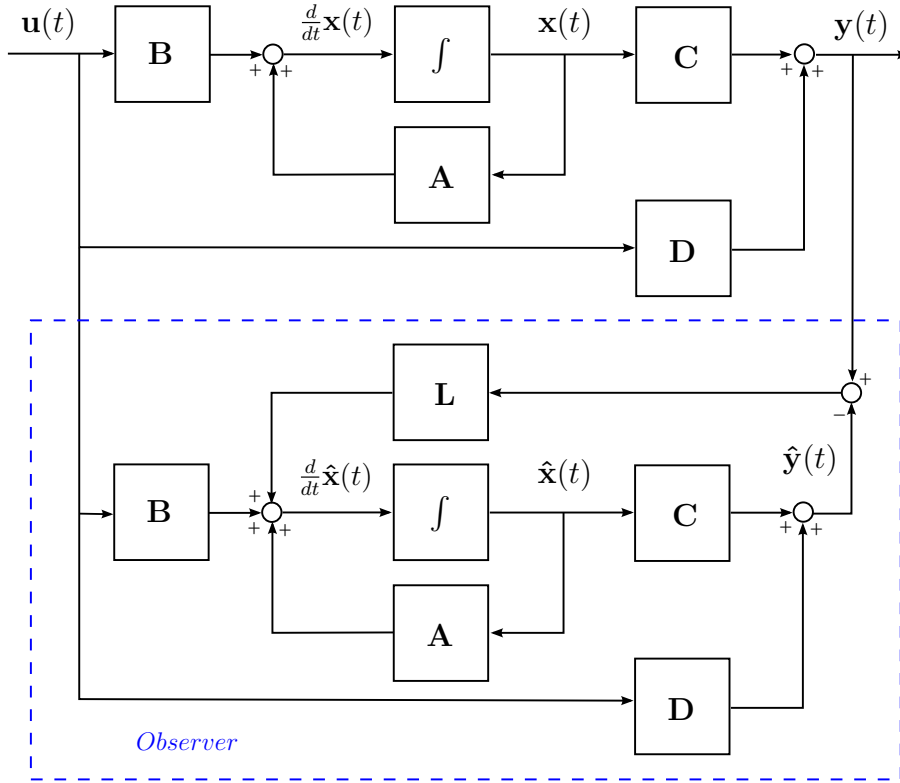
$$\mathbf{y}(t) = \mathbf{C}\mathbf{x}(t) + \mathbf{D}\mathbf{u}(t) \quad (3.20)$$

is given by

$$\frac{d}{dt}\hat{\mathbf{x}}(t) = \mathbf{A}\hat{\mathbf{x}}(t) + \mathbf{B}\mathbf{u}(t) + \mathbf{L}(\mathbf{y}(t) - \mathbf{C}\hat{\mathbf{x}}(t)) \quad (3.21)$$

where  $\hat{\mathbf{x}}$  denotes the estimate of the state  $\mathbf{x}$ . The matrix  $\mathbf{L}$  is the observer gain matrix and is to be determined as part of the observer design procedure.

The block diagram of a Luenberger observer is shown in Fig. 3.13


 Figure 3.13: *Observer with augmented system block diagram*

The observer has two inputs,  $u(t)$  and  $y(t)$ , and one output,  $\hat{x}$ . The goal of the observer is to provide an estimate  $\hat{x}$  so that  $\hat{x}$  tends to  $x$  as  $t$  tends to infinity. As  $x(t_0)$  is unknown, an initial estimate  $x(t_0)$  should be provided to the observer. Define the observer estimation error as

$$\varepsilon_{obs}(t) = \mathbf{x}(t) - \hat{\mathbf{x}}(t) \quad (3.22)$$

The design of the observer should produce  $\varepsilon_{obs}(t) \rightarrow 0$  as  $t \rightarrow \infty$ . One of the main results of systems theory is that if the system is completely observable, we can always find  $\mathbf{L}$  so that the tracking error is asymptotically stable, as desired [14].

Taking the time-derivative of the estimation error ends up in

$$\frac{d}{dt}\varepsilon_{obs}(t) = \frac{d}{dt}\mathbf{x}(t) - \frac{d}{dt}\hat{\mathbf{x}}(t) \quad (3.23)$$

which can be transformed by inserting (3.19) and (3.21) into (3.23) and assuming  $\mathbf{D}$  is zero.

$$\frac{d}{dt}\varepsilon_{obs}(t) = \underbrace{\mathbf{A}\mathbf{x}(t) + \mathbf{B}\mathbf{u}(t)}_{(3.19)} - \underbrace{\mathbf{A}\hat{\mathbf{x}}(t) + \mathbf{B}\mathbf{u}(t) + \mathbf{L}(\mathbf{y}(t) - \mathbf{C}\hat{\mathbf{x}}(t))}_{(3.21)} \quad (3.24)$$

$$\frac{d}{dt}\varepsilon_{obs}(t) = (\mathbf{A} - \mathbf{L}\mathbf{C})\varepsilon_{obs}(t) \quad (3.25)$$

It can be guaranteed that  $\varepsilon_{obs}(t)$  tends to 0 as  $t$  tends to infinity for any initial tracking error  $\varepsilon_{obs}(t_0)$  if the characteristic equation

$$\det(p\mathbf{I} - (\mathbf{A} - \mathbf{LC})) = 0 \quad (3.26)$$

has all its roots in the left half-plane. Therefore, the observer design process reduces to finding the matrix  $\mathbf{L}$  such that the roots of the characteristic equation lie in the left half-plane. This can always be accomplished if the system is completely observable [14].

### 3.2.2.8 Robustness

Designing highly accurate systems in the presence of significant plant uncertainty is a classical design problem. Going back to the early 1930s, the theoretical bases to solve this problem can be found in the works of H. S. Black and H. W. Bode, when this problem was referred to as the sensitivities design problem. Since then an important amount of literature has been published about the design of systems that are subject to large process uncertainties [14].

An objective of the designer should be to obtain a system that performs adequately over a large range of uncertain parameters. The goal of robust system's design is to retain assurance of system performance in spite of model inaccuracies and changes. A system is robust when the system has acceptable changes in performance due to model changes or inaccuracies, when it is durable, hardy, and resilient. A robust control system is identified by exhibiting the desired performance despite the presence of significant process uncertainties [14].

**Definition 5.** Sensitivity The minimum signal power that can be distinguished from the random fluctuations in the output of a measuring system caused by noise inherent in the system. [17]

**Definition 6.** A control system is robust when it has low sensitivities, it is stable over the range of parameter variations, and the performance continues to meet the specifications in the presence of a set of changes in the system parameters [14].

**Definition 7.** Robustness is the low sensitivity to effects such as disturbances, measurement noise, or unmodeled dynamics, that are not considered in the analysis and design phase [14].

The system should be able to withstand these neglected effects when performing the tasks for which it was designed [14].

## 3.3 Parameter estimation

This section is based on [23]. Parameter estimation is the process of using observations from a dynamic system to develop mathematical models that adequately represent the system characteristics [23]. The model that is assumed consists of a

finite set of parameters, which are estimated using one of the various estimation techniques. Fundamentally, the approach is based on minimization of the error between the model response and actual system's response. With the advent of high-speed digital computers, more complex and sophisticated techniques like filter error method and innovative methods based on artificial neural networks find increasing use in parameter estimation problems [23].

The idea behind modeling an engineering system or a process is to improve its performance or to design a control system.

Dynamic systems abound in the real-life practical environment in a variety of systems that can be categorized in biological, mechanical, electrical, civil, chemical, aerospace, road traffic and others. Understanding the dynamic behavior of these systems, as mentioned before, is one of the primary interests to scientists as well as engineers. Mathematical modeling via parameter estimation is one of the ways that leads to deeper understanding of the system's characteristics. These parameters often describe the stability and control behavior of the system [23].

Estimation of these parameters from the input-output data of the system is an important step in the analysis of the dynamic system. By all means, analysis can be referred as the process of obtaining the system response to a specific input, given the knowledge of the model representing the system [23], but within this method, the knowledge of the mathematical model and its parameters is vital. This can end up falling into the known category of "inverse problems" where the knowledge of the dynamical system is actually derived from the input-output data of the system. Opening or starting the discussion about the uniqueness of the identified model and establishing the adequacy of the estimated model parameters on the analyst. Nevertheless, there are several criteria available for establishing the adequacy and validity of such estimated parameters and models. Parameter estimation is based on the minimization of some criterion, and this criterion itself can serve as one of the means to establish the adequacy of the identified model [23].

The parameters of the model are adjusted through iteration until the time when the responses of the model match closely with the measured outputs of the system under investigation in the sense specified by the minimization criterion. It must be emphasized here that though a good match is necessary, it is not the sufficient condition for achieving good estimates [23]. A simplified block diagram of the parameter estimation is shown in Fig. 3.14.

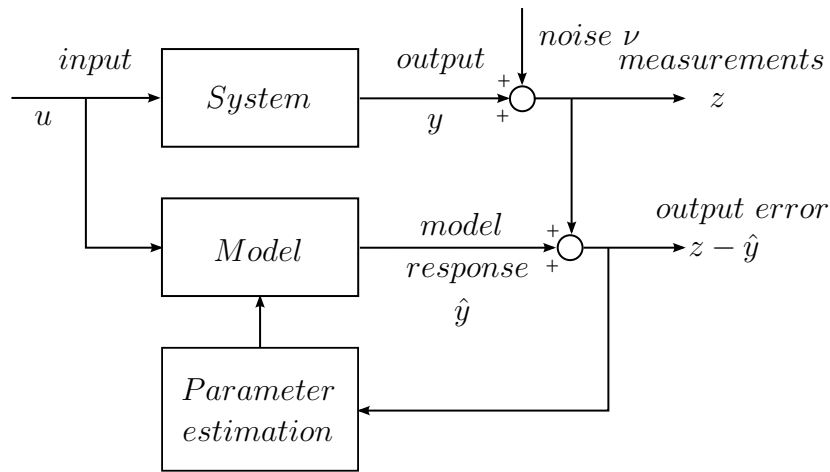


Figure 3.14: *Simplified block diagram of the estimation procedure [23]*

As early as 1795, Gauss dealt with the motion of the planets and concerned himself with the prediction of their trajectories, using only a few parameters in the process to describe these motions, making pioneering contributions to the problem of parameter estimation of the dynamic systems. He invented the least squares parameter estimation method as a special case of the so-called maximum likelihood type method, though he did not name it [23]. Commonly, the estimation of the parameters of dynamic systems and the state-estimation is done by using Kalman filtering algorithms. In this thesis, forms of both methods, least squares and Kalman filtering are used.

The parameter error can be obtained if the true parameter value is known, which does not happen in real-life scenarios. However, the parameter estimation algorithms can be checked and/or validated with simulated data, which is generated using the true parameter values of the system. For the real data situations, assumptions about the error in estimated values of the parameters can be made based on some statistical properties [23]. Mostly, the approach to use the output error is appealing from the point of view of matching of the measured and estimated or predicted model output responses.

### 3.3.1 Kalman filtering

In 1960, R.E. Kalman published his famous paper describing a recursive solution to the discrete-data linear filtering problem. Since that time, due in large part to advances in digital computing, the Kalman filter has been the subject of extensive research and application, particularly in the area of autonomous or assisted navigation [34].

The Kalman filter is a set of mathematical equations that provides an efficient computational (recursive) means to estimate the state of a process, in a way that minimizes the mean of the squared error. The filter is very powerful in several aspects: it supports estimations of past, present, and even future states, and it can do so even when the precise nature of the modeled system is unknown [34].



Although most dynamic systems are continuous-time, the Kalman filter is an extremely popular filtering method and is best discussed using the discrete-time model. In addition, in the sequel, it will be seen that the solution of the Kalman filter requires handling of the Riccati equation, which is easier to handle in discrete form rather than in continuous-time form.

The basic principle of the method is predicting the value of an state and then correcting the measurement that was done. The time update equations can also be thought of as predictor equations, while the measurement update equations can be thought of as corrector equations. Indeed the final estimation algorithm resembles that of a predictor-corrector algorithm for solving numerical problems [34] as shown in Fig. 3.15

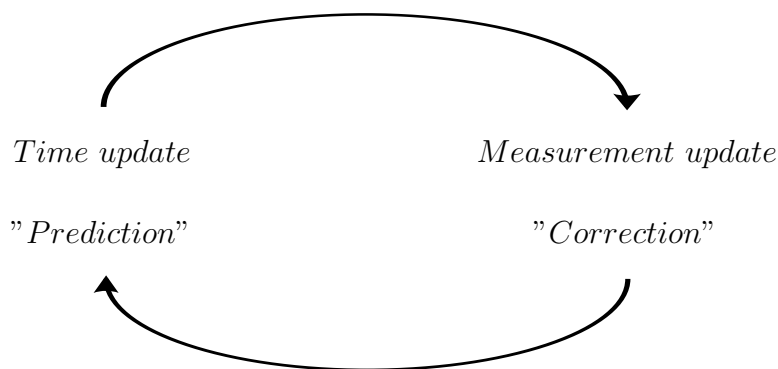


Figure 3.15: *The ongoing discrete Kalman filter cycle [34]*

In deriving the equations for the Kalman filter, the goal is to find an equation that computes an a posteriori state estimate as a linear combination of an a priori estimate and a weighted difference between an actual measurement and a measurement prediction. Where the difference is called the measurement innovation or residual. The residual reflects the discrepancy between the predicted measurement and the actual measurement. A residual of zero means that the two are in complete agreement.

The Kalman filter estimates a process by using a form of feedback control: the filter estimates the process state at some time and then obtains feedback in the form of noisy measurements [34]. As such, the equations for the Kalman filter fall into two groups: time update equations and measurement update equations.

The time update equations are responsible for projecting forward in time the current state and error covariance estimates to obtain the priori estimates for the next time step. The measurement update equations are responsible for the feedback, or for incorporating a new measurement into the priori estimate to obtain an improved a posteriori estimate [34].

### 3.3.2 Least squares parameter estimation method

The least squares (LS) estimation method was invented by Karl Gauss in 1809 and independently by Legendre in 1806 [23]. Gauss was interested in predicting the

motions of the planets using just measurements obtaining or inventing the least squares method. It is a well established and easy to understand method. Still, to date, many problems center on this basic approach. The least squares method is a special case of the well-known maximum likelihood estimation method for linear systems with Gaussian noise [23].

In general, least squares methods can be used with both linear as well as nonlinear problems. They are also applicable to multiple input multiple output dynamic systems. Least squares techniques can be applied to the online parameter identification or to the offline parameter identification.

The measurement equation model is assumed to have the following form:

$$\mathbf{y} = \varphi^\top \theta + \nu \quad (3.27)$$

where  $\mathbf{y}$  is a  $m \times 1$  vector of true outputs and  $\varphi$  is a  $m \times n$  matrix or vector that denotes the measurements or data, usually affected by noise, of the unknown parameters.  $\theta$  is a  $n \times 1$  vector of the unknown parameters and  $\nu$  represents the measurement noise which is assumed to be zero mean and Gaussian. This model is called the measurement equation model, since it forms a relationship between the measurements and the parameters of a system. [23]

It is said that the estimation theory and the methods have a data-dependent nature, since the measurements used for estimation are invariably noisy [23]. But these noisy measurements are used in the estimation method to improve upon the initial estimate of the parameters that characterize the signal or system.

For this method, it is assumed that the system parameters do not rapidly change with time, thereby assuring an almost stationary behavior of the plant or the process parameters, or at least during the measurement period [23]. This should not be confused with the requirement of non-steady input-output data over the period for which the data is collected for parameter estimation. This means that during the measurement period there should be some activity.

The least squares method is considered a deterministic approach to the estimation problem. There is then chose an estimator of  $\theta$  that minimizes the sum of the squares of the error. Or that minimizes the well-known "cost function"

$$J = \frac{1}{2} \sum_{k=1}^N v^2[k] = \frac{1}{2} (\mathbf{y} - \varphi^\top \theta)^\top (\mathbf{y} - \varphi^\top \theta) \quad (3.28)$$

Here  $J$  is a cost function and  $v$  is the residual error at time  $k$ . It is noticed that  $\nu$  is neglected for the cost function.

There are several methods based on the least squares estimation, so the implementation depends on the chosen method, but there are properties that are shown in every one. To read more up on the topic, please check [22].



# Chapter 4

## Methodology

In this chapter the four main sections of the solution's approach to determine if it is possible to detect mechanical faults in wind turbines with the estimation of the low speed shaft's mechanical constants are developed. The main information sources for the thesis are published books and scientific articles and master's thesis developed on the research group.

### 4.1 Mechanical modeling of wind turbines

In this section only the basic mechanical components are considered to describe the modeling of a wind turbine with direct drive. The section is based on [3] and [13].

#### 4.1.1 Turbine

The turbine with its three blades, as shown in Fig. 3.4, is the one in charge of transforming the wind's energy into rotational energy. As explained in section 3.1.2, the turbine has a radius,  $r_T$  [m] and it spans defining an area described by

$$A_T := \pi \cdot r_T^2 \quad [\text{m}^2] \quad (4.1)$$

in this case, this area is assumed as the total area. The nacelle area,  $A_G$  [m<sup>2</sup>], can be neglected due to its small value compared to the turbine area.

Any change in the wind speed will be reflected in the whole system. And it is possible to obtain a relation between the wind speed and the rotational speed, known as the tip speed,  $\lambda$  [1].

The tip speed is the ratio between the tangential speed of the tip of a blade,  $w_T \cdot r_T$ , and the actual wind speed,  $v_W$ . The tip speed is related to the efficiency of the wind turbine, varying on the blade design. The higher the tip speeds is, higher noise levels are produced and stronger blades are required due to large centrifugal forces [33].

The equation that describes the tip speed is

$$\lambda := \frac{r_T \cdot \omega_T}{v_W} \quad (4.2)$$

The tip speed,  $\lambda$ , is a key variable in the control of wind turbines because it allows the wind turbine to operate in the optimum point to obtain the maximum possible power from the wind. It is important to note that even without the knowledge of the tip speed, the turbine is allowed to operate at the optimal point by physics.

There is also an optimal tip speed,  $\lambda_{opt}$  [1] or  $\lambda^*$  [1], that stays the same for every wind speed. Working as a constant reference.

Besides  $\lambda$ , the pitch angle,  $\beta$ , needs to be considered as another control variable due to the importance associated to angle changes in the overall functioning of the wind turbine. The slightest change in the pitch angle means the incident wind flow in the rotor blades is increased or decreased.

The relationship between these two variables and the wind turbine performance is further explained with the power coefficient and the turbine torque.

#### 4.1.1.1 Power coefficient

The power coefficient,  $c_P$  [1], is described as the amount of mechanical power,  $p_T$  [W], that can be obtained from the wind's power,  $p_W$  [W]. It comes as a result of the relation between the pitch angle,  $\beta$ , and the tip speed,  $\lambda$ .

The Betz factor,  $c_{P,Betz}$  is the theoretical value of the power coefficient, or its maximum. It is used as the power coefficient reference and it has a value of  $\frac{16}{27}$  or 0,59 approximately.

The actual power obtained from the wind is given by

$$p_W(t) = \frac{1}{2} \cdot \rho \cdot \pi \cdot r_T^3 \cdot v_W(t)^2 \quad (4.3)$$

In this equation it needs to be considered the air's density,  $\rho$  [kg/m<sup>3</sup>].

As mentioned before, the power coefficient has a direct impact on the overall turbine power, which can be obtained applying the power coefficient to the wind power as

$$p_T(\lambda, \beta) = c_P(\lambda, \beta) \cdot p_W(t) \leq c_{P,Betz} \cdot p_W(t) \quad (4.4)$$

From the direct relation between the power coefficient and the turbine's power, the maximum power from the wind turbine can be obtained at the maximum  $c_P$ , shown in Fig. 4.1 as the graph's maximum.

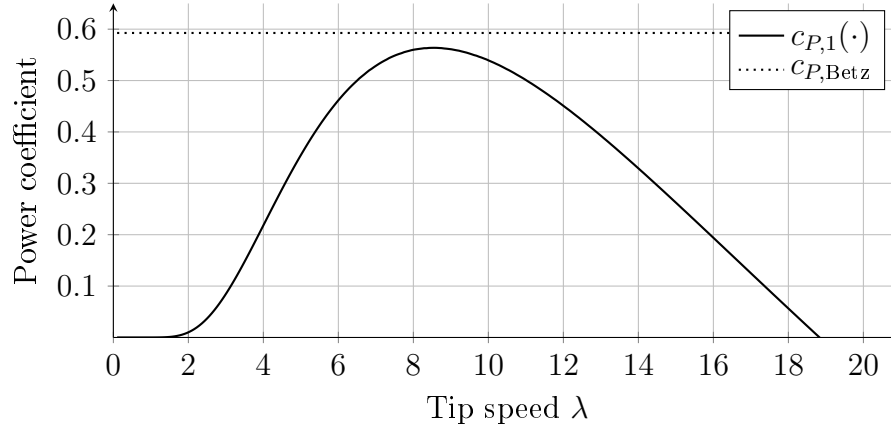


Figure 4.1: Power coefficient for a 2 MW wind turbine, see (4.5)

**Approximation of the power coefficient** The power coefficient can be divided into two depending on the pitch angle,  $\beta$ :

- $c_{P,1}$ : In this case there is no pitch system and the value of the power coefficient at any specific  $\lambda$  can be obtain with the equation

$$c_{P,1}(\lambda) := \max \left\{ \left[ 46.4 \cdot \left( \frac{1}{\lambda} - 0.01 \right) - 2 \right] \cdot e^{-15.6 \cdot \left( \frac{1}{\lambda} - 0.01 \right)}; 0 \right\} \quad (4.5)$$

$c_{P,1}$  has a maximum located in  $\lambda^*$ , which is given by the derivative of the equation (4.5).

$$\frac{d}{d\lambda} c_{P,1}(\lambda) = 0 \quad (4.6)$$

- $c_{P,2}$ : This specific wind turbine has a pitch system, and the value of the power coefficient is given by

$$c_{P,2}(\beta, \lambda) := \max \left\{ \left[ 151 \cdot \left( \frac{1}{\lambda - 0,02\beta} - \frac{0,003}{\beta^3 + 1} \right) - 0,58\beta - 0,002 \cdot \beta^{2,14} - 13,2 \right] \cdot \exp \left( -18,4 \cdot \left( \frac{1}{\lambda - 0,02\beta} - \frac{0,003}{\beta^3 + 1} \right) \right); 0 \right\} \quad (4.7)$$

$c_{P,2}$  has also a maximum located in  $\lambda^*$ , which is given by the derivative of the equation (4.5).

$$\frac{d}{d\lambda} c_{P,2}(\beta, \lambda) = 0, \quad \beta = 0 \quad (4.8)$$

#### 4.1.1.2 Turbine torque

While the turbine is converting the kinetic wind energy in rotational energy, a torque is being generated on the drive train that leads to an acceleration and rotation of

the generator shaft.

As power, torque and rotational speed are related in

$$p_T(t) = m_T(t) \cdot \omega_T(t) \quad (4.9)$$

from here,  $m_T$  can be obtained using (4.3) and (4.4).

$$m_T(t) = \frac{p_T(t)}{\omega_T(t)} = \frac{1}{2} \cdot \rho \cdot \pi \cdot r_T^2 \cdot v_W(t)^3 \cdot \frac{c_P(\beta, \lambda)}{\omega_T(t)} \quad (4.10)$$

The turbine torque can be defined as a function of  $m_T(v_W, \beta, \lambda)$  or as  $m_T(v_W, \beta, \omega_T)$ . Both of them can be used because of the relationship given by the power coefficient and (4.2).

As those relationships are established, the direct relation between the power coefficient  $c_P$ , tip speed  $\lambda$ , and pitch angle  $\beta$  is shown.

### 4.1.2 Transmission

The transmission is the part of the wind turbine in charge of transmitting the mechanical power from the driving shaft to the driven one.

Most of the simple wind turbine gear box consists of two main shafts, the low speed shaft which is basically connected with the wind turbine blades, and the second one which is called the high speed shaft connected directly to the generator [3].

The turbine rotational speed,  $\omega_T$ , is much slower than the machine's rotational speed,  $\omega_M$  [ $\frac{\text{rad}}{\text{s}}$ ]. The relation between rotational speeds is called gearbox ratio,  $g_r$  [1].

$$g_r := \frac{\omega_M}{\omega_T} \geq 1 \quad (4.11)$$

**Assumption 1.** For a direct drive, the gear ratio is 1.

The present thesis shows two different mathematical modeling approaches that are commonly used to model the mechanical system. The two techniques are explained and detailed with the assumptions used in order to distinguish the differences and hence the consequences of each modeling.

**Assumption 2.** Elimination of the inertias from: the low speed shaft  $\Theta_{LS}$  [ $\text{kg m}^2$ ] and the high speed shaft  $\Theta_{HS}$  [ $\text{kg m}^2$ ]

**Assumption 3.** The gearbox inertia,  $\Theta_{GB}$  [ $\text{kg m}^2$ ], is included in the total machine's inertia,  $\Theta_M$  [ $\text{kg m}^2$ ], as

$$\Theta_M = \Theta_{M_0} + \Theta_{GB} \quad (4.12)$$

**Assumption 4.** Static friction is always neglected.

## 4.1.2.1 One-mass system

The transmission system in the wind turbine has two sides, as mentioned before, the turbine side and the machine side. Each side has a rotational speed, a torque and an inertia.

The one-mass system (1MS) is the one that consists of one inertia  $\Theta$  [kg m<sup>2</sup>] that is the sum of all of the coupled masses, and a gear ratio  $g_r$ . In this case, the mechanical system is driven by the turbine's torque  $m_T$  [N m] and it is subject to the machine's torque  $m_M$  [N m].

**Assumption 5.** Dynamic friction is neglected for the one-mass system.

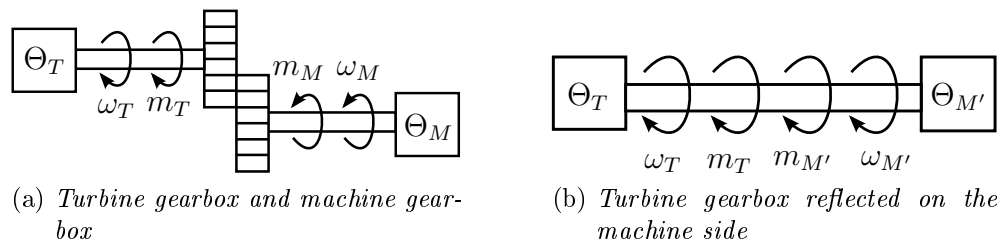


Figure 4.2: Gearbox transmission in a wind turbine, based on [13, p.18]

As shown in Fig. 4.2, the turbine side in (a) is described with the turbine's rotational speed,  $\omega_T$ , turbine's inertia,  $\Theta_T$  [kg m<sup>2</sup>], and turbine's torque,  $m_T$ . On the other side, the machine's variables are the machine's rotational speed,  $\omega_M$ , machine's inertia,  $\Theta_M$  [kg m<sup>2</sup>], and machine's torque,  $m_M$ .

Both sides can be reflected on the other one to obtain relations that will describe the system. In this case, the machine's side is the one reflected on the turbine's side. As this is done and the turbine's variables are the same, it applies

$$\omega_{T'} = \omega_T \quad , \quad m_{T'} = m_T \quad \text{and} \quad \Theta_{T'} = \Theta_T \quad (4.13)$$

Not the same happens to the machine's variables, which change to  $\omega_{M'}$ ,  $\Theta_{M'}$  and  $m_{M'}$  and the values need to be deducted. The starting point for deductions is the conservation of energy in the drive train in (4.14) and the power conservation in (4.15)

$$\forall t \geq 0 : \quad \frac{1}{2} \cdot \left( \Theta_T \cdot \omega_T(t)^2 + \Theta_M \cdot \omega_M(t)^2 \right) = \frac{1}{2} \cdot \left( \Theta_T \cdot \omega_T(t)^2 + \Theta_{M'} \cdot \omega_{M'}(t)^2 \right) \quad (4.14)$$

$$\forall t \geq 0 : \quad m_M(t) \cdot \omega_M(t) = m_{M'}(t) \cdot \omega_{M'}(t) \quad (4.15)$$

By relating the variables, the system can be described as a direct drive system, so the shaft speed is the same for both sides in Fig. 4.2 (b). Due to this,  $\omega_{M'}(t) = \omega_T(t)$



and (4.11),  $m_{M'}(t)$  can be obtained

$$\forall t \geq 0: \quad \omega_{M'}(t) = \omega_T(t) = \frac{\omega_M(t)}{g_r} \quad (4.16)$$

$$m_{M'}(t) = g_r \cdot m_M(t) \quad (4.17)$$

To find out the total inertia of the system, both inertias need to be added, but  $\Theta_{M'}$  [kg m<sup>2</sup>] is still undefined. It can be deduced

$$\Theta_{M'} \stackrel{(4.14)}{=} \Theta_M \cdot \frac{\omega_M(t)^2}{\omega_{M'}(t)^2} \stackrel{(4.16)}{=} \Theta_M \cdot \frac{\omega_M(t)^2}{\frac{\omega_M(t)^2}{g_r^2}} = g_r^2 \cdot \Theta_M \quad (4.18)$$

$$\Theta = \Theta_T + \Theta_{M'} = \Theta_T + g_r^2 \cdot \Theta_M \quad (4.19)$$

Finally, it is possible to obtain a simple model that describes the wind turbine in a one-mass system

$$\frac{d}{dt} \omega_M(t) = \frac{1}{\Theta} \cdot \left( m_T(t) + m_{M'}(t) \right) = \frac{1}{\Theta} \cdot \left( m_T(t) + g_r \cdot m_M(t) \right), \quad \omega_M(0) = \omega_{M,0} \quad (4.20)$$

From this simple model,  $\omega_M(t)$  is the output and feedback variable,  $\Theta$  is a known value,  $m_T(t)$  is given by (4.10),  $g_r$  is given by (4.11), and  $m_M(t)$  is described by the electrical modeling of the generator.

#### 4.1.2.2 Two-mass system

Two inertias coupled by a harmonic drive can be considered as an elastic two-mass system [20, p.16].

In particular, most controllers are considered more adapted for high-flexibility wind turbines that cannot be properly modeled with a one mass model. Besides, it is shown that the two-mass model can show flexible modes in the gear train model that cannot be done using the one mass model [3].

So the two-mass system (2MS) consists of two inertias, the machine's inertia  $\Theta_M$  [kg m<sup>2</sup>] and the turbine's inertia  $\Theta_T$  [kg m<sup>2</sup>]. From the coupling, there is a low speed shaft stiffness  $c_S$  [ $\frac{\text{Nm}}{\text{rad}}$ ] and low speed shaft damping  $d_S$  [ $\frac{\text{Nm s}}{\text{rad}}$ ] associated. The coupling may, as well, include a gear ratio  $g_r$  [1].

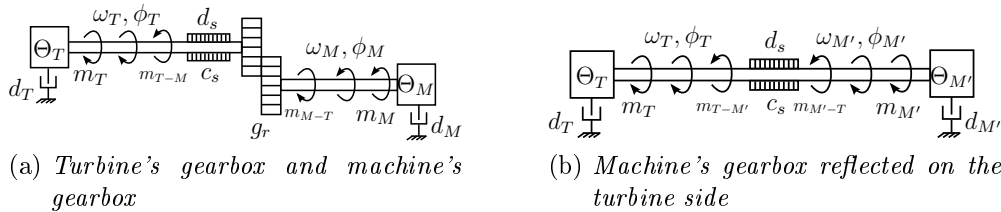


Figure 4.3: *Two-mass system in a wind turbine*

The essential assumptions of this model are:

**Assumption 6.** A turbine damping effect  $d_T$  [ $\frac{\text{Nms}}{\text{rad}}$ ] and a machine damping effect  $d_M$  [ $\frac{\text{Nms}}{\text{rad}}$ ] exist and are considered.

**Assumption 7.** The impact of the high speed shaft stiffness  $c_{HS}$  [ $\frac{\text{Nm}}{\text{rad}}$ ] and damping  $d_{HS}$  [ $\frac{\text{Nms}}{\text{rad}}$ ] exist, but are not considered.

In this two-mass model system, there are two ways to obtain the state variable that describes the system shown in Fig. 4.3.

**Case I** To obtain the model that is described in Fig. 4.3, it is necessary to relate the machine side to the turbine, as shown on Fig. 4.3 (b). From this moment on, the gear ratio can be related as

$$g_r = \frac{\omega_M(t)}{\omega_{M'}(t)} = \frac{\phi_M(t)}{\phi_{M'}(t)} = \frac{m_{M'-T}(t)}{m_{M-T}(t)} \quad \text{and} \quad g_r^2 = \frac{\Theta_{M'}}{\Theta_M} = \frac{d_{M'}}{d_M} \quad (4.21)$$

With Assumption 2, Assumption 3, Assumption 4, Assumption 6, Assumption 7, and the Newton's second law for rotating systems, the mathematical model for the turbine shown in Fig. 4.3 (b) is described by

$$\Theta_T \cdot \frac{d}{dt} \omega_T(t) + d_T \omega_T(t) = m_T(t) - m_{T-M'}(t), \quad \omega_T(0) = \omega_{T,0} \quad (4.22)$$

There are two torques, the torque produced by the turbine on the machine,  $m_{T-M}$  [Nm], and the torque produced by the machine on the turbine,  $m_{M-T}$  [Nm]. These torques are related by the gear ratio,  $g_r$ .

$$m_{M-T} = -\frac{m_{T-M}}{g_r} \quad (4.23)$$

In Fig. 4.3 (b), two torques are as well present, but in terms of the related machine. Transforming the variables in the torque produced by the turbine on the related machine,  $m_{T-M'}$  [Nm], and the torque produced by the related machine on the turbine,  $m_{M'-T}$  [Nm]

To describe  $m_{T-M'}$ , as shown in Fig. 4.3 (b), it is necessary to include the angle of the turbine  $\phi_T$  [rad] and the angle of the related machine's shaft  $\phi_{M'}$  [rad].

Applying Assumption 2, Assumption 4, Assumption 6, Assumption 7; the torque produced by the turbine on the machine is reduced to

$$m_{T-M'}(t) = d_s \cdot (\omega_T(t) - \omega_{M'}(t)) + c_s \cdot (\phi_T(t) - \phi_{M'}(t)) \quad (4.24)$$

For the machine's mathematical model the same procedure is used to obtain it

$$\Theta_{M'} \cdot \frac{d}{dt} \omega_{M'}(t) + d_{M'} \omega_{M'}(t) = m_{M'}(t) - m_{M'-T}(t), \quad \omega_{M'}(0) = \omega_{M',0} \quad (4.25)$$

To describe  $m_{M'-T}$ , the same method used to describe  $m_{T-M'}$  is used

$$\begin{aligned} m_{M'-T}(t) &= d_s \cdot (\omega_{M'}(t) - \omega_T(t)) + c_s \cdot (\phi_{M'}(t)\phi_T(t)) \\ &= -m_{T-M'} \end{aligned} \quad (4.26)$$

Using the relations and equations presented, the final equations to describe the model can be resumed as

$$\frac{d}{dt}\omega_T(t) = \frac{1}{\Theta_T}(m_T(t) - m_{T-M'}(t) - d_T\omega_T(t)), \quad \omega_T(0) = \omega_{T,0} \quad (4.27)$$

$$\begin{aligned} g_r^j \Theta_M \cdot \frac{d}{dt} \frac{\omega_M(t)}{g_r} &= g_r \cdot m_M(t) - m_{T-M'}(t) - g_r^j \cdot d_M \cdot \frac{\omega_M(t)}{g_r} \\ \frac{d}{dt}\omega_M(t) &= \frac{g_r \cdot m_M(t)}{g_r \cdot \Theta_M} - \frac{m_{T-M'}(t)}{g_r \cdot \Theta_M} - \frac{g_r^j \cdot d_M \cdot \omega_M(t)}{g_r \cdot \Theta_M} \\ \frac{d}{dt}\omega_M(t) &= \frac{1}{\Theta_M} \left( m_M(t) + \frac{m_{T-M'}(t)}{g_r} - d_M\omega_M(t) \right), \quad \omega_M(0) = \omega_{M,0} \end{aligned} \quad (4.28)$$

To relate the variables in this model, it is necessary to derive (4.24) with respect to the time to obtain

$$\begin{aligned} \frac{d}{dt}m_{T-M'}(t) &= d_s \left( \frac{d}{dt}\omega_T(t) - \frac{d}{dt}\omega_{M'}(t) \right) + c_s \left( \frac{d}{dt}\phi_T(t) - \frac{d}{dt}\phi_{M'}(t) \right) \\ &= d_s \left( \frac{d}{dt}\omega_T(t) - \frac{d}{dt}\omega_{M'}(t) \right) + c_s(\omega_T(t) - \omega_{M'}(t)) \\ &\stackrel{(4.21)}{=} d_s \left( \frac{d}{dt}\omega_T(t) - \frac{d}{dt} \frac{\omega_M(t)}{g_r} \right) + c_s \left( \omega_T(t) - \frac{\omega_M(t)}{g_r} \right) \end{aligned} \quad (4.29)$$

After substituting values using (4.27) and (4.28) in (4.29)

$$\begin{aligned} \frac{d}{dt}m_{T-M'}(t) &= \left( c_s - \frac{d_s \cdot d_T}{\Theta_T} \right) \omega_T(t) + \left( \frac{-c_s\Theta_M + d_M \cdot d_s}{g_r \cdot \Theta_M} \right) \omega_M(t) + \frac{d_s}{\Theta_T} m_T(t) + \\ &\quad \left( \frac{-d_s(\Theta_M \cdot g_r^2 + \Theta_T)}{g_r^2 \Theta_T \Theta_M} \right) m_{T-M'}(t) + \frac{d_s}{g_r \Theta_M} m_M(t), \quad m_{T-M'}(0) = m_{T-M',0} \end{aligned} \quad (4.30)$$

The state variable system derived is

$$\frac{d}{dt}\mathbf{x}(t) = \mathbf{A} \cdot \mathbf{x}(t) + \mathbf{b} \cdot m_M(t) + \mathbf{b}_d \cdot m_T(t)$$

$$\mathbf{y}(t) = \mathbf{C} \cdot \mathbf{x}(t)$$

where the state vector for this model is  $\mathbf{x}(t) = (\omega_T(t), \omega_M(t), m_{T-M'}(t))^T \in \mathbb{R}^{3 \times 1}$ , with:  $\mathbf{A} \in \mathbb{R}^{3 \times 3}$ ,  $\mathbf{b} \in \mathbb{R}^{3 \times 1}$ ,  $\mathbf{b}_d \in \mathbb{R}^{3 \times 1}$  and  $\mathbf{C} \in \mathbb{R}^{3 \times 3}$ .

and the system can be represented as

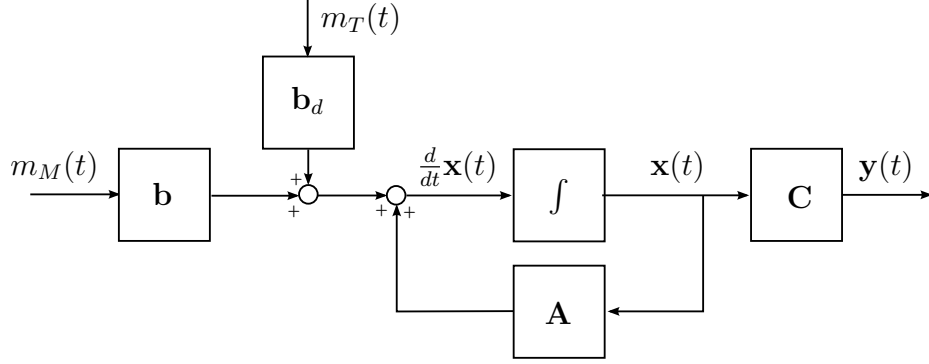


Figure 4.4: *Two mass system block diagram*

Each matrix can be referenced as

$$\mathbf{A} := \begin{bmatrix} a_{11} & a_{12} & a_{13} \\ a_{21} & a_{22} & a_{23} \\ a_{31} & a_{32} & a_{33} \end{bmatrix}, \quad \mathbf{b} := \begin{bmatrix} b_{11} \\ b_{21} \\ b_{31} \end{bmatrix}, \quad \mathbf{b}_d := \begin{bmatrix} b_{d11} \\ b_{d21} \\ b_{d31} \end{bmatrix} \quad (4.31)$$

$$\mathbf{C} := \begin{bmatrix} c_{11} & c_{12} & c_{13} \\ c_{21} & c_{22} & c_{23} \\ c_{31} & c_{32} & c_{33} \end{bmatrix} \quad (4.32)$$

The matrix form of the state variables can be expressed as:

$$\frac{d}{dt} \mathbf{x}(t) = \begin{bmatrix} -\frac{d_T}{\Theta_T} & 0 & -\frac{1}{\Theta_T} \\ 0 & -\frac{d_M}{\Theta_M} & \frac{1}{g_r \cdot \Theta_M} \\ c_s - \frac{d_s \cdot d_T}{\Theta_T} & -\frac{c_s \Theta_M + d_M \cdot d_s}{g_r \cdot \Theta_M} & -\frac{d_s (\Theta_M \cdot g_r^2 + \Theta_T)}{g_r^2 \Theta_T \Theta_M} \end{bmatrix} \mathbf{x}(t) + \begin{bmatrix} 0 \\ \frac{1}{\Theta_M} \\ \frac{d_s}{g_r \cdot \Theta_M} \end{bmatrix} m_M(t) + \begin{bmatrix} \frac{1}{\Theta_T} \\ 0 \\ \frac{d_s}{\Theta_T} \end{bmatrix} m_T(t) \quad (4.33)$$

$$\mathbf{y}(t) = \begin{bmatrix} 1 & 0 & 0 \\ 0 & 1 & 0 \\ 0 & 0 & 1 \end{bmatrix} \mathbf{x}(t) \quad (4.34)$$

This case of the two mass system model is considered to be the most commonly used way to describe a two-mass system [3].

**Case II** Using the previous assumptions and, as well as before, the Newton's second law for rotating systems, the mathematical model for the turbine shown in

Fig. 4.3 (b) from reflecting the variables from the machine's side to the turbine's side in Fig. 4.3 (a), is described by

$$\Theta_T \cdot \frac{d}{dt} \omega_T(t) + d_T \omega_T(t) = m_T(t) - m_{T-M'}(t), \quad \omega_T(0) = \omega_{T,0} \quad (4.35)$$

For machine's mathematical model the same procedure is used to obtain it

$$\Theta_{M'} \cdot \frac{d}{dt} \omega_{M'}(t) + d_{M'} \omega_{M'}(t) = m_{M'}(t) - m_{M'-T}(t), \quad \omega_{M'}(0) = \omega_{M',0} \quad (4.36)$$

In this case,  $m_{T-M'}$  [N m] and  $m_{M'-T}$  [N m] are the torques produced by the turbine on the related machine and the torque produced by the related machine on the turbine respectively, and are described as

$$m_{T-M'}(t) = d_s \cdot (\omega_T(t) - \omega_{M'}(t)) + c_s \cdot (\phi_T(t) - \phi_{M'}(t)) \quad (4.37)$$

$$\begin{aligned} m_{M'-T}(t) &= d_s \cdot (\omega_{M'}(t) - \omega_T(t)) + c_s \cdot (\phi_{M'}(t) - \phi_T(t)) \\ &= -d_s \cdot (\omega_T(t) - \omega_{M'}(t)) - c_s \cdot (\phi_T(t) - \phi_{M'}(t)) \\ &\stackrel{(4.37)}{=} -m_{T-M'}(t) \end{aligned} \quad (4.38)$$

From this equations, a new relation can be obtained using the angular displacement between the turbine's angle  $\phi_T$  [rad] and the machine's angle  $\phi_M$  [rad].

$$\Delta\phi_{T-M}(t) = \phi_T(t) - \phi_{M'}(t) \stackrel{(4.21)}{=} \phi_T(t) - \frac{\phi_M(t)}{g_r} \quad (4.39)$$

After obtaining this relations, it is possible to describe  $\frac{d}{dt} \omega_T(t)$  and  $\frac{d}{dt} \omega_{M'}(t)$  using (4.37), (4.39) and (4.38) as

$$\Theta_T \cdot \frac{d}{dt} \omega_T(t) = m_T(t) - d_s \cdot (\omega_T(t) - \omega_{M'}(t)) - c_s \cdot \Delta\phi_{T-M}(t) - d_T \omega_T(t) \quad (4.40)$$

$$\Theta_{M'} \cdot \frac{d}{dt} \omega_{M'}(t) = m_{M'}(t) + d_s \cdot (\omega_T(t) - \omega_{M'}(t)) + c_s \cdot \Delta\phi_{T-M}(t) - d_{M'} \omega_{M'}(t) \quad (4.41)$$

Because of the addition of terms and variables in the model description, it is neces-

sary to express all states in terms of  $M'$  in terms of  $M$  using (4.21)

$$\begin{aligned}\Theta_T \cdot \frac{d}{dt} \omega_T(t) &= m_T(t) - d_s \cdot \left( \omega_T(t) - \frac{\omega_M(t)}{g_r} \right) - c_s \cdot \Delta \phi_{T-M}(t) - d_T \omega_T(t) \\ \frac{d}{dt} \omega_T(t) &= \frac{1}{\Theta_T} \left( m_T(t) - d_s \cdot \left( \omega_T(t) - \frac{\omega_M(t)}{g_r} \right) - c_s \cdot \Delta \phi_{T-M}(t) - d_T \omega_T(t) \right)\end{aligned}\tag{4.42}$$

$$\begin{aligned}g_r^2 \cdot \Theta_M \cdot \frac{d}{dt} \frac{\omega_M(t)}{g_r} &= g_r \cdot m_M(t) + d_s \left( \omega_T(t) - \frac{\omega_M(t)}{g_r} \right) + c_s \cdot \Delta \phi_{T-M}(t) - g_r^2 \cdot d_M \cdot \frac{\omega_M(t)}{g_r} \\ g_r \cdot \Theta_M \cdot \frac{d}{dt} \omega_M(t) &= \left( g_r \cdot m_M(t) + d_s \left( \omega_T(t) - \frac{\omega_M(t)}{g_r} \right) + c_s \cdot \Delta \phi_{T-M}(t) - g_r \cdot d_M \cdot \omega_M(t) \right) \\ \frac{d}{dt} \omega_M(t) &= \left( \frac{g_r \cdot m_M(t)}{g_r \cdot \Theta_M} + d_s \left( \frac{\omega_T(t)}{g_r \cdot \Theta_M} - \frac{\omega_M(t)}{g_r^2 \cdot \Theta_M} \right) + \frac{c_s \cdot \Delta \phi_{T-M}(t)}{g_r \cdot \Theta_M} - \frac{g_r \cdot d_M \cdot \omega_M(t)}{g_r \cdot \Theta_M} \right) \\ \frac{d}{dt} \omega_M(t) &= \frac{1}{\Theta_M} \left( m_M(t) + d_s \left( \frac{\omega_T(t)}{g_r} - \frac{\omega_M(t)}{g_r^2} \right) + \frac{c_s \cdot \Delta \phi_{T-M}(t)}{g_r} - d_M \cdot \omega_M(t) \right)\end{aligned}\tag{4.43}$$

In this case the state variable system derived is

$$\begin{aligned}\frac{d}{dt} \mathbf{x}(t) &= \mathbf{A} \cdot \mathbf{x}(t) + \mathbf{b} \cdot m_M(t) + \mathbf{b}_d \cdot m_T(t) \\ \mathbf{y}(t) &= \mathbf{C} \cdot \mathbf{x}(t)\end{aligned}$$

The system can be represented as shown in Fig. 4.4 and The state vector for this model is  $\mathbf{x}(t) = (\omega_T(t), \omega_M(t), \Delta \phi_{T-M}(t))^T \in \mathbb{R}^{3 \times 1}$ ; with:  $\mathbf{A} \in \mathbb{R}^{3 \times 3}$ ,  $\mathbf{b} \in \mathbb{R}^{3 \times 1}$ ,  $\mathbf{b}_d \in \mathbb{R}^{3 \times 1}$  and  $\mathbf{C} \in \mathbb{R}^{3 \times 3}$ . The matrices can be referenced as shown in case I with (4.31) and (4.32).

Now, by differentiating (4.39) with respect to time, rearranging (4.42) and (4.43) in terms of  $\frac{d}{dt} \omega_T(t)$  and  $\frac{d}{dt} \omega_M(t)$  respectively, the matrix form of the state variables can be expressed as:

$$\frac{d}{dt} \mathbf{x}(t) = \begin{bmatrix} -\frac{(d_s+d_T)}{\Theta_T} & \frac{d_s}{g_r \cdot \Theta_T} & -\frac{c_s}{\Theta_T} \\ \frac{d_s}{g_r \cdot \Theta_M} & -\frac{(d_s+g_r^2 \cdot d_M)}{g_r^2 \cdot \Theta_M} & \frac{c_s}{g_r \cdot \Theta_M} \\ 1 & -\frac{1}{g_r} & 0 \end{bmatrix} \mathbf{x}(t) + \begin{bmatrix} 0 \\ \frac{1}{\Theta_M} \\ 0 \end{bmatrix} m_M(t) + \begin{bmatrix} \frac{1}{\Theta_T} \\ 0 \\ 0 \end{bmatrix} m_T(t)\tag{4.44}$$

$$\mathbf{y}(t) = \begin{bmatrix} 1 & 0 & 0 \\ 0 & 1 & 0 \\ 0 & 0 & 1 \end{bmatrix} \mathbf{x}(t)\tag{4.45}$$

From the discussion made by [7], it can be concluded that a wind turbine can be reduced to an effective two-mass model with an acceptable accuracy, and also that more than two-mass model may be more appropriate for short-time phenomena as transient stability analysis during faults. The choice of choosing the two-mass model with a flexible low-speed shaft is motivated by the fact that the low speed shaft encounters a torque  $g_r$ -times greater than the high-speed shaft torque that turns  $g_r$ -times quicker than the low-speed shaft. As the low-speed shaft encounters a higher torque, it is subject to more deviation and it is more convenient to take it into consideration. And, besides that, the use of two flexible shafts leads to a more complex model not really well adapted for controllers design. And as many authors report, general models can be largely simplified to be used in a control system [7], [25].

## 4.2 Speed control for the one-mass system

This section is based on [7] and [13]. The control applied to the model obtained in (4.20) is a speed control. The control is used aiming to obtain the maximum power from the wind.

At all times, the turbine's power is given by the turbine's torque times the turbine's rotational speed (see (4.9)).

As shown in Fig. 3.5, it must be true that at regions I and IV, the machine's power is 0. In region III, the nominal turbine's power should be achieved at any given time, being the turbine's power described by

$$p_{T,nom}(t) = m_{T,nom}(t) \cdot \omega_{T,nom}(t) > 0 \quad [\text{W}] \quad (4.46)$$

Where  $m_{T,nom}$  [N m] is the nominal turbine's torque and  $\omega_{T,nom}$  [ $\frac{\text{rad}}{\text{s}}$ ] is the nominal turbine's rotational speed.

In region II, the machine's power is less than the nominal value, and as  $c_{P,1}$  is being used, there is no pitch angle.

$$p_T(t) = m_T(t) \cdot \omega_T(t) < p_{T,nom} \quad (4.47)$$

The basic speed control for a wind turbine is given by the block diagram in Fig. 4.5

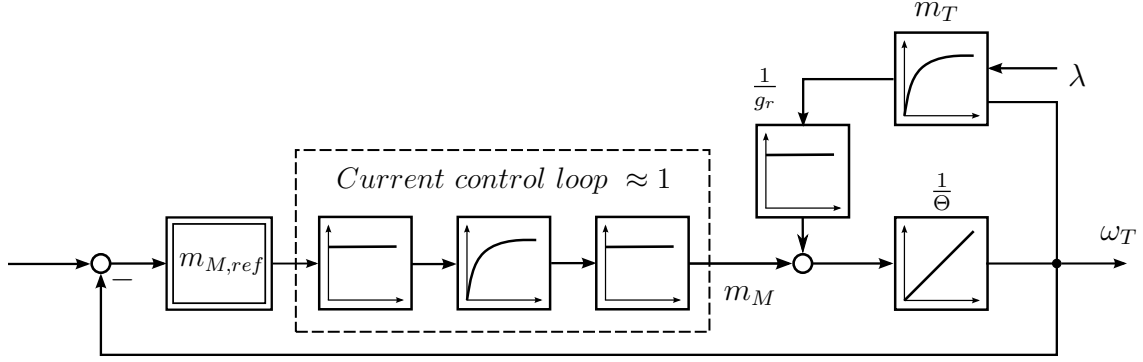


Figure 4.5: Block diagram for a basic speed control in a wind turbine with a direct drive

For this control it is necessary that some conditions are true and some assumptions to be considered such as the following:

**Assumption 8.** The turbine is working in the region II, see Fig. 3.5

$$\forall t \geq 0 : \quad v_{nom} > v_W(t) \geq v_{cut-in} > 0 \quad \text{and} \quad \omega_T(t) > \omega_{T,min} > 0 \quad (4.48)$$

**Assumption 9.** It is assumed that the speed control is fast enough to, ideally, apply

$$\forall t \geq 0 : \quad m_{M,ref}(t) = m_M(t) \quad (4.49)$$

**Assumption 10.** Variables used with a star exponent (\*) are taking into consideration as nominal values.

**Assumption 11.** The wind turbine is supposed to be working in region II, so the turbine's power can be calculated as

$$p_T(v_W, \lambda) = p_T(v_W, \lambda) = c_P(\lambda) \cdot \frac{1}{2} \cdot \rho \cdot \pi \cdot r_T^2 \cdot v_W(t)^3 \quad (4.50)$$

$$p_T(v_W, \lambda) \leq c_P(\lambda^*) \cdot p_T(t) \quad (4.51)$$

From this new equations and relations, (4.20) can be transformed into:

$$\frac{d}{dt} \omega_T(t) = \frac{1}{\Theta} \cdot \left( \frac{m_T(v_W, \omega_T)}{g_r} + m_M(t) \right) = \frac{1}{\Theta} \cdot \left( \frac{m_T(v_W, \omega_T)}{g_r} + m_{M,ref}(t) \right) \quad (4.52)$$

The speed control implementation has two necessary terms. There is a constant named  $K_p^*$  and the square value of the rotational speed. The combination of both gives us the variable  $m_{M,ref}(t)$  shown in Fig. 4.5 and 4.49

$$m_{M,ref} = -K_p^* \cdot \omega_T(t)^2 \quad (4.53)$$

In this control, the constant value of  $K_p^*$  is assumed as

$$K_p^* = \frac{\rho \cdot \pi \cdot r_T^5}{2 \cdot g_r} \cdot \frac{c_{P,1}(\lambda^*)}{(\lambda^*)^3} \quad (4.54)$$



## 4.3 Observer design for the two-mass system

After obtaining the model that describes the two-mass system in (4.44) and (4.45), the design of an observer for the turbine's torque  $m_T$  is necessary to work as a sensor for the variable. As the turbine's torque is not a state of the model, it is going to be treated as a disturbance since it can be assumed that through time, it should be kept as a constant.

### 4.3.1 Augmented system, observability and reachability

Using [10] as a guide, in this case a disturbance observer is designed to estimate the unknown value of the turbine torque  $m_T(t)$ . In this case, the disturbance observer is going to be used as a sensor since  $m_T(t)$  is not usually measured and it is necessary for further steps. For doing this, an augmented system of (4.44) and (4.45) is introduced with an additional (virtual) disturbance state  $x_d$  [10]. This augmented system is going to be the basis for the observer and controller design

#### 4.3.1.1 Augmented system

The disturbance can be defined as

$$d(t) = d_0 + \bar{d}(t) = m_T(t) \quad (4.55)$$

with  $d_0$  as a constant and  $\bar{d}(t)$  as the variable part of the disturbance. From this moment on, it is possible to introduce the virtual disturbance state  $\frac{d}{dt}x_d(t) = 0$  with an initial value  $x_d(0) = d_0$ . The augmented state vector corresponds to  $\mathbf{x}' = (\mathbf{x}^\top, x_d)^\top$  and the augmented system is given by

$$\frac{d}{dt}\mathbf{x}'(t) = \underbrace{\begin{bmatrix} \mathbf{A} & \mathbf{b}_d \\ \mathbf{0}_3^\top & 0 \end{bmatrix}}_{:=\mathbf{A}' \in \mathbb{R}^{4 \times 4}} \mathbf{x}'(t) + \underbrace{\begin{pmatrix} \mathbf{b} \\ 0 \end{pmatrix}}_{:=\mathbf{b}' \in \mathbb{R}^{4 \times 1}} u(t) + \underbrace{\begin{pmatrix} \mathbf{b}_d \\ 0 \end{pmatrix}}_{:=\mathbf{b}'_d \in \mathbb{R}^{4 \times 1}} \bar{d}(t) \quad (4.56)$$

$$\mathbf{y}(t) = \underbrace{\begin{pmatrix} \mathbf{C} & \mathbf{0}_3 \end{pmatrix}}_{:=\mathbf{C}' \in \mathbb{R}^{3 \times 4}} \mathbf{x}'(t) \quad (4.57)$$

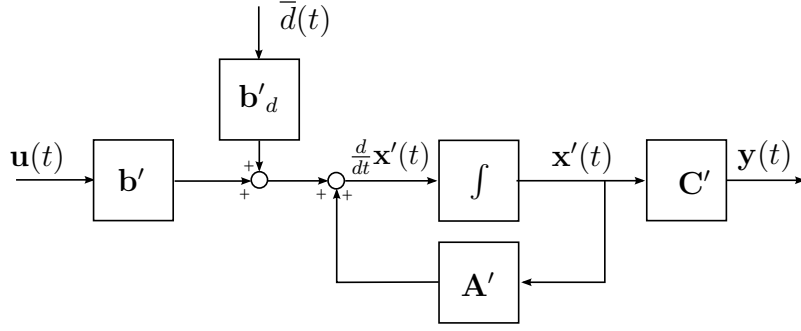
with  $\mathbf{0}_k$  as a vector of zeros with  $k$ -rows.

The system is now described as

$$\frac{d}{dt}\mathbf{x}'(t) = \mathbf{A}'\mathbf{x}'(t) + \mathbf{b}'\mathbf{u}(t) + \mathbf{b}'_d\bar{d}(t) \quad (4.58)$$

$$\mathbf{y}(t) = \mathbf{C}'\mathbf{x}'(t) \quad (4.59)$$

and represented as


 Figure 4.6: *Augmented system block diagram*

Each matrix can be assumed as

$$\mathbf{A}' := \begin{bmatrix} a'_{11} & a'_{12} & a'_{13} & a'_{14} \\ a'_{21} & a'_{22} & a'_{23} & a'_{24} \\ a'_{31} & a'_{32} & a'_{33} & a'_{34} \\ a'_{41} & a'_{42} & a'_{43} & a'_{44} \end{bmatrix}, \quad \mathbf{b}' := \begin{bmatrix} b'_{11} \\ b'_{21} \\ b'_{31} \\ b'_{41} \end{bmatrix}, \quad \mathbf{b}'_d := \begin{bmatrix} b'_{d11} \\ b'_{d21} \\ b'_{d31} \\ b'_{d41} \end{bmatrix} \quad (4.60)$$

$$\mathbf{C}' := \begin{bmatrix} c'_{11} & c'_{12} & c'_{13} & c'_{14} \\ c'_{21} & c'_{22} & c'_{23} & c'_{24} \\ c'_{31} & c'_{32} & c'_{33} & c'_{34} \end{bmatrix} \quad (4.61)$$

With the new variables, the resultant matrix are

$$\mathbf{A}' = \begin{bmatrix} -\frac{(d_s+d_T)}{\Theta_T} & \frac{d_s}{g_r \cdot \Theta_T} & -\frac{c_s}{\Theta_T} & \frac{1}{\Theta_T} \\ \frac{d_s}{g_r \cdot \Theta_M} & -\frac{(d_s+g_r^2 \cdot d_M)}{g_r^2 \cdot \Theta_M} & \frac{c_s}{g_r \cdot \Theta_M} & 0 \\ 1 & -\frac{1}{g_r} & 0 & 0 \\ 0 & 0 & 0 & 0 \end{bmatrix}, \quad \mathbf{b}' = \begin{bmatrix} 0 \\ \frac{1}{\Theta_M} \\ 0 \\ 0 \end{bmatrix}, \quad \mathbf{b}'_d = \begin{bmatrix} \frac{1}{\Theta_T} \\ 0 \\ 0 \\ 0 \end{bmatrix} \quad (4.62)$$

$$\mathbf{C}' = \begin{bmatrix} 1 & 0 & 0 & 0 \\ 0 & 1 & 0 & 0 \\ 0 & 0 & 1 & 0 \end{bmatrix} \quad (4.63)$$

#### 4.3.1.2 Observability and controllability

For the observability and controllability of the system, it is necessary to obtain matrix S and M, given as

$$\mathbf{S} := \begin{bmatrix} \mathbf{C}' \\ \mathbf{C}'\mathbf{A}' \\ \mathbf{C}'\mathbf{A}'^2 \\ \vdots \\ \mathbf{C}'\mathbf{A}'^{m-1} \end{bmatrix} \quad (4.64)$$

$$\mathbf{M} := \begin{bmatrix} \mathbf{b}' & \mathbf{A}'\mathbf{b}' & \mathbf{A}'^2\mathbf{b}' & \dots & \mathbf{A}'^{m-1}\mathbf{b}' \end{bmatrix} \quad (4.65)$$

A  $n$ -th order system, with squared matrices, is observable when the determinant of  $\mathbf{S}$  is  $\neq 0$  and controllable when the determinant of  $\mathbf{M}$  is  $\neq 0$ . If matrices are not squared, the system is observable and controllable if the rank of the matrices is  $n$  (see [29, Th. 9.5, Th. 9.11]).

In this case, the rank of each matrix is maximum 4, so the matrix can be represented as follows to analyze them.

$$\mathbf{S} = \begin{bmatrix} \mathbf{C}' \\ \mathbf{C}'\mathbf{A}' \\ \mathbf{C}'\mathbf{A}'^2 \\ \mathbf{C}'\mathbf{A}'^3 \end{bmatrix} = \begin{bmatrix} 1 & 0 & 0 & 0 \\ 0 & 1 & 0 & 0 \\ 0 & 0 & 1 & 0 \\ \frac{-(d_s+d_T)}{\Theta_T} & \frac{d_s}{g_r \cdot \Theta_T} & \frac{-c_s}{\Theta_T} & \frac{1}{\Theta_T} \\ \vdots & \vdots & \vdots & \vdots \end{bmatrix} \quad (4.66)$$

$$\mathbf{M} = \begin{bmatrix} \mathbf{b}' & \mathbf{A}'\mathbf{b}' & \mathbf{A}'^2\mathbf{b}' & \mathbf{A}'^3\mathbf{b}' \end{bmatrix} \quad (4.67)$$

Note that the rank of  $\mathbf{S}$  is, indeed, 4 as long as  $\frac{1}{\Theta_T} \neq 0$ , which means the system is always observable since 4 independent equations are obtained. In the controllability matrix, since it is not yet necessary, it was computed through the symbolic toolbox of MATLAB to obtain its rank. Due to the nature of the  $\mathbf{b}'$  matrix, the maximum rank of  $\mathbf{M}$  in this case is 3, which means that at least one of the states not controllable. And through the computation it was confirmed that the rank of the matrix is 3.

### 4.3.2 Disturbance observer design

**Convention 1.** The usage of  $(\hat{\phantom{x}})$  over any of the variables introduced before, corresponds to a equivalent variable in the disturbance observer design.

Based on (4.56) and (4.57), it is possible to obtain a generic Luenberger observer to estimate the unknown disturbance  $x_d$  through the state  $\hat{x}_d$ . The observer that is going to be designed corresponds to:

$$\frac{d}{dt}\hat{\mathbf{x}}'(t) = \mathbf{A}'\hat{\mathbf{x}}'(t) + \mathbf{b}'\mathbf{u}(t) + \hat{\mathbf{u}}_{obs}(t) \quad (4.68)$$

$$\hat{\mathbf{y}}(t) = \mathbf{C}'\hat{\mathbf{x}}'(t) \quad (4.69)$$

The last term, known as  $\hat{\mathbf{u}}_{obs}$ , is the observer's feedback and works as a correction value that contains the difference between the measured output and the estimated output.

$$\hat{\mathbf{u}}_{obs} = \mathbf{L}(\mathbf{y}(t) - \mathbf{C}'\hat{\mathbf{x}}'(t)) = \mathbf{L}(\mathbf{y}(t) - \hat{\mathbf{y}}(t)) = \mathbf{L}\mathbf{C}'(\mathbf{x}'(t) - \hat{\mathbf{x}}'(t)) \quad (4.70)$$

The correction term helps reducing the effects of the difference between the dynamic

model and the real system. Where  $\mathbf{L} \in \mathbb{R}^{4 \times 3}$  is a matrix that works as a weight matrix.

The error dynamics in the state estimation can be obtained, defining the observer's error  $\varepsilon_{obs}$  as

$$\varepsilon_{obs}(t) := \mathbf{x}'(t) - \hat{\mathbf{x}}'(t) \quad (4.71)$$

By differencing (4.71) in time,

$$\frac{d}{dt}\varepsilon_{obs}(t) = \underbrace{\frac{d}{dt}\mathbf{x}'(t)}_{(4.58)} - \underbrace{\frac{d}{dt}\hat{\mathbf{x}}'(t)}_{(4.68)}$$

$$\frac{d}{dt}\varepsilon_{obs}(t) = \mathbf{A}'(\mathbf{x}'(t) - \hat{\mathbf{x}}'(t)) + \mathbf{b}'_d \bar{d}(t) - \mathbf{L}\mathbf{C}'(\mathbf{x}'(t) - \hat{\mathbf{x}}'(t))$$

the error dynamics result in

$$\frac{d}{dt}\varepsilon_{obs}(t) = (\underbrace{\mathbf{A}' - \mathbf{L}\mathbf{C}'}_{:=\mathbf{A}_{obs} \in \mathbb{R}^{4 \times 4}})\varepsilon_{obs}(t) + \mathbf{b}'_d \bar{d}(t) \quad (4.72)$$

In this design,  $\mathbf{A}_{obs}$  is obtained as

$$\begin{aligned} \mathbf{A}_{obs} &= \begin{bmatrix} a_{obs11} & a_{obs12} & a_{obs13} & a_{obs14} \\ a_{obs21} & a_{obs22} & a_{obs23} & a_{obs24} \\ a_{obs31} & a_{obs32} & a_{obs33} & a_{obs34} \\ a_{obs41} & a_{obs42} & a_{obs43} & a_{obs44} \end{bmatrix} \\ &= \begin{bmatrix} a'_{11} & a'_{12} & a'_{13} & a'_{14} \\ a'_{21} & a'_{22} & a'_{23} & a'_{24} \\ a'_{31} & a'_{32} & a'_{33} & a'_{34} \\ a'_{41} & a'_{42} & a'_{43} & a'_{44} \end{bmatrix} - \begin{bmatrix} l_{11} & l_{12} & l_{13} \\ l_{21} & l_{22} & l_{23} \\ l_{31} & l_{32} & l_{33} \\ l_{41} & l_{42} & l_{43} \end{bmatrix} \begin{bmatrix} c'_{11} & c'_{12} & c'_{13} & c'_{14} \\ c'_{21} & c'_{22} & c'_{23} & c'_{24} \\ c'_{31} & c'_{32} & c'_{33} & c'_{34} \end{bmatrix} \\ &= \begin{bmatrix} -\frac{(d_s+d_T)}{\Theta_T} & \frac{d_s}{g_r \cdot \Theta_T} & -\frac{c_s}{\Theta_T} & \frac{1}{\Theta_T} \\ \frac{d_s}{g_r \cdot \Theta_M} & -\frac{(d_s+g_r^2 \cdot d_M)}{g_r^2 \cdot \Theta_M} & \frac{c_s}{g_r \cdot \Theta_M} & 0 \\ 1 & -\frac{1}{g_r} & 0 & 0 \\ 0 & 0 & 0 & 0 \end{bmatrix} - \begin{bmatrix} l_{11} & l_{12} & l_{13} \\ l_{21} & l_{22} & l_{23} \\ l_{31} & l_{32} & l_{33} \\ l_{41} & l_{42} & l_{43} \end{bmatrix} \begin{bmatrix} 1 & 0 & 0 & 0 \\ 0 & 1 & 0 & 0 \\ 0 & 0 & 1 & 0 \end{bmatrix} \\ &= \begin{bmatrix} -\frac{(d_s+d_T)}{\Theta_T} & \frac{d_s}{g_r \cdot \Theta_T} & -\frac{c_s}{\Theta_T} & \frac{1}{\Theta_T} \\ \frac{d_s}{g_r \cdot \Theta_M} & -\frac{(d_s+g_r^2 \cdot d_M)}{g_r^2 \cdot \Theta_M} & \frac{c_s}{g_r \cdot \Theta_M} & 0 \\ 1 & -\frac{1}{g_r} & 0 & 0 \\ 0 & 0 & 0 & 0 \end{bmatrix} - \begin{bmatrix} l_{11} & l_{12} & l_{13} & 0 \\ l_{21} & l_{22} & l_{23} & 0 \\ l_{31} & l_{32} & l_{33} & 0 \\ l_{41} & l_{42} & l_{43} & 0 \end{bmatrix} \end{aligned} \quad (4.73)$$

Finally resulting in

$$\mathbf{A}_{obs} = \begin{bmatrix} -\frac{(d_s+d_T)}{\Theta_T} - l_{11} & \frac{d_s}{g_r \cdot \Theta_T} - l_{12} & -\frac{c_s}{\Theta_T} - l_{13} & \frac{1}{\Theta_T} \\ \frac{d_s}{g_r \cdot \Theta_M} - l_{21} & -\frac{(d_s+g_r^2 \cdot d_M)}{g_r^2 \cdot \Theta_M} - l_{22} & \frac{c_s}{g_r \cdot \Theta_M} - l_{23} & 0 \\ 1 - l_{31} & -\frac{1}{g_r} - l_{32} & -l_{33} & 0 \\ -l_{41} & -l_{42} & -l_{43} & 0 \end{bmatrix} \quad (4.74)$$

The observer can be represented as

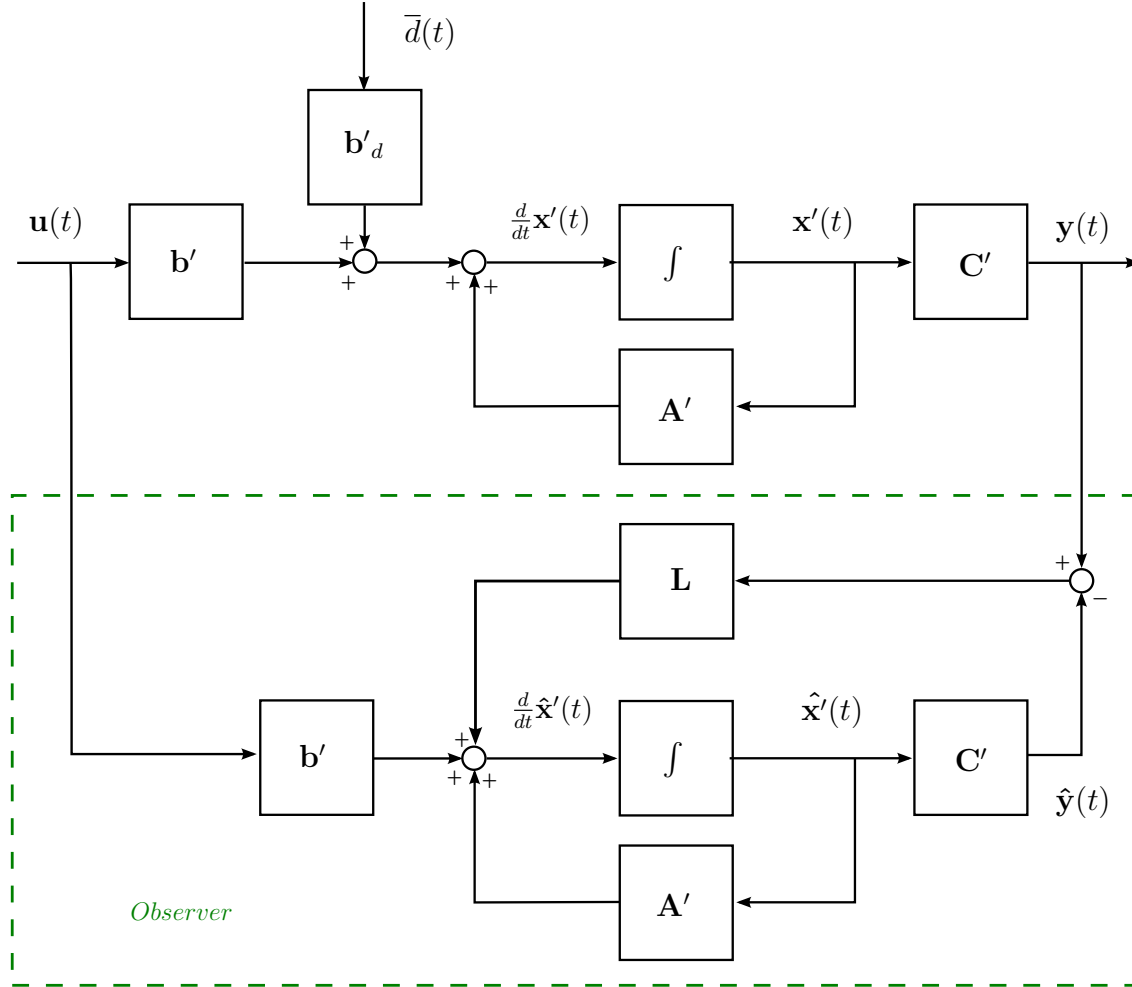


Figure 4.7: Observer with augmented system block diagram

#### 4.3.2.1 Observer design by pole placement

In this case, the observer dynamics shown in (4.71) are asymptotically stable if all of the values in  $\mathbf{A}_{obs}$  are in the imaginary half plane, that means, that their real part is negative.

The observer poles are given by

$$\det(z\mathbf{I}_4 - \mathbf{A}_{obs}) = 0 \quad (4.75)$$

with  $\mathbf{I}_4$  as a 4x4 identity matrix.

$$\begin{aligned} z\mathbf{I}_4 - \mathbf{A}_{obs} &= z \begin{bmatrix} 1 & 0 & 0 & 0 \\ 0 & 1 & 0 & 0 \\ 0 & 0 & 1 & 0 \\ 0 & 0 & 0 & 1 \end{bmatrix} - \begin{bmatrix} a_{obs11} & a_{obs12} & a_{obs13} & a_{obs14} \\ a_{obs21} & a_{obs22} & a_{obs23} & a_{obs24} \\ a_{obs31} & a_{obs32} & a_{obs33} & a_{obs34} \\ a_{obs41} & a_{obs42} & a_{obs43} & a_{obs44} \end{bmatrix} \\ &= \begin{bmatrix} z & 0 & 0 & 0 \\ 0 & z & 0 & 0 \\ 0 & 0 & z & 0 \\ 0 & 0 & 0 & z \end{bmatrix} - \begin{bmatrix} -\frac{(d_s+d_T)}{\Theta_T} - l_{11} & \frac{d_s}{g_r \cdot \Theta_T} - l_{12} & -\frac{c_s}{\Theta_T} - l_{13} & \frac{1}{\Theta_T} \\ \frac{d_s}{g_r \cdot \Theta_M} - l_{21} & -\frac{(d_s+g_r^2 \cdot d_M)}{g_r^2 \cdot \Theta_M} - l_{22} & \frac{c_s}{g_r \cdot \Theta_M} - l_{23} & 0 \\ 1 - l_{31} & -\frac{1}{g_r} - l_{32} & -l_{33} & 0 \\ -l_{41} & -l_{42} & -l_{43} & 0 \end{bmatrix} \\ &= \begin{bmatrix} z + \frac{(d_s+d_T)}{\Theta_T} + l_{11} & -\frac{d_s}{g_r \cdot \Theta_T} + l_{12} & \frac{c_s}{\Theta_T} + l_{13} & -\frac{1}{\Theta_T} \\ -\frac{d_s}{g_r \cdot \Theta_M} + l_{21} & z + \frac{(d_s+g_r^2 \cdot d_M)}{g_r^2 \cdot \Theta_M} + l_{22} & -\frac{c_s}{g_r \cdot \Theta_M} + l_{23} & 0 \\ -1 + l_{31} & \frac{1}{g_r} + l_{32} & z + l_{33} & 0 \\ l_{41} & l_{42} & l_{43} & z \end{bmatrix} \end{aligned} \quad (4.76)$$

And the values needed are fixed by the polynomial

$$P_{desired}(z) = (z - p_1)(z - p_2)(z - p_3)(z - p_4) \quad (4.77)$$

It is possible to simplify (4.76) choosing the value of some of the observer gains based on the relation between states, such as

$$\begin{aligned} l_{12} = a'_{12} &= \frac{d_s}{g_r \cdot \Theta_T}, & l_{13} = a'_{13} &= -\frac{c_s}{\Theta_T}, & l_{21} = a'_{21} &= -\frac{d_s}{g_r^2 \cdot \Theta_M}, & l_{23} = a'_{23} &= \frac{c_s}{g_r \cdot \Theta_M}, \\ l_{31} = a'_{31} &= 1, & l_{32} = a'_{32} &= -\frac{1}{g_r}, & l_{42} &= 0 & \text{and} & l_{43} = 0 \end{aligned}$$

Applying this relations to the current  $z\mathbf{I}_4 - \mathbf{A}_{obs}$  matrix, the resulting matrix is

$$z\mathbf{I}_4 - \mathbf{A}_{obs} = \begin{bmatrix} z + \frac{(d_s+d_T)}{\Theta_T} + l_{11} & 0 & 0 & -\frac{1}{\Theta_T} \\ 0 & z + \frac{(d_s+g_r^2 \cdot d_M)}{g_r^2 \cdot \Theta_M} + l_{22} & 0 & 0 \\ 0 & 0 & z + l_{33} & 0 \\ l_{41} & 0 & 0 & z \end{bmatrix} \quad (4.78)$$

Using the symbolic toolbox of MatLab, the coefficients from  $\det(z\mathbf{I}_4 - \mathbf{A}_{obs})$  should be now compared with the ones of the desired polynomial  $P_{desired}(z)$  in (4.77), obtaining

that

$$l_{11} = a'_{11} - p_2 - p_3, \quad l_{22} = a'_{22} - p_1, \quad l_{33} = -p_4, \quad \text{and} \quad l_{41} = \frac{p_2 \cdot p_3}{a'_{14}} \quad (4.79)$$

With this relations, it is possible to get the final  $\mathbf{L}$  matrix with all of the observer's gains

$$\mathbf{L} = \begin{bmatrix} l_{11} & a'_{12} & a'_{13} \\ a'_{21} & l_{22} & a'_{23} \\ a_{31} & a'_{32} & l_{33} \\ l_{41} & 0 & 0 \end{bmatrix} = \begin{bmatrix} -\frac{(d_s+d_T)}{\Theta_T} - p_2 - p_3 & \frac{d_s}{g_r \Theta_T} & -\frac{c_s}{\Theta_T} \\ \frac{d_s}{g_r \Theta_M} & -\frac{(d_s+g_r^2 \cdot d_M)}{g_r^2 \Theta_M} - p_1 & \frac{c_s}{g_r \Theta_M} \\ 1 & -\frac{1}{g_r} & -p_4 \\ \Theta_T \cdot p_2 \cdot p_3 & 0 & 0 \end{bmatrix} \quad (4.80)$$

After obtaining the final  $\mathbf{L}$  matrix for the observer,  $\mathbf{A}_{obs}$  can be described as

$$\mathbf{A}_{obs} = \begin{bmatrix} p_2 + p_3 & 0 & 0 & -\frac{1}{\Theta_T} \\ 0 & p_1 & 0 & 0 \\ 0 & 0 & p_4 & 0 \\ -\Theta_T \cdot p_2 \cdot p_3 & 0 & 0 & 0 \end{bmatrix} \quad (4.81)$$

The values for  $p_i$  with  $i = 1, 2, 3, 4$  are found through tests to see if the observer is working correctly.

Due to the amount of cancellations in the design of this observer, a disturbance observer design by LQR with stability margin is also stated, for further comparison between the results.

#### 4.3.2.2 Disturbance observer design by LQR with stability margin

In this design, based on [11, Sec IV], as well as in the one done by pole placement previously, it is necessary that the  $\mathbf{L}$  matrix values are chosen for the values of  $(\mathbf{A}' - \mathbf{L}\mathbf{C}')$  to be on the left side of the complex half plane.

It is noted for this design that  $\det(\mathbf{A}' - \mathbf{L}\mathbf{C}') = \det(\mathbf{A}'^\top - \mathbf{C}'^\top \mathbf{L}^\top)$ , with this, and considering the dual system [27, Sec. 7.1.2] with a dual state  $\hat{x}_q$  and dual input  $\hat{u}_q$ , the design of a Linear Quadratic Regulator (LQR) [27, Sec. 10.4.5] with respect to the cost function can be started

$$J_o = \int_0^{\infty} e^{2\alpha_o t} (\hat{x}_q(t)^\top \mathbf{Q}_o \hat{x}_q(t) + \hat{u}_q(t)^\top \mathbf{R}_o \hat{u}_q(t)) dt \quad (4.82)$$

A stability margin  $\alpha_o \geq 0$  is stated, as well as the weighting matrices  $\mathbf{Q}_o$  and  $\mathbf{R}_o$

$$0 \leq \mathbf{Q}_o = \mathbf{Q}_o^\top \in \mathbb{R}^{4 \times 4} \quad \text{and} \quad 0 \leq \mathbf{R}_o = \mathbf{R}_o^\top \in \mathbb{R}^{3 \times 3} \quad (4.83)$$

A dual system with dual state and dual input can be explained using the error dynamics in the observer design 4.72.

The optimal feedback gain matrix  $\mathbf{L}$  is obtained using [27, Sec. 10.4.5] and the equation described as

$$\mathbf{L} = (\mathbf{R}_o^{-1} \mathbf{C}' \mathbf{P}_o^{-1}) \quad (4.84)$$

Where a third weighting matrix is introduced and defined as  $0 \leq \mathbf{P}_o = \mathbf{P}_o^\top \in \mathbb{R}^4$ , additionally it solves the Riccati equation as

$$(\mathbf{A}' + \alpha_o \mathbf{I}_4) \mathbf{P}_o + \mathbf{P}_o (\mathbf{A}' + \alpha_o \mathbf{I}_4)^\top - \mathbf{P}_o \mathbf{C}'^\top \mathbf{R}_o^{-1} \mathbf{C}' \mathbf{P}_o + \mathbf{Q}_o = \mathbf{O}_{4 \times 4} \quad (4.85)$$

Where  $\mathbf{O}_{4 \times 4}$  is a  $4 \times 4$  zero matrix and  $\mathbf{I}_4$  is a  $4 \times 4$  identity matrix.

It is important to know what each matrix means and how it affects the overall performance of the observer as well as what is the role of the stability margin. The matrix  $\mathbf{R}_o$  is related to the characteristics of noise measurements,  $\mathbf{Q}_o$  is associated with the confidence in the system model and  $\mathbf{P}_o$  represents the mean-squared error or covariance of the initial conditions. The stability margin itself corresponds to a value, decided by the designer, which sets up a place in the negative imaginary half plane from which the poles of the system are placed to assure the stability of the system. [2].

**Observability** As analyzed before, the  $\mathbf{S}$  matrix shown in (4.64) is used by substituting  $\mathbf{A}'$  with  $(\mathbf{A}' + \alpha_o \cdot \mathbf{I}_4)$ . The maximum rank of the  $\mathbf{S}$  matrix is still 4 as before, and the rank obtained with the mentioned substitution is 4. With this, we can assure all of the states in the system are observable.

## 4.4 Parameter estimation

After obtaining a stable and well functioning observer for the turbine's torque  $m_T$  as shown in Chapter 4.2, the proceeding part will be to estimate the value of unknown parameters to establish a fault detection pattern. There are four main mechanical parameters that can be estimated: the low-speed shaft's damping  $d_s$ , the low-speed shaft's stiffness  $c_s$ , the turbine's damping  $d_T$  and the machine's damping  $d_M$ , as shown in Fig. 4.3. Initially it is desired to estimate the four of them and an Extended Kalman Filter (EKF) is proposed for the parameter estimation.

It is important to note that it is assumed that there is a very precise wind measurement and that the  $c_{P,1}$  curve fits the reality perfectly so that the turbine's torque that is used is the precise one. This is noted because in the past chapter, the whole idea is to obtain a precise turbine's torque observer, variable that is needed for the parameter estimation.



### 4.4.1 Overall nonlinear model

To implement the EKF it is necessary to obtain a nonlinear state space model that will follow the form

$$\frac{d}{dt}\mathbf{x} = \mathbf{g}(\mathbf{x}, \mathbf{u}), \quad \mathbf{x}_0 \in \mathbb{R}^7 \quad \text{and} \quad \mathbf{y} = \mathbf{h}(\mathbf{x}) \quad (4.86)$$

The new state vector  $\mathbf{x}$  will include the present states and new ones, or the ones that are going to be estimated. The output or measurement vector is known as  $\mathbf{y}$  and the input vector as  $\mathbf{u}$ . The overall nonlinear model works as an augmented system to add the parameters as states.

$$\mathbf{x} = (\omega_T(t), \omega_M(t), \Delta\phi_{T-M}(t), d_s(t), c_s(t), d_T(t), d_M(t))^\top \in \mathbb{R}^7 \quad (4.87)$$

$$\mathbf{y} = (\omega_T(t), \omega_M(t), \Delta\phi_{T-M}(t))^\top \in \mathbb{R}^3 \quad (4.88)$$

$$\mathbf{u} = (m_M(t), m_T(t))^\top \in \mathbb{R}^2 \quad (4.89)$$

The nonlinear model can be transformed or adapted the three basic state equations (see (4.39), (4.42) and (4.43)). In these three state equations, the parameters are adapted from constants to time varying function. For example, the low speed shaft's damping  $d_s$  changed from a constant to  $d_s(t)$  which means it is now changing through time, as shown in (4.90).

$$\mathbf{g}(\mathbf{x}, \mathbf{u}) = \begin{bmatrix} \frac{1}{\Theta_T} \left( m_T(t) - d_s(t) \left( \omega_T(t) - \frac{\omega_M(t)}{g_r} \right) - c_s(t) \Delta\phi_{T-M}(t) - d_T(t) \omega_T(t) \right) \\ \frac{1}{\Theta_M} \left( m_M(t) + d_s(t) \left( \frac{\omega_T(t)}{g_r} - \frac{\omega_M(t)}{g_r^2} \right) + \frac{c_s(t) \Delta\phi_{T-M}(t)}{g_r} - d_M(t) \omega_M(t) \right) \\ \omega_T - \frac{\omega_M}{g_r} \\ 0 \\ 0 \\ 0 \\ 0 \end{bmatrix} \quad (4.90)$$

$$\mathbf{h}(\mathbf{x}) = \begin{bmatrix} 1 & 0 & 0 & 0 & 0 & 0 & 0 \\ 0 & 1 & 0 & 0 & 0 & 0 & 0 \\ 0 & 0 & 1 & 0 & 0 & 0 & 0 \end{bmatrix} \quad (4.91)$$

### 4.4.2 Discretization

To apply the EKF method, it is necessary to have a discrete system. The system, defined in (4.39), (4.42) and (4.43) is now discretized using the Euler method [21,

p.9-11] with a sample time  $T_S$  [s] sufficiently small as  $0 < T_S \ll 1$ .

The Euler method itself describes a function  $\vartheta(t)$  as

$$\vartheta(t) \approx \vartheta(kT_S) := \vartheta[k], k \in \mathbb{N} \quad (4.92)$$

From the method it is stated that the derived function can be defined as

$$\frac{d}{dt}\vartheta(t) \approx \frac{\vartheta[k+1] - \vartheta[k]}{T_S} \quad (4.93)$$

The three basic state equations are now defined as:

$$\omega_T[k+1] = \left[1 - \frac{T_S d_s[k]}{\Theta_T} - \frac{T_S d_T[k]}{\Theta_T}\right] \omega_T[k] + \frac{T_S d_s[k] \omega_M[k]}{g_r \Theta_T} - \frac{T_S c_s[k] \Delta \phi_{T-M}[k]}{\Theta_T} + \frac{T_S m_T[k]}{\Theta_T} \quad (4.94)$$

$$\omega_M[k+1] = \frac{T_S d_s[k] \omega_T[k]}{g_r \Theta_M} + \left[1 - \frac{T_S d_s[k]}{g_r^2 \Theta_M} - T_S d_M[k]\right] \omega_M[k] + \frac{T_S c_s[k] \Delta \phi_{T-M}[k]}{g_r \Theta_M} + \frac{T_S m_M[k]}{\Theta_M} \quad (4.95)$$

$$\Delta \phi_{T-M}[k+1] = T_S \omega_T[k] - \frac{T_S \omega_M[k]}{g_r} + \Delta \phi_{T-M}[k] \quad (4.96)$$

And the equations that describe the parameters, which are constants so their derivatives are zero as shown in (4.90), are stated as

$$d_s[k+1] = d_s[k] \quad (4.97)$$

$$c_s[k+1] = c_s[k] \quad (4.98)$$

$$d_T[k+1] = d_T[k] \quad (4.99)$$

$$d_M[k+1] = d_M[k] \quad (4.100)$$

After the Euler method was applied to the state variables and solved for  $\mathbf{x}[k+1]$  the resultant system can be defined as

$$\mathbf{x}[k+1] = \mathbf{A}_k \cdot \mathbf{x}[k] + \mathbf{B}_k \cdot \mathbf{u}[k] \quad (4.101)$$

$$\mathbf{y}[k] = \mathbf{C}_k \cdot \mathbf{x}[k] \quad (4.102)$$

With the matrices  $\mathbf{A}_k \in \mathbb{R}^{7 \times 7}$ ,  $\mathbf{B}_k \in \mathbb{R}^{7 \times 2}$  and  $\mathbf{C}_k \in \mathbb{R}^{3 \times 7}$  defined as

$$\mathbf{A}_k := T_S \begin{bmatrix} \frac{1}{T_S} - \frac{d_s[k] + d_T[k]}{\Theta_T} & \frac{d_s[k]}{g_r \Theta_T} & -\frac{c_s[k]}{\Theta_T} & -\frac{g_r \omega_T[k] + \omega_M[k]}{g_r \Theta_T} & -\frac{\Delta \phi_{T-M}[k]}{\Theta_T} & -\frac{\omega_T[k]}{\Theta_T} & 0 \\ \frac{d_s[k]}{g_r \Theta_M} & \frac{1}{T_S} - \frac{d_s[k] + g_r^2 d_M[k]}{g_r^2 \Theta_M} & \frac{c_s[k]}{g_r \Theta_M} & \frac{g_r \omega_T[k] - \omega_M[k]}{g_r^2 \Theta_M} & \frac{\Delta \phi_{T-M}[k]}{g_r \Theta_M} & 0 & -\frac{\omega_M[k]}{g_r^2 \Theta_M} \\ 1 & -\frac{1}{g_r} & \frac{1}{T_S} & 0 & 0 & 0 & 0 \\ 0 & 0 & 0 & \frac{1}{T_S} & 0 & 0 & 0 \\ 0 & 0 & 0 & 0 & \frac{1}{T_S} & 0 & 0 \\ 0 & 0 & 0 & 0 & 0 & \frac{1}{T_S} & 0 \\ 0 & 0 & 0 & 0 & 0 & 0 & \frac{1}{T_S} \end{bmatrix} \quad (4.103)$$

$$\mathbf{B}_k := T_S \begin{bmatrix} \frac{1}{\Theta_T} & 0 \\ 0 & \frac{1}{\Theta_M} \\ 0 & 0 \\ 0 & 0 \\ 0 & 0 \\ 0 & 0 \\ 0 & 0 \end{bmatrix} \quad (4.104)$$

$$\mathbf{C}_k := \begin{bmatrix} 1 & 0 & 0 & 0 & 0 & 0 & 0 \\ 0 & 1 & 0 & 0 & 0 & 0 & 0 \\ 0 & 0 & 1 & 0 & 0 & 0 & 0 \end{bmatrix} \quad (4.105)$$

For further reference about the discretization, see [29, p.385].

### 4.4.3 Extended Kalman Filter

Based on [2]. Initially, the EKF is an extension of the Kalman filter but it is applied to nonlinear systems. The EKF is based on a discrete nonlinear system model. For the discretization of the system, the Euler method with a sampling time  $T_s[s]$  is used in the continuous model obtained in (4.44) and (4.45).

The nonlinear discrete model of the wind turbine can be written as

$$\mathbf{x}[k+1] = \mathbf{x}[k] + T_S \mathbf{g}(\mathbf{x}[k], \mathbf{u}[k]) + \mathbf{w}[k] \quad (4.106)$$

$$\mathbf{y}[k] = \mathbf{h}(\mathbf{x}[k]) + \mathbf{v}[k] \quad (4.107)$$

where  $\mathbf{w}[k] \in \mathbb{R}^{7 \times 7}$  and  $\mathbf{v}[k] \in \mathbb{R}^{3 \times 7}$  are included in the model system and correspond to uncertainties and measurement noise, respectively. For simplicity [2], it is assumed that the covariance matrices of the system are constant, which means that for all  $k \in \mathbb{N}$

$$\mathbf{Q} := E\{\mathbf{w}[k]\mathbf{w}[k]^\top\} \geq 0 \quad \text{and} \quad \mathbf{R} := E\{\mathbf{v}[k]\mathbf{v}[k]^\top\} \geq 0 \quad (4.108)$$

The EKF algorithm is shown next, and it achieves an optimal state estimation by

minimizing the covariance of the estimation error for each time instant or the known cost function, as shown in (4.82), with the correspondant relations between variables.

#### 4.4.3.1 Extended Kalman Filter algorithm

**Step 1:** Initialization for  $k = 0$

$$\hat{\mathbf{x}}[0] = E\{\mathbf{x}_0\},$$

$$\mathbf{P}_0 := \mathbf{P}[0] = E\{(\mathbf{x}_0 - \hat{\mathbf{x}}_0)(\mathbf{x}_0 - \hat{\mathbf{x}}_0)^\top\}$$

$$\mathbf{K}_0 := \mathbf{K}[0] = \mathbf{P}[0]\mathbf{C}[0]^\top (\mathbf{C}[0]\mathbf{P}[0]\mathbf{C}[0]^\top + \mathbf{R})^{-1}$$

with  $\mathbf{C}[k] := \left. \frac{\partial \mathbf{h}(\mathbf{x})}{\partial \mathbf{x}} \right|_{\hat{\mathbf{x}}^-[k]}$  and  $\hat{\mathbf{x}}^-[k]$  being the previous measurement.

**Step 2:** Time update

(a) State prediction

$$\hat{\mathbf{x}}^-[k] = \mathbf{g}[\hat{\mathbf{x}}[k-1], \mathbf{u}[k-1]]$$

(b) Prediction of the error covariance matrix

$$\mathbf{P}^-[k] = \mathbf{A}[k]\mathbf{P}[k-1]\mathbf{A}[k]^\top + \mathbf{Q}$$

with  $\mathbf{A}[k] := \left. \frac{\partial \mathbf{f}(\mathbf{x}, \mathbf{u})}{\partial \mathbf{x}} \right|_{\hat{\mathbf{x}}^-[k]}$

**Step 3:** Observability check

$$n[k] := \text{rank}(\mathbf{S}_o[k]) \text{ with } \mathbf{S}_o \text{ as in (4.109)}$$

**Step 4:** The Kalman gain is computed

$$\mathbf{K}[k] = \mathbf{P}^-[k]\mathbf{C}[k]^\top (\mathbf{C}[k]\mathbf{P}^-[k]\mathbf{C}[k]^\top + \mathbf{R})^{-1}$$

**Step 5:** Known as the correction step, in here the measurement is updated for  $k \geq 1$

(a) The estimation is updated

$$\hat{\mathbf{x}}[k] = \hat{\mathbf{x}}^-[k] + \mathbf{K}[k](\mathbf{y}[k] - \mathbf{h}(\hat{\mathbf{x}}^-[k]))$$

(b) The error covariance matrix is updated

$$\mathbf{P}[k] = \mathbf{P}^-[k] - \mathbf{K}[k]\mathbf{C}[k]\mathbf{P}^-[k]$$

**Step 6:** Return to Step 2 with  $\mathbf{C}[k]$

The choice of these matrices,  $\mathbf{P}_0$ ,  $\mathbf{Q}$  and  $\mathbf{R}$  is a crucial step during the design of the EKF because they affect the performance and the convergence of the EKF [2]. Usually, the three of them are chosen to be diagonal matrices. The covariance matrix  $\mathbf{P}_0$  represents the covariances of the initial conditions and determines the initial amplitude of the transient behavior of the estimation process. The matrix  $\mathbf{Q}$  describes the confidence with the system model, which means that large values in  $\mathbf{Q}$  indicate a low confidence with the system model and will increase the matrix gain to give a better/faster measurement update. The matrix  $\mathbf{R}$  is related to the measurement noise characteristics. Increasing the values of  $\mathbf{R}$  indicates that measured signals are heavily affected by noise and, therefore, are of little confidence. Consequently, the Kalman gain will decrease yielding a slower response.

**Observability** Observability, as well as before, analyzing the rank of the matrix  $\mathbf{S}_o$

$$\mathbf{S}_o = \begin{bmatrix} \mathbf{C}_d \\ \mathbf{C}_d \mathbf{A}_d \\ \mathbf{C}_d \mathbf{A}_d^2 \\ \vdots \\ \mathbf{C}_d \mathbf{A}_d^{n-1} \end{bmatrix} \quad (4.109)$$

So after the discretization, the corresponding  $\mathbf{A}_k$  and  $\mathbf{C}_k$  are

$$\mathbf{A}_k = T_S \begin{bmatrix} \frac{1}{T_S} - \frac{d_s[k] + d_T[k]}{\Theta_T} & \frac{d_s[k]}{g_r \Theta_T} & -\frac{c_s[k]}{\Theta_T} & -\frac{g_r \omega_T[k] - \omega_M[k]}{g_r \Theta_T} & -\frac{\Delta \phi_{T-M}[k]}{\Theta_T} & -\frac{\omega_T}{\Theta_T} & 0 \\ \frac{d_s[k]}{g_r \Theta_M} & \frac{1}{T_S} - \frac{g_r \Theta_T}{d_s[k] + g_r^2 d_M[k]} & \frac{c_s[k]}{\Theta_M} & \frac{g_r \omega_T[k] - \omega_M[k]}{g_r^2 \Theta_M} & \frac{\Delta \phi_{T-M}[k]}{g_r \Theta_M} & 0 & -\frac{\omega_M}{g_r^2 \Theta_M} \\ 1 & -\frac{1}{g_r} & \frac{1}{T_S} & 0 & 0 & 0 & 0 \\ 0 & 0 & 0 & \frac{1}{T_S} & 0 & 0 & 0 \\ 0 & 0 & 0 & 0 & \frac{1}{T_S} & 0 & 0 \\ 0 & 0 & 0 & 0 & 0 & \frac{1}{T_S} & 0 \\ 0 & 0 & 0 & 0 & 0 & 0 & \frac{1}{T_S} \end{bmatrix} \quad (4.110)$$

$$\mathbf{C}_k = \begin{bmatrix} 1 & 0 & 0 & 0 & 0 & 0 & 0 \\ 0 & 1 & 0 & 0 & 0 & 0 & 0 \\ 0 & 0 & 1 & 0 & 0 & 0 & 0 \end{bmatrix} \quad (4.111)$$

with both of this matrices, the observability for the system can be checked. For this matter, the matrix  $\mathbf{S}_o$  results in

$$\mathbf{S}_o = \begin{bmatrix} 1 & 0 & 0 & 0 & 0 & 0 & 0 \\ 0 & 1 & 0 & 0 & 0 & 0 & 0 \\ 0 & 0 & 1 & 0 & 0 & 0 & 0 \\ 0 & 0 & 0 & 1 & -\frac{g_r \Delta \phi_{T-M}[k]}{\omega_M[k] - g_r \omega_T[k]} & 0 & \frac{\omega_M[k]}{\omega_M[k] - g_r \omega_T[k]} \\ 0 & 0 & 0 & 0 & 0 & 1 & \frac{1}{g_r} \\ 0 & 0 & 0 & 0 & 0 & 0 & 0 \\ 0 & 0 & 0 & 0 & 0 & 0 & 0 \\ \vdots & \vdots & \vdots & \vdots & \vdots & \vdots & \vdots \end{bmatrix} \quad (4.112)$$

As the maximum rank was 7, but the rank obtained for this matrix was 5, two parameters are not observable. After considering the importance of the estimation of all the parameters, it is decided to check if  $d_s$  and  $c_s$  are observable at the same time since  $d_T$  and  $d_M$  are being neglected.

Assuming the new state vector is  $(\omega_T(t), \omega_M(t), \Delta \phi_{T-M}(t), d_s(t), c_s(t))^T \in \mathbb{R}^5$ , and using the same equations described before, the new  $\mathbf{A}_k$  and  $\mathbf{C}_k$  matrices are

$$\mathbf{A}_d = T_S \begin{bmatrix} \frac{1}{T_S} - \frac{d_s[k] + d_T[k]}{\Theta_T} & \frac{d_s[k]}{g_r \Theta_T} & -\frac{c_s[k]}{\Theta_T} & -\frac{g_r \omega_T[k] - \omega_M[k]}{g_r \Theta_T} & -\frac{\Delta \phi_{T-M}[k]}{\Theta_T} \\ \frac{d_s[k]}{g_r \Theta_M} & \frac{1}{T_S} - \frac{d_s[k] + g_r^2 d_M[k]}{g_r^2 \Theta_M} & \frac{c_s[k]}{\Theta_M} & \frac{g_r \omega_T[k] - \omega_M[k]}{g_r^2 \Theta_M} & \frac{\Delta \phi_{T-M}[k]}{g_r \Theta_M} \\ 1 & -\frac{1}{g_r} & \frac{1}{T_S} & 0 & 0 \\ 0 & 0 & 0 & \frac{1}{T_S} & 0 \\ 0 & 0 & 0 & 0 & \frac{1}{T_S} \end{bmatrix} \quad (4.113)$$

$$\mathbf{C}_d = \begin{bmatrix} 1 & 0 & 0 & 0 & 0 \\ 0 & 1 & 0 & 0 & 0 \\ 0 & 0 & 1 & 0 & 0 \end{bmatrix} \quad (4.114)$$

with both of this new matrices, the observability for the system can be checked. For this matter, the matrix  $\mathbf{S}_o$  results in

$$\mathbf{S}_o = \begin{bmatrix} 1 & 0 & 0 & 0 & 0 \\ 0 & 1 & 0 & 0 & 0 \\ 0 & 0 & 1 & 0 & 0 \\ 0 & 0 & 0 & 1 & -\frac{g_r \Delta \phi_{T-M}[k]}{\omega_M[k] - g_r \omega_T[k]} \\ \vdots & \vdots & \vdots & \vdots & \vdots \end{bmatrix} \quad (4.115)$$

Once more, the maximum rank was 5 and the rank obtained is 4. Which means only one of the two parameters can be observed at a time since they are linearly dependent. Due to this it is decided to move from an Extended Kalman Filter to a Recursive Least Square method with a different sampling method to solve the static

observability problem.

#### 4.4.4 Recursive Least Squares (RLS)

Based on [26]. The recursive method of least squares was also created by Gauss (1809) [23]. First applications of this technique to dynamic systems have been presented by Lee (1964) and Albert and Sittler (1965) [22]. In this specific method, different from a non-recursive method of least squares, the new parameter estimates should be available during the measurement, after each sample step. So previous measurements do not have to be stored.

The RLS algorithm is used in this thesis to implement the estimation of the mechanical parameters of a wind turbine. The RLS algorithm with a forgetting factor compromises the convergence rate of the estimated parameters and the filtering effect on the measurement noise [26]. The RLS algorithm is described by the following equations:

$$\hat{\theta}[k] = \hat{\theta}[k-1] + \mathbf{K}[k](\mathbf{y}[k] - \varphi^\top[k]\hat{\theta}[k-1]) \quad (4.116)$$

$$\mathbf{K}[k] = \mathbf{P}[k-1]\varphi[k](\gamma\mathbf{I} + \varphi^\top[k]\mathbf{P}[k-1]\varphi[k])^{-1} \quad (4.117)$$

$$\mathbf{P}[k] = \frac{1}{\gamma}(\mathbf{I} - \mathbf{K}[k]\varphi^\top[k])\mathbf{P}[k-1] \quad (4.118)$$

where the system's description for the parameter estimation is given by

$$\mathbf{y} = \varphi^\top\theta \quad (4.119)$$

In here,  $\mathbf{y}$  and  $\varphi^\top$  are the output and states;  $\theta$  and  $\hat{\theta}$  are the real and estimated parameter vectors respectively.  $\gamma$  is a positive forgetting factor, which is chosen less than 1.  $\mathbf{P}$  is the covariance matrix and  $\mathbf{K}$  the correcting factor for the next measurement.

In order to start the recursive method of least squares, the initial values for  $\hat{\theta}$  and  $\mathbf{K}$  must be known, but also can be initialized to 0.

A small forgetting factor results in fast convergence rate of the parameter estimation but large noise level in estimated values. Therefore, a proper forgetting factor should be chosen to achieve a trade-off between the convergence rate and the noise level. Usually, 0.95 is chosen.

To choose and define the output, states and parameter matrices, the following steps are taken.

1. Define the equations that are going to be used for the method

$$\frac{\omega_T[k+1] - \omega_T[k]}{T_S} = \frac{m_T[k]}{\Theta_T} - \frac{\omega_T[k] \cdot d_s[k]}{\Theta_T} + \frac{\omega_M[k] \cdot d_s[k]}{g_r\Theta_T} - \frac{\Delta\phi_{T-M}[k] \cdot c_s[k]}{\Theta_T} \quad (4.120)$$

$$\frac{\omega_M[k+1] - \omega_M[k]}{T_S} = \frac{m_M[k]}{\Theta_M} + \frac{\omega_T[k] \cdot d_s[k]}{g_r \Theta_M} - \frac{\omega_M[k] \cdot d_s[k]}{g_r^2 \Theta_T} + \frac{\Delta\phi_{T-M}[k] \cdot c_s[k]}{g_r \Theta_M} \quad (4.121)$$

2. Choose the parameters and identify them in the stated equations in the previous step. These parameters are from now on known as  $\theta$

$$\frac{\omega_T[k+1] - \omega_T[k]}{T_S} = \frac{m_T[k]}{\Theta_T} - \frac{\omega_T[k] \cdot d_s[k]}{\Theta_T} + \frac{\omega_M[k] \cdot d_s[k]}{g_r \Theta_T} - \frac{\Delta\phi_{T-M}[k] \cdot c_s[k]}{\Theta_T} \quad (4.122)$$

$$\frac{\omega_M[k+1] - \omega_M[k]}{T_S} = \frac{m_M[k]}{\Theta_M} + \frac{\omega_T[k] \cdot d_s[k]}{g_r \Theta_M} - \frac{\omega_M[k] \cdot d_s[k]}{g_r^2 \Theta_T} + \frac{\Delta\phi_{T-M}[k] \cdot c_s[k]}{g_r \Theta_M} \quad (4.123)$$

3. Identify which terms in the stated equation do not depend directly on the chosen parameters. These terms are now the output vector  $\mathbf{y}$ .

$$\frac{\omega_T[k+1] - \omega_T[k]}{T_S} = \frac{m_T[k]}{\Theta_T} - \frac{\omega_T[k] \cdot d_s[k]}{\Theta_T} + \frac{\omega_M[k] \cdot d_s[k]}{g_r \Theta_T} - \frac{\Delta\phi_{T-M}[k] \cdot c_s[k]}{\Theta_T} \quad (4.124)$$

$$\frac{\omega_M[k+1] - \omega_M[k]}{T_S} = \frac{m_M[k]}{\Theta_M} + \frac{\omega_T[k] \cdot d_s[k]}{g_r \Theta_M} - \frac{\omega_M[k] \cdot d_s[k]}{g_r^2 \Theta_T} + \frac{\Delta\phi_{T-M}[k] \cdot c_s[k]}{g_r \Theta_M} \quad (4.125)$$

4. Separate the terms that are affected directly by the chosen parameters. This terms constitute the state or data matrix  $\varphi^\top$ .

$$\frac{\omega_T[k+1] - \omega_T[k]}{T_S} = \frac{m_T[k]}{\Theta_T} - \frac{\omega_T[k] \cdot d_s[k]}{\Theta_T} + \frac{\omega_M[k] \cdot d_s[k]}{g_r \Theta_T} - \frac{\Delta\phi_{T-M}[k] \cdot c_s[k]}{\Theta_T} \quad (4.126)$$

$$\frac{\omega_M[k+1] - \omega_M[k]}{T_S} = \frac{m_M[k]}{\Theta_M} + \frac{\omega_T[k] \cdot d_s[k]}{g_r \Theta_M} - \frac{\omega_M[k] \cdot d_s[k]}{g_r^2 \Theta_T} + \frac{\Delta\phi_{T-M}[k] \cdot c_s[k]}{g_r \Theta_M} \quad (4.127)$$

5. Arrange the selected terms into the corresponding matrices.

$$\theta = \begin{bmatrix} d_s[k] \\ c_s[k] \end{bmatrix} \quad (4.128)$$



$$\mathbf{y} = \begin{bmatrix} \frac{\omega_T[k+1]-\omega_T[k]}{T_S} - \frac{m_T[k]}{\Theta_T} \\ \frac{\omega_M[k+1]-\omega_M[k]}{T_S} - \frac{m_M[k]}{\Theta_M} \end{bmatrix} \quad (4.129)$$

$$\varphi^T = \begin{bmatrix} -\frac{g_r\omega_T[k]-\omega_M[k]}{g_r\Theta_T} - \frac{\Delta\phi_{T-M}[k]}{\Theta_T} \\ \frac{g_r\omega_T[k]-\omega_M[k]}{g_r^2\Theta_M} - \frac{\Delta\phi_{T-M}[k]}{g_r\Theta_M} \end{bmatrix} \quad (4.130)$$

#### 4.4.4.1 Principle of the estimation

In the last section while the EKF was being implemented, it is shown a weak observability for the four parameters estimation of the wind turbine, even for the two main ones  $d_s$  and  $c_s$ .

To achieve the convergence of the estimator, it is proposed the consideration of the sinusoidal injected signal as the sampling principle. An example sampling of the d-axis is shown in Fig. 4.8

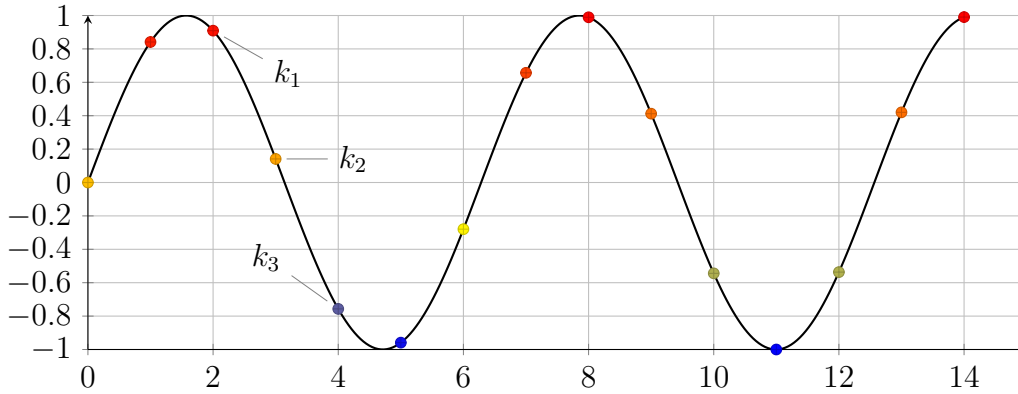


Figure 4.8: *Sampling principle*

Where  $k_1$  and  $k_2$  denote two different sampling instants for the estimator. So considering the model of the wind turbine at the sampling instants  $k_1$  and  $k_2$ , it is obtained

$$\begin{bmatrix} \frac{\omega_T[k_1+1]-\omega_T[k_1]}{T_S} - \frac{m_T[k_1]}{\Theta_T} \\ \frac{\omega_T[k_2+1]-\omega_T[k_2]}{T_S} - \frac{m_T[k_2]}{\Theta_T} \\ \frac{\omega_M[k_1+1]-\omega_M[k_1]}{T_S} - \frac{m_M[k_1]}{\Theta_M} \\ \frac{\omega_M[k_2+1]-\omega_M[k_2]}{T_S} - \frac{m_M[k_2]}{\Theta_M} \end{bmatrix} = \begin{bmatrix} -\frac{g_r\omega_T[k_1]-\omega_M[k_1]}{g_r\Theta_T} - \frac{\Delta\phi_{T-M}[k_1]}{\Theta_T} \\ -\frac{g_r\omega_T[k_2]-\omega_M[k_2]}{g_r\Theta_T} - \frac{\Delta\phi_{T-M}[k_2]}{\Theta_T} \\ \frac{g_r\omega_T[k_1]-\omega_M[k_1]}{g_r^2\Theta_M} - \frac{\Delta\phi_{T-M}[k_1]}{g_r\Theta_M} \\ \frac{g_r\omega_T[k_2]-\omega_M[k_2]}{g_r^2\Theta_M} - \frac{\Delta\phi_{T-M}[k_2]}{g_r\Theta_M} \end{bmatrix} \cdot \begin{bmatrix} d_s \\ c_s \end{bmatrix} \quad (4.131)$$

Equation (4.119) holds under the assumption that the time interval between two adjacent points  $k_1$  and  $k_2$  is relatively small so that the parameter variation during the sampling time interval can be neglected [26]. This assumption can be fulfilled by achieving two conditions: choosing a relative fast sampling time for the estimator

so that the variation between two adjacent points is small, and using small injected signal which causes a negligible influence on the parameters.

In this case, observability should be checked as well, but in this method, it is analysed through the matrix  $\mathbf{B}$ . And the basic conditions for the observability are that the discriminant of  $\mathbf{B}$  is different from zero or that the rank of  $\mathbf{B}$  matches the size of the matrix itself. [26]

$$\mathbf{B} = \begin{bmatrix} -\frac{g_r \omega_T[k_1] - \omega_M[k_1]}{g_r \Theta_T} & -\frac{\Delta \phi_{T-M}[k_1]}{\Theta_T} \\ -\frac{g_r \omega_T[k_2] - \omega_M[k_2]}{g_r \Theta_T} & -\frac{\Delta \phi_{T-M}[k_2]}{\Theta_T} \\ \frac{g_r \omega_T[k_1] - \omega_M[k_1]}{g_r^2 \Theta_M} & \frac{\Delta \phi_{T-M}[k_1]}{g_r \Theta_M} \\ \frac{g_r \omega_T[k_2] - \omega_M[k_2]}{g_r^2 \Theta_M} & \frac{\Delta \phi_{T-M}[k_2]}{g_r \Theta_M} \end{bmatrix} \quad (4.132)$$

It is simple to find out that the rank of the matrix  $\mathbf{B}$  is 2, if the rotational speeds  $\omega_T[k]$  and  $\omega_M[k]$  are different from each other or and if  $\Delta \phi_{T-M}[k]$  is not zero. Therefore, it can be assumed that there is at least one sampling pattern that guarantees the parameter identifiability for the sinusoidal current injection. In order to achieve a fast convergence time for the parameter estimation, more sampling points can be chosen within one period of the injected sinusoidal signal.



# Chapter 5

## Analysis and results

In this chapter, the main simulations that were designed as well as the necessary steps to get to the shown results are included. Simulations for the working one and two mass system, speed control, observer designs and parameter estimator are shown.

### 5.1 Speed control for the one-mass system

The control previously explained in section 4.2 is implemented in Simulink using equations for variables  $\lambda$ ,  $c_{P,1}$ ,  $m_T$ ,  $g_r$ ,  $\Theta$ ,  $\frac{d}{dt}\omega_T(t)$ ,  $K_P^*$  and  $m_{M,ref}$ , given by (4.2), (4.5), (4.10), (4.11), (4.18), (4.19), (4.16), (4.52), and (4.53); respectively. For the correct simulation of a basic wind turbine, assuming as basic a wind turbine with a one mass system, some constants are needed.

For this thesis, the simulations are being carried on for a 2 MW wind turbine. The needed constants and data assumed from a 2 MW wind turbine and air conditions were taken from [13]. For this and further simulations, a fixed step solver Runge-Kutta (ode4) for Simulink was used.

Table 5.1: *Wind turbine and air conditions for simulation*

Description	Symbol	Value with units
Sample time	$s_T$	$20 \times 10^{-3}$ s
Air density	$\rho$	1.293 kg/m <sup>3</sup>
Turbine's radius	$r_T$	40 m
Optimal tip speed	$\lambda^*$	8.506
Optimal power coefficient	$c_{P,1}^*$	0.558
Turbine's inertia	$\Theta_T$	$8.6 \times 10^6$ kg m <sup>2</sup>
Machine's inertia	$\Theta_M$	$1.3 \times 10^6$ kg m <sup>2</sup>
Speed Controller gain	$K_P^*$	$188.73 \times 10^5$ kg m <sup>2</sup>
Gear ratio	$g_r$	1
Constant wind's speed	$v_W$	$4 \frac{\text{m}}{\text{s}}$

The basic equations and constants were set in Simulink by the use of blocks and Matlab functions for the correct implementation of the simulation.

The control variables: tip speed ratio ( $\lambda$ ), the turbine's rotational speed ( $\omega_T$ ), machine's torque ( $m_M$ ), turbine's torque ( $m_T$ ) and power coefficient ( $c_{P,1}$ ) were graphed to check the system and control's response. The data obtained is displayed in Fig. 5.1.

In the first graph, a constant wind speed is shown. In graph 2, the optimal tip speed ratio  $\lambda^*$  and the tip speed ratio through time  $\lambda(t)$  are shown, displaying the converging behavior of the system by reaching the expected value of the tip speed ratio with a constant wind speed.

About the power coefficient, as well as in the previous graph, the optimal  $c_{P,1}^*$  and the through time  $c_{P,1}(t)$  response are shown in graph 3. Where the same behavior is displayed, the power coefficient through time reaches the optimal value.

The graph 4, the turbine's rotational speed  $\omega_T(t)$  is shown. In this graph it can be noticed the initial value of the integrator as 1 and how it reaches a stable value around  $0.86 \frac{\text{rad}}{\text{s}}$ .

And, in graph 5, the turbine's torque  $m_T(t)$  and machine's torque  $m_M(t)$  through time are shown. As it is shown in the model, it is assumed that both of them are the same and the simulation displays the assumption.

In all 4 of the 5 graphs, it is shown the working control system for the turbine as all of the variables end up converging to the expected value.

The tip speed ratio and the power coefficient reach their optimal values, the turbine's rotational speed reaches a constant value and the torques converge to the exact same value.

In these initial simulations, the initial values are not the system's initial values just to illustrate the correct functioning of the control and overall system.

This behavior obtained is set as a standard for following behavior with the two-mass system with constant wind speed, with the correct initial values.

## 5.1. SPEED CONTROL FOR THE ONE-MASS SYSTEM

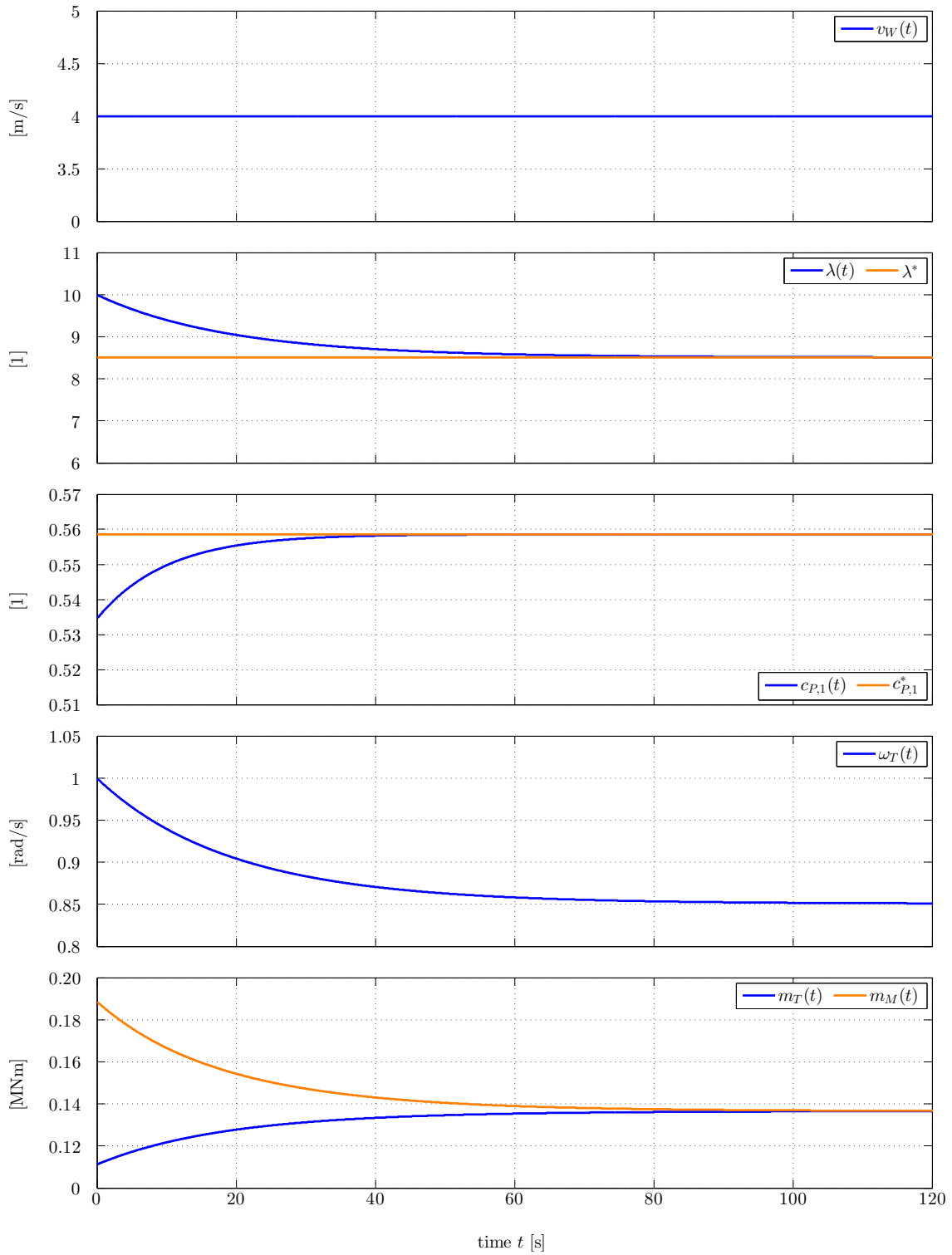


Figure 5.1: *Wind speed, tip speed ratio, power coefficient, turbine's rotational speed and torques simulation results of a one-mass system*

### 5.1.1 Disturbance observer design for the two-mass system

The two-mass system was implemented in the Simulink simulation using the initial equations that characterized each of the states as in (4.44) and (4.45). As for the observer designed, it was implemented in the Simulink simulation using (4.68) and (4.69) and the correspondent values of  $\mathbf{A}'$ ,  $\mathbf{b}'$ ,  $\mathbf{C}'$  and  $\mathbf{L}$  as shown in (4.62), (4.63) and (4.80).

Some constants are also assumed from data of a 2 MW wind turbine and air conditions. All the needed values were taken from [13]. And as well as before, a fixed step solver Runge-Kutta (ode4) was used for the simulation.

Table 5.2: *Wind turbine and air conditions for two-mass system simulation*

Description	Symbol	Value with units
Sample time	$s_T$	$20 \times 10^{-3}$ s
Air density	$\rho$	1.293 kg/m <sup>3</sup>
Turbine's radius	$r_T$	40 m
Optimal tip speed	$\lambda^*$	8.506
Optimal power coefficient	$c_{P,1}^*$	0.558
Low-speed shaft damping	$d_s$	$1.35 \times 10^7 \frac{\text{N m s}}{\text{rad}}$
Low-speed shaft stiffness	$c_s$	$2.36 \times 10^9 \frac{\text{N m}}{\text{rad}}$
Turbine's damping	$d_T$	$0 \frac{\text{N m s}}{\text{rad}}$
Machine's damping	$d_M$	$0 \frac{\text{N m s}}{\text{rad}}$
Turbine's inertia	$\Theta_T$	$8.6 \times 10^6$ kg m <sup>2</sup>
Machine's inertia	$\Theta_M$	$1.3 \times 10^6$ kg m <sup>2</sup>
Speed Controller gain	$K_P^*$	$188.73 \times 10^5$ kg m <sup>2</sup>
Gear ratio	$g_r$	1
Constant wind's speed	$v_W$	$4 \frac{\text{m}}{\text{s}}$

The block diagram for the disturbance observer is shown in Fig. 5.2

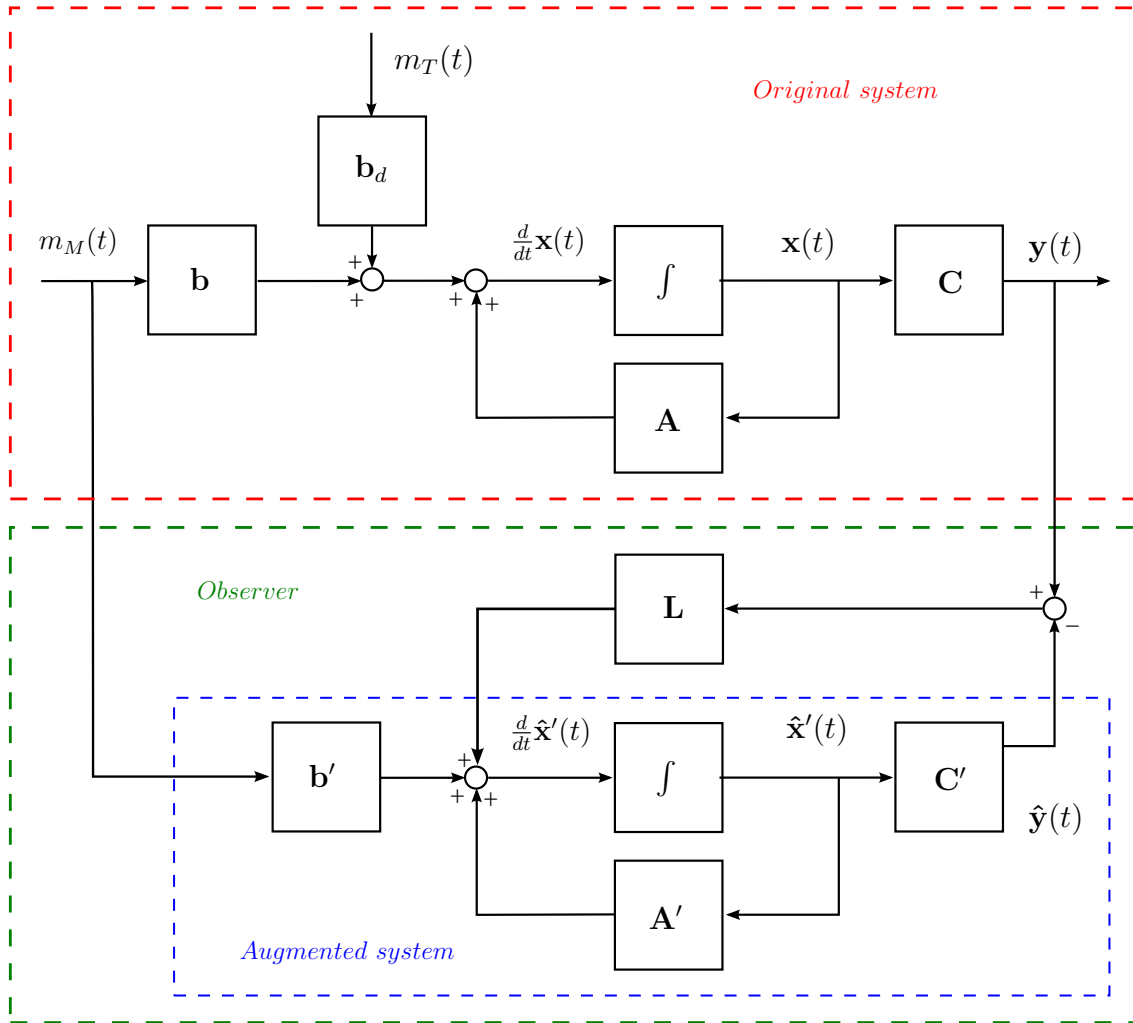


Figure 5.2: Original system and observer with augmented system block diagram

### 5.1.1.1 Disturbance observer design by pole placement

To decide on the observer gains' values, after implementing the diagram shown in Fig. 5.2, an initial  $\mathbf{L}$  matrix is calculated with all the poles set in -1.

The initial gain matrix  $\mathbf{L}$  corresponds to

$$\mathbf{L} = \begin{bmatrix} 0.4302 & 1.5698 & -2.7442 \\ 10.3846 & -9.3846 & 1.8154 \\ 1 & -1 & 1 \\ 8600000 & 0 & 0 \end{bmatrix}$$

The results obtained with the poles in -1 are good, but there is a small retardation in the answer of the observer. The decision made after some tests is to place the poles as further as possible for the observer to have the quickest and closer response to the original turbine torque that is now treated as the "disturbance".



The best result is obtained when the poles are placed in:

$$p_1 = p_2 = p_3 = p_4 = -10$$

The values are all negative for the response to be stable as explained in the introduction, where the poles of the system should be placed on the left side of the imaginary half plane. The values are also chosen accordingly to the variable they are dependent on:  $p_1$  is related to the machine's rotational speed error,  $p_2$  and  $p_3$  relate to the turbine's rotational speed error, and  $p_4$  is related to the angle displacement error.

**Simulation results** The main point of the simulations is to show the working observer for the turbine's torque and the original turbine's torque as a reference. The following graphs will also show the conditions on which the turbine is working and that directly affect the turbine's torque such as wind speed, tip speed ratio and power coefficient. In the same way, the three basic states and the difference between the original and the observed states are shown.

Initially, the system is simulated using the diagram shown in 5.2 and a constant wind speed. The initial values for each of the variables have been set for the simulation to be as truthful as possible.

The results that show the wind turbine's conditions such as wind speed, tip speed ratio and power coefficient are shown in the first three graphs in Fig. 5.3. As well as the rotational speeds and angle displacement for the turbine and machine in the original system and the observed one, the two states,  $\mathbf{y}(t)$  and  $\hat{\mathbf{y}}(t)$ , are compared in the last three graphs in Fig. 5.3. It is shown, a constant wind speed with some small disturbances that stay constant for small periods of time just to show, as well, the correct functioning of the controller and the overall behavior of the wind turbine. In both graphs 2 and 3, the tip speed ratio and power coefficient react to the disturbance, but the system quickly absorbs and controls it.

As for turbine's and machine's rotational speeds and angle displacement, shown in graphs 4, 5 and 6, the observer follows through all of the changes as they happen. Which is also shown in graphs 2, 3 and 4 in Fig. 5.4 where the differences between the original and observed states are displayed. About the rotational speeds, there are some small changes in the measurements with every disturbance which can be assumed as normal. It is noticeable, that both of the rotational speeds react basically the same, turning this behavior into a zero or really small value in the angle displacement variable.

The same behavior is shown in graphs 5 and 6 in Fig. 5.4 where the original and observed turbine's torque are stated. The observed system follows through the changes, and there are some big differences between the observed and original system in every disturbance. After the disturbance is made, the observed system quickly adapts and keeps of following the original system.

## 5.1. SPEED CONTROL FOR THE ONE-MASS SYSTEM

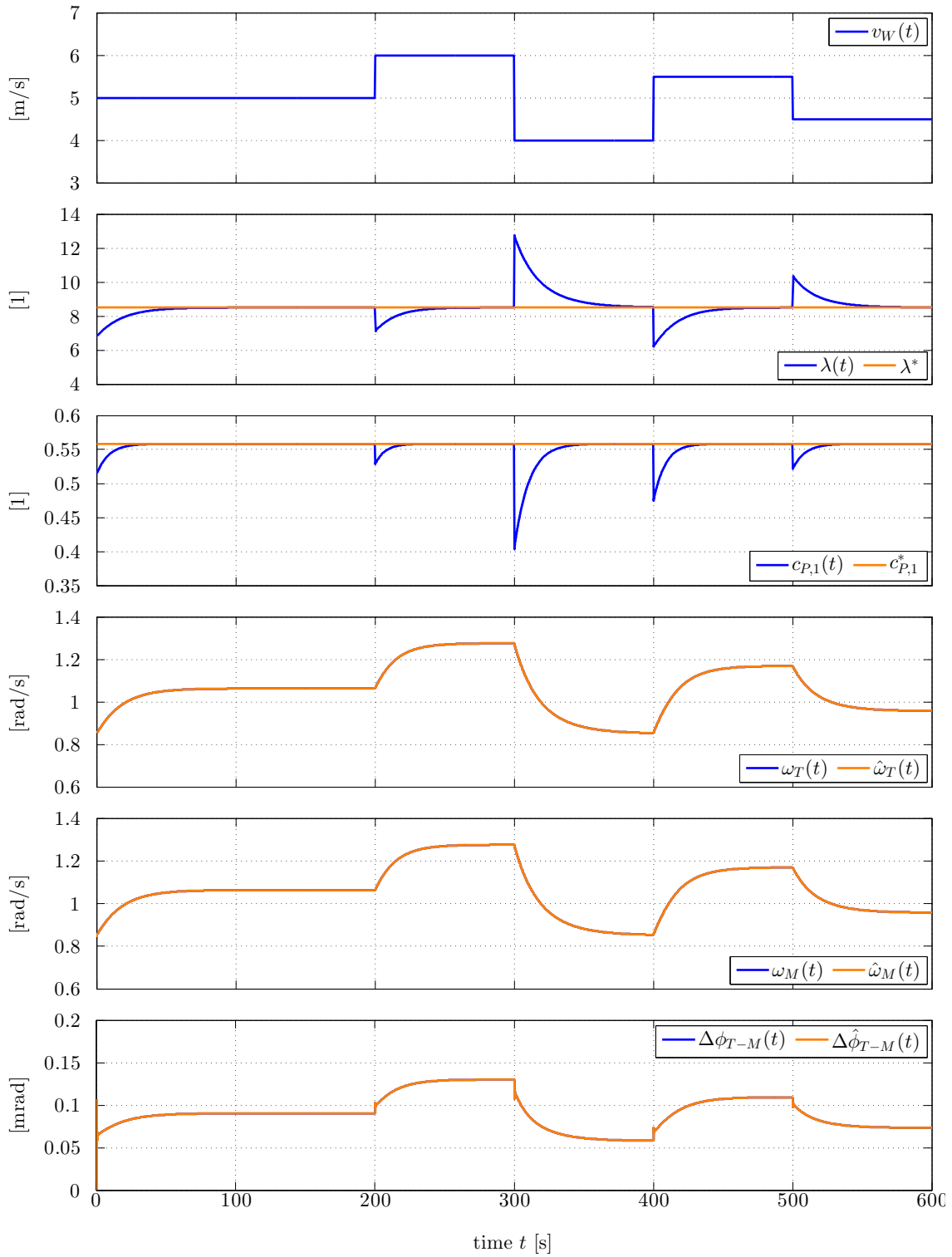


Figure 5.3: *Simulation results for the wind speed, tip speed ratio, power coefficient, original and observed rotational speeds and angle displacement in a wind turbine with a two-mass system with a constant wind speed input and a observer designed by pole placement*

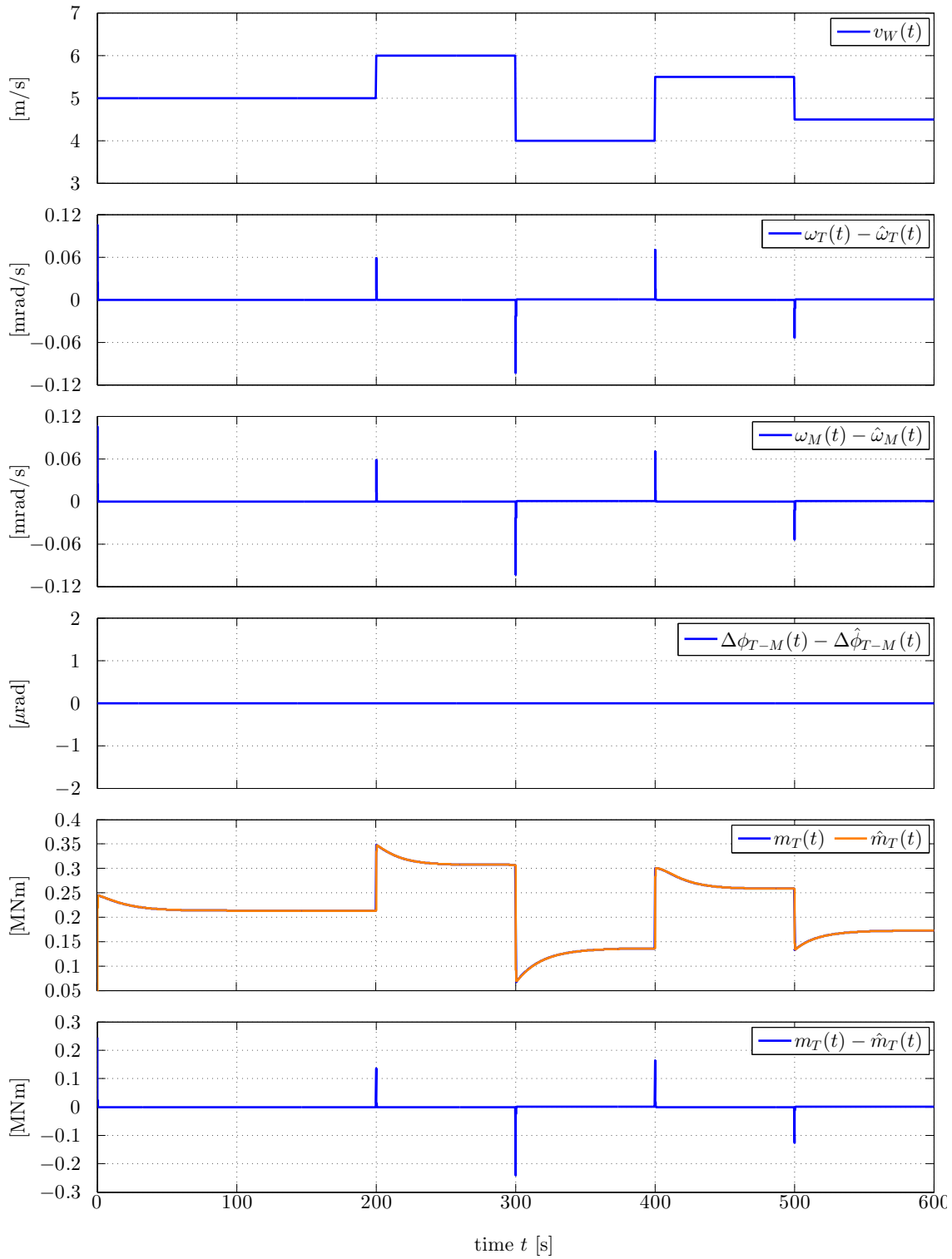


Figure 5.4: Simulation results for the wind speed, the difference between the original system and the observed system for the rotational speeds and angle displacement, the original turbine's torque and the observed one and the difference between them in a wind turbine with a two-mass system with a constant wind speed input and a observer designed by pole placement

After obtaining what can be considered as a good response from the observer and overall system with a constant wind speed, a wind speed profile is added to the simulation. Where the following results are obtained.

As well as before, the two states,  $\mathbf{y}(t)$  and  $\hat{\mathbf{y}}(t)$ , are compared in Fig. 5.5. The graphs shown in Fig. 5.5 corresponds to the wind speed, tip speed ratio and power coefficient in the first three graphs. In the fourth, fifth and sixth graphs, the original system's response and the observed system's response are shown. The fourth graph corresponds to the the turbine's rotational speed  $\omega_T$ , the machine's rotational speed  $\omega_M$  in the fifth one, and the angle displacement between the turbine and the related machine  $\phi_{T-M}$  in the sixth one.

It can be observed in Fig. 5.5 how the tip speed ratio and power coefficient react to the wind profile. It is noted that the tip speed ratio constantly fluctuates around the optimal tip speed ratio value, and that the power coefficient constantly reaches the maximum power coefficient value for this wind turbine.

Physics can be used to explain the relation between these two variables, and that every time the tip speed ratio equals the optimal tip speed ratio, the power coefficient reaches its maximum value.

As for the three basic states, the rotational speeds for the turbine and machine and the angle displacement, the observed system follows through the original almost perfectly. The difference between both values for the three states are shown in Fig. 5.6. The difference between the observed and original systems for the rotational speeds are almost the same, as before, ending up in a zero value in the angle displacement variable. This is shown in graphs 2, 3 and 4 of Fig. 5.6.

As well as before, in Fig. 5.6 the first graph corresponds to the wind speed. The second, third and fourth graphs correspond to the difference between the original system and the observed one,  $\mathbf{y}(t)$  and  $\hat{\mathbf{y}}(t)$ , in the three main states:  $\omega_T$ ,  $\omega_M$  and  $\Delta\phi_{T-M}$ . In the fifth graph the original turbine's torque and the observed one are shown, as well as the difference between them in the sixth graph.

About the observer response, it seems to follow through the changes of the original turbine's torque quite good, showing a small difference, less than a 15 percent between the original and observed responses.

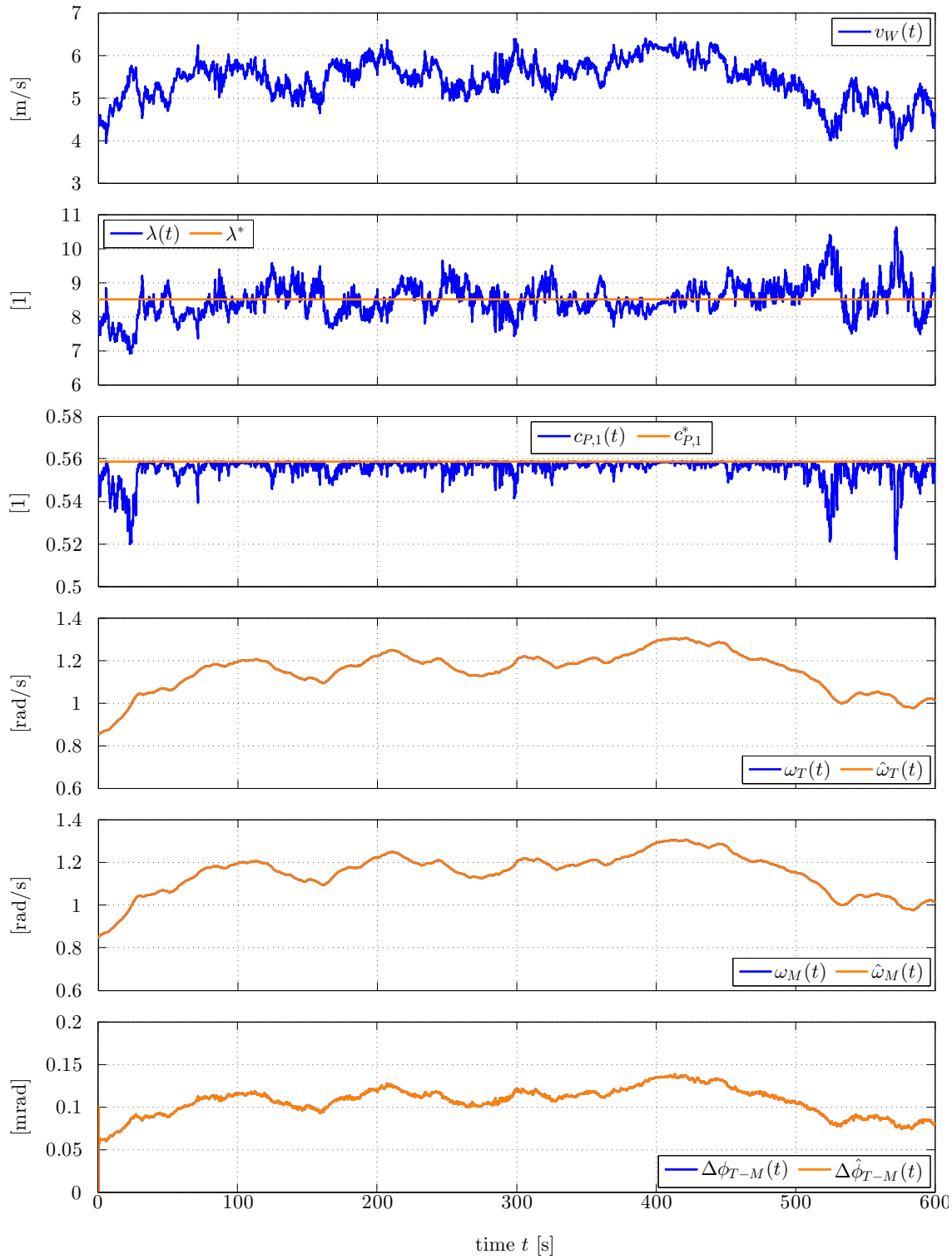


Figure 5.5: Simulation results for the wind speed, tip speed ratio, power coefficient, original and observed rotational speeds and angle displacement in a wind turbine with a two-mass system with a wind profile input and an observer designed by pole placement

## 5.1. SPEED CONTROL FOR THE ONE-MASS SYSTEM

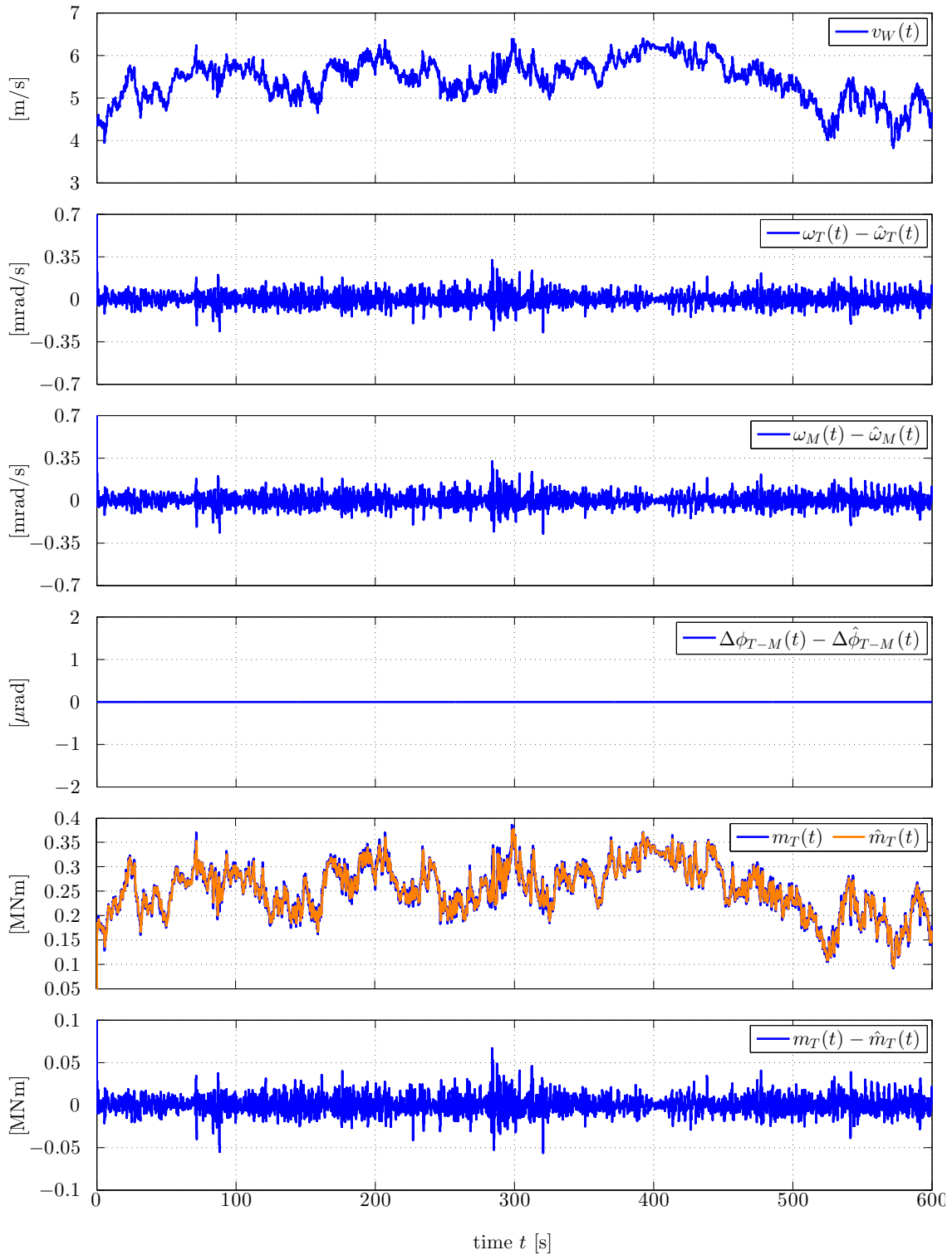


Figure 5.6: *Simulation results for the wind speed, the difference between the original system and the observed system for the rotational speeds and angle displacement, the original turbine's torque and the observed one and the difference between them in a wind turbine with a two-mass system with a wind profile input and an observer designed by pole placement*

### 5.1.1.2 Disturbance observer design by LQR with stability margin

For the observer to work correctly, it is crucial to chose the values of the design weighting matrices  $\mathbf{R}_o$  and  $\mathbf{Q}_o$ , as well as the stability margin  $\alpha_0$ .

Initially, the matrices are chosen as

$$\mathbf{R}_o = \begin{bmatrix} 1 & 0 & 0 \\ 0 & 1 & 0 \\ 0 & 0 & 1 \end{bmatrix} \quad (5.1)$$

$$\mathbf{Q}_o = \begin{bmatrix} 1 & 0 & 0 & 0 \\ 0 & 1 & 0 & 0 \\ 0 & 0 & 1 & 0 \\ 0 & 0 & 0 & 1 \end{bmatrix} \quad (5.2)$$

After solving (4.84) and (4.85), the resultant  $\mathbf{L}$  matrix is

$$\mathbf{L} = 1 \times 10^7 \cdot \begin{bmatrix} 0.000000351910945 & -0.000000206094948 & -0.000000003453908 \\ -0.000000206094948 & 0.000002962789615 & 0.000000040766102 \\ -0.000000003453908 & 0.000000040766102 & 0.000000002623445 \\ 3.077542334623121 & 2.299738362124113 & 0.027062094727349 \end{bmatrix} \quad (5.3)$$

Using [6] to tune the design matrices  $\mathbf{R}_o$  and  $\mathbf{Q}_o$ . Increasing  $\mathbf{Q}_o$  would indicate the presence of either heavy system noise or increased parameter uncertainty. An increment of the elements of  $\mathbf{Q}_o$  will likewise increase the EKF gain, resulting in a faster filter dynamic. Although, large values in  $\mathbf{Q}_o$  are also related to a low confidence in the model. On the other hand, matrix  $\mathbf{R}_o$  is associated measurement noise. Increasing the values of the elements of  $\mathbf{R}_o$  will mean that the measurements are affected by noise and thus they are of little confidence. Consequently the filter gain  $\mathbf{L}$  will decrease, yielding poorer transient response [6]. As the relation between the two of them is what matters in the design,  $\mathbf{R}_o$  can be assumed as a diagonal matrix of ones and  $\mathbf{Q}_o$  should also be a diagonal, but with small values on it.

Consequently, the matrices used ended up being

$$\mathbf{Q}_o = \begin{bmatrix} 1 \times 10^{-6} & 0 & 0 \\ 0 & 1 \times 10^{-6} & 0 \\ 0 & 0 & 1 \times 10^{-6} \end{bmatrix} \quad (5.4)$$

$$\mathbf{R}_o = \begin{bmatrix} 1 & 0 & 0 & 0 \\ 0 & 1 & 0 & 0 \\ 0 & 0 & 1 & 0 \\ 0 & 0 & 0 & 1 \end{bmatrix} \quad (5.5)$$

And the stability margin  $\alpha_0$  was chosen to be 10, the same value chosen before for

the pole placement design.

**Simulation results** As well as in the past simulations, the system is simulated using the diagram shown in 5.2 and to start with, a constant wind speed, from which the following results are obtained.

The two states,  $y(t)$  and  $\hat{y}(t)$  are compared in the fourth, fifth and sixth graphs in Fig. 5.7. In Fig. 5.7 as well, the response of the wind speed, tip speed ratio and power coefficient are shown in graphs 1, 2 and 3, respectively.

The fourth graph shown in Fig. 5.7 corresponds to the turbine's rotational speed  $\omega_T$ , the fifth one to the machine's rotational speed  $\omega_M$ , and the sixth one to the angle displacement between the turbine and the related machine  $\Delta\phi_{T-M}$ .

The overall behavior of the wind turbine is the same as the previous observer design graphs since those did not change. As for the observed system, it can be noted in Fig. 5.7 that this systems follows through the changes of the original one quite closely. This can be shown in graphs 4, 5 and 6 of Fig. 5.7 where the original and observed system response are compared using the turbine and machine's rotational speeds and the angle displacement variables.

After obtaining  $y(t)$  and  $\hat{y}(t)$ , the difference between them is graphed in graphs 2, 3 and 4 in Fig. 5.8. Where the big differences happen when the disturbances in the constant wind speed happens. With this observer, there is a difference between the rotational speeds, ending up in a difference in the angle displacement. Which was actually expected.

The results from the disturbance observer designed work as expected, with an error below 10 percent. The results are shown in graph number 5 and 6 in Fig. 5.8.

After obtaining a good response from the observer with a constant wind speed, a wind speed profile is added to the simulation(see first graph in Fig. 5.9). Where the following results are obtained: the two states,  $y(t)$  and  $\hat{y}(t)$ , are compared in Fig. 5.9 where the turbine's rotational speed  $\omega_T$ , the machine's rotational speed  $\omega_M$ , and the angle displacement between the turbine and the related machine  $\phi_{T-M}$  in the fourth, fifth and sixth graphs are shown. In the second and third graphs in Fig. 5.9 the response of the tip speed ratio and power coefficient are shown.

The difference between the results of  $y(t)$  and  $\hat{y}(t)$ , is shown in Fig. 5.10, where the difference in the turbine's rotational speeds  $\omega_T$  can be found in the second graph, the difference in the machine's rotational speeds  $\omega_M$  in the third one, and the angle displacement difference between the turbine and the related machine  $\phi_{T-M}$  in the fourth one.

The disturbance observer designed and its response is also shown in Fig. 5.10. In the fifth graph in Fig. 5.10 the response of the original system and the observed one is shown, as well as the difference between them in the sixth graph.

In this case, when the wind profile is used to test the disturbance observer designed by LQR with a stability margin, basically the same results from the constant wind speed are obtained. The observer follows through and the difference between the observed and original system is quite small.



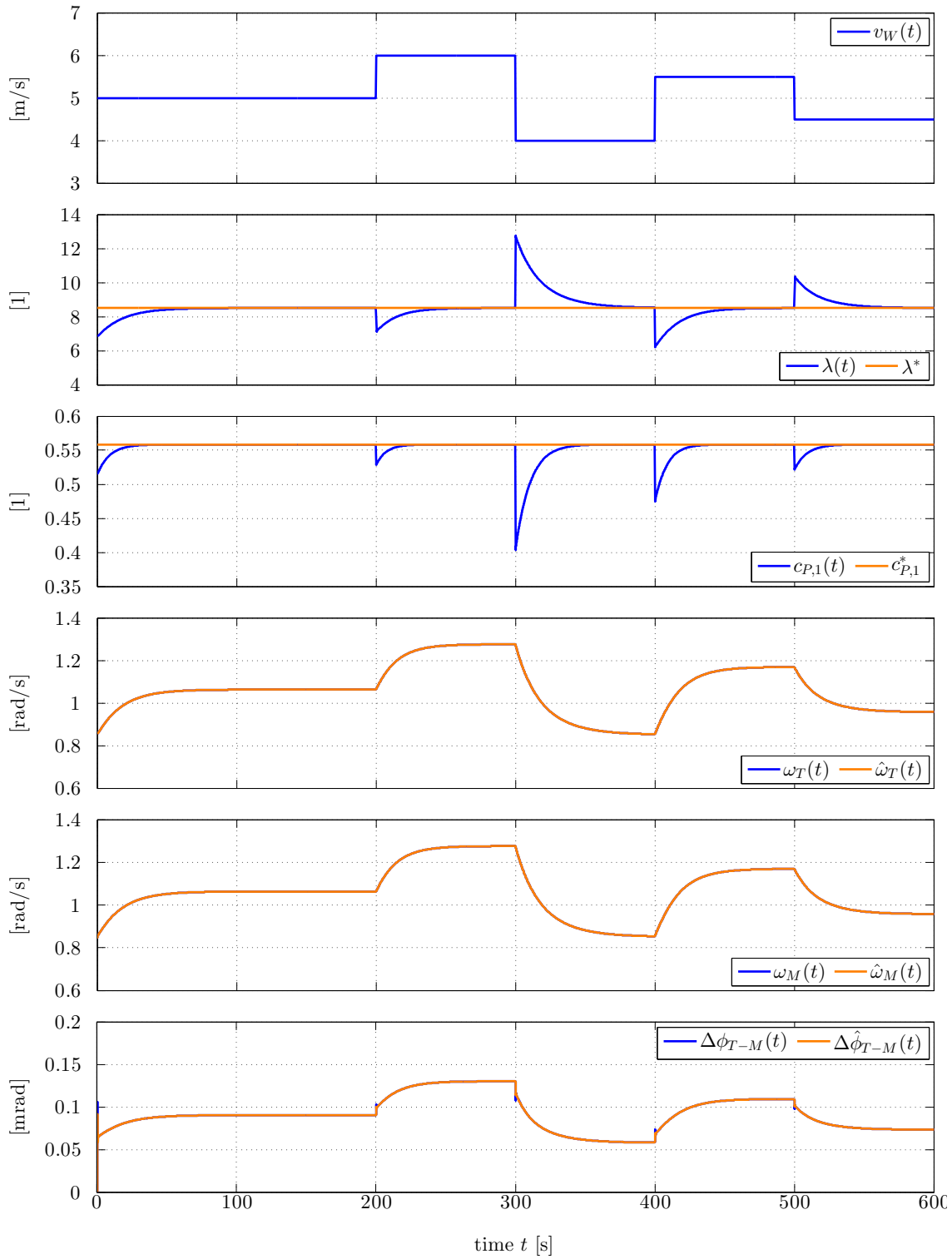


Figure 5.7: Simulation results for the wind speed, tip speed ratio, power coefficient, original and observed rotational speeds and angle displacement in a wind turbine with a two-mass system with a constant wind speed input and a observer designed by LQR

## 5.1. SPEED CONTROL FOR THE ONE-MASS SYSTEM

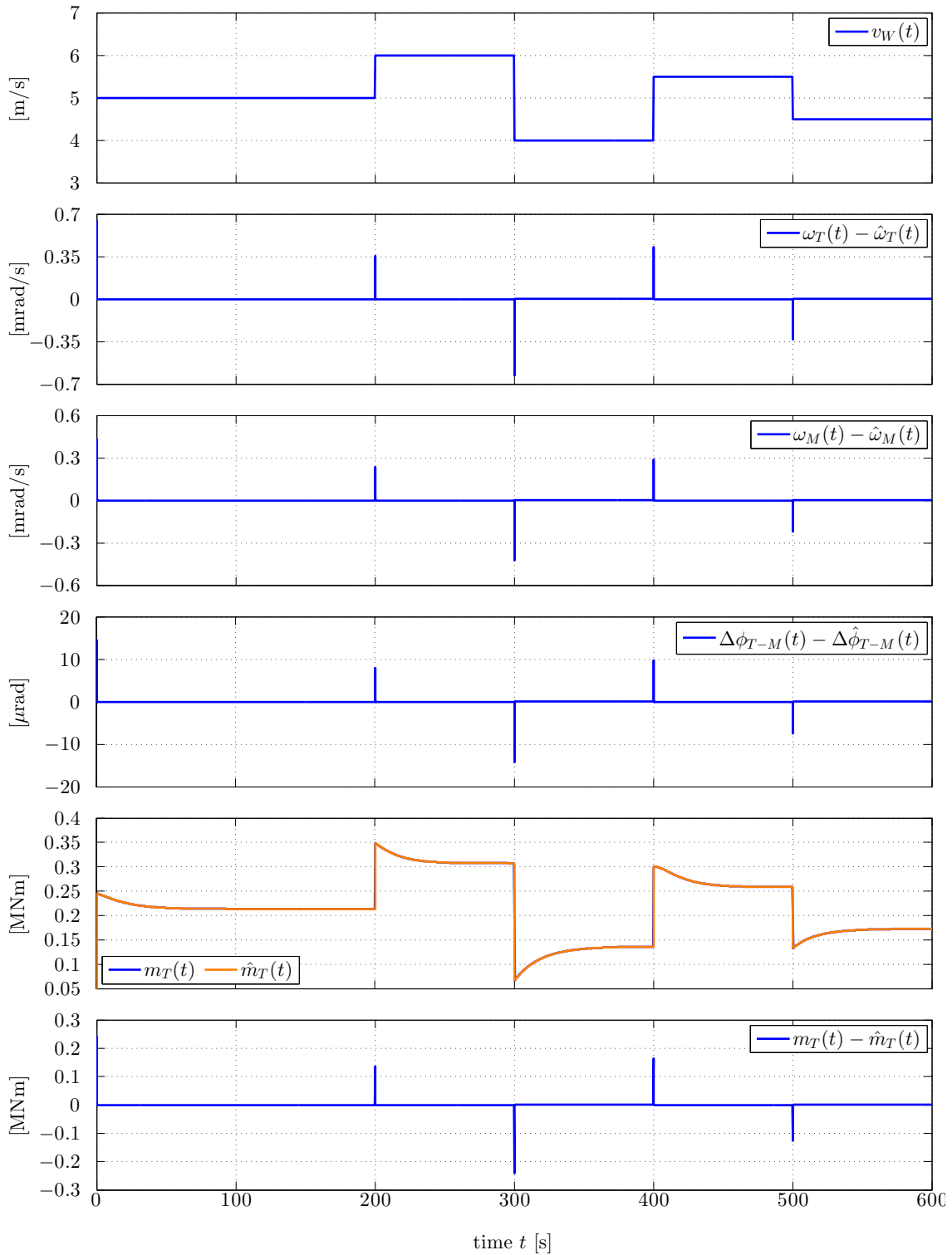


Figure 5.8: *Simulation results for the wind speed, the difference between the original system and the observed system for the rotational speeds and angle displacement, the original turbine's torque and the observed one and the difference between them in a wind turbine with a two-mass system with a constant wind speed input and an observer designed by LQR*

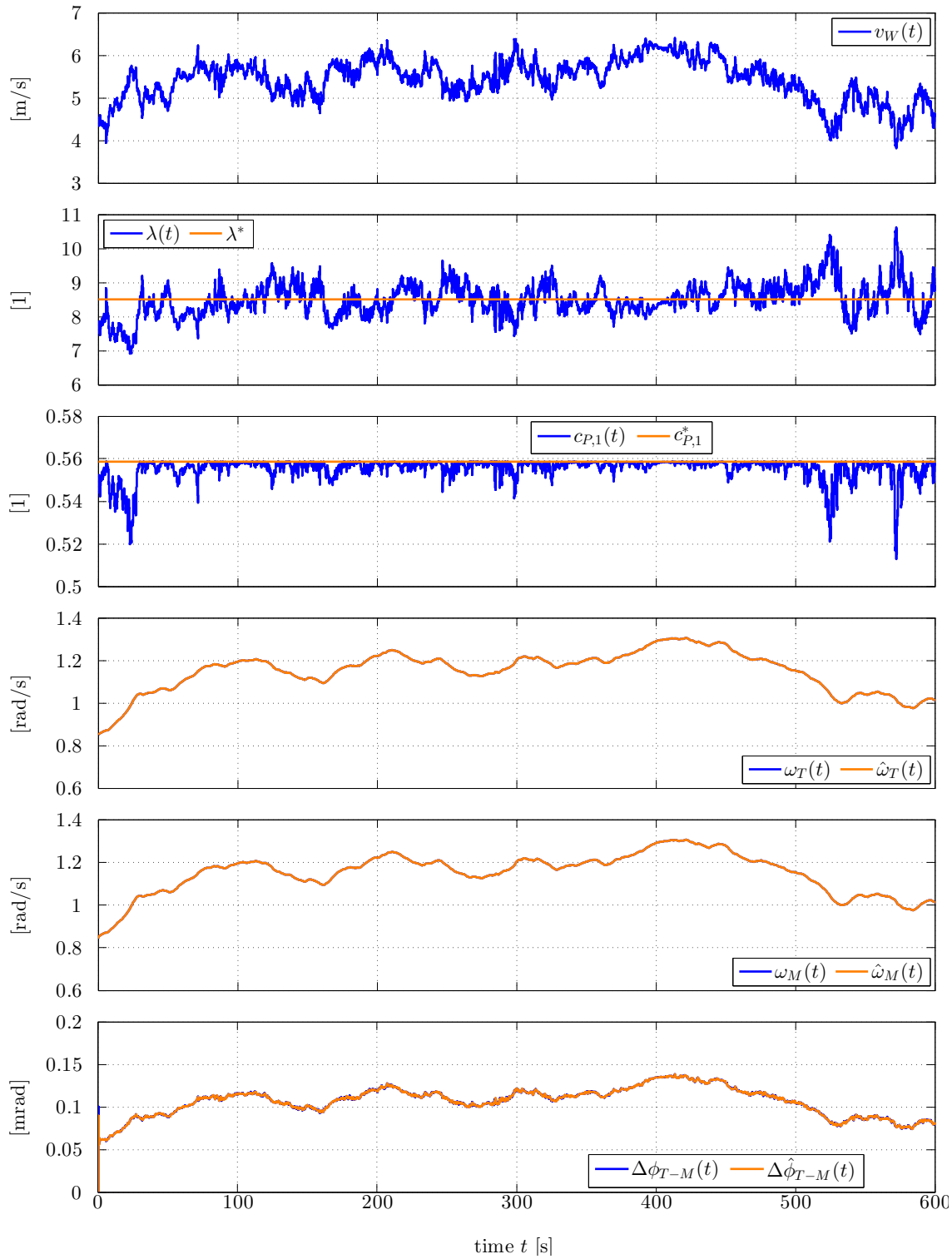


Figure 5.9: *Simulation results for the wind speed, tip speed ratio, power coefficient, original and observed rotational speeds and angle displacement in a wind turbine with a two-mass system with a wind profile input and a observer designed by LQR*

## 5.1. SPEED CONTROL FOR THE ONE-MASS SYSTEM

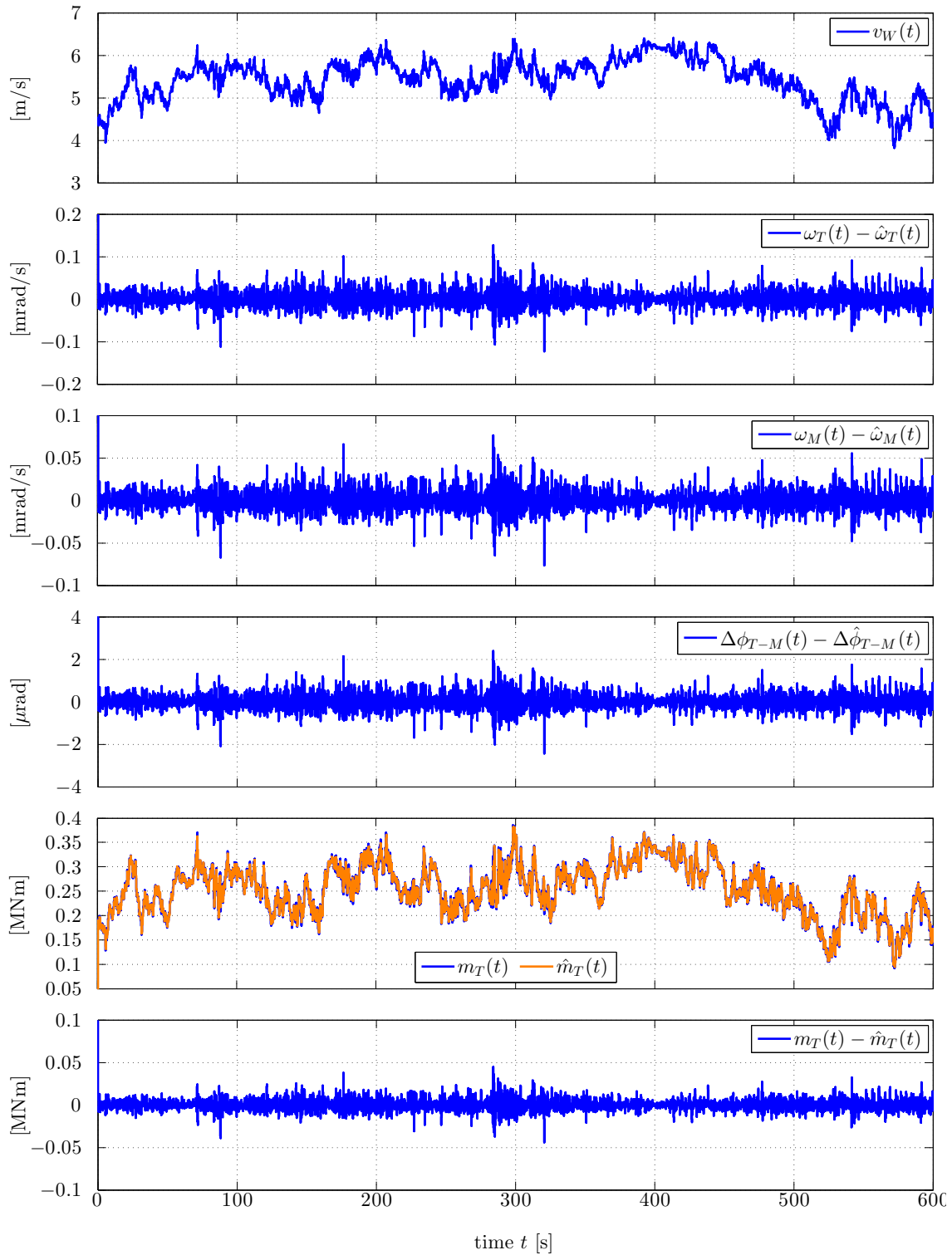


Figure 5.10: *Simulation results for the wind speed, the difference between the original system and the observed system for the rotational speeds and angle displacement, the original turbine's torque and the observed one and the difference between them in a wind turbine with a two-mass system with a wind profile input and a observer designed by LQR*

### 5.1.1.3 Comparison between disturbance observer design by pole place and by LQR with stability margin

It is shown in Fig. 5.11 the two observed responses for the original system's turbine's torque are shown, as well as the difference between them. The one labeled under  $m_{T_{PP}}$  refers to the one designed by pole placement and the one labeled under  $m_{T_{LQR}}$  refers to the one designed by LQR method with a stability margin.

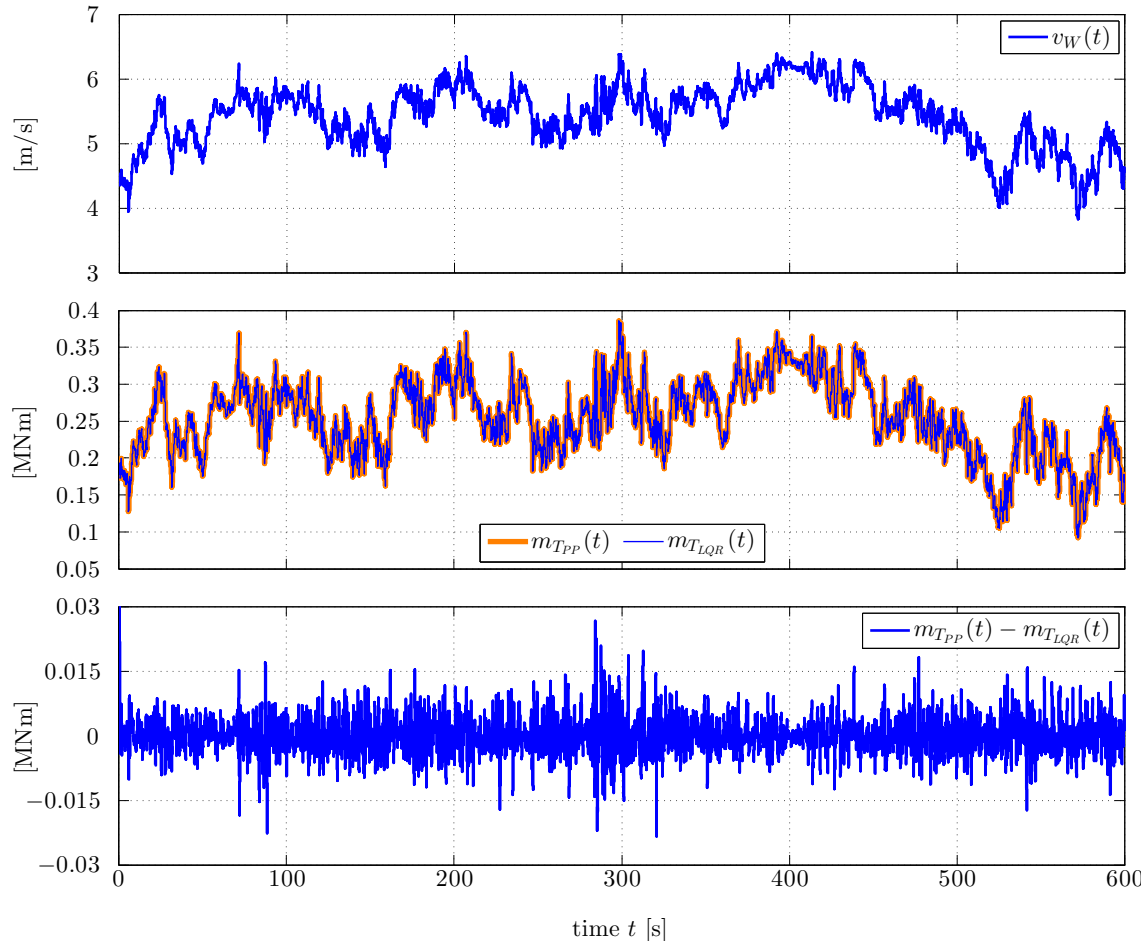


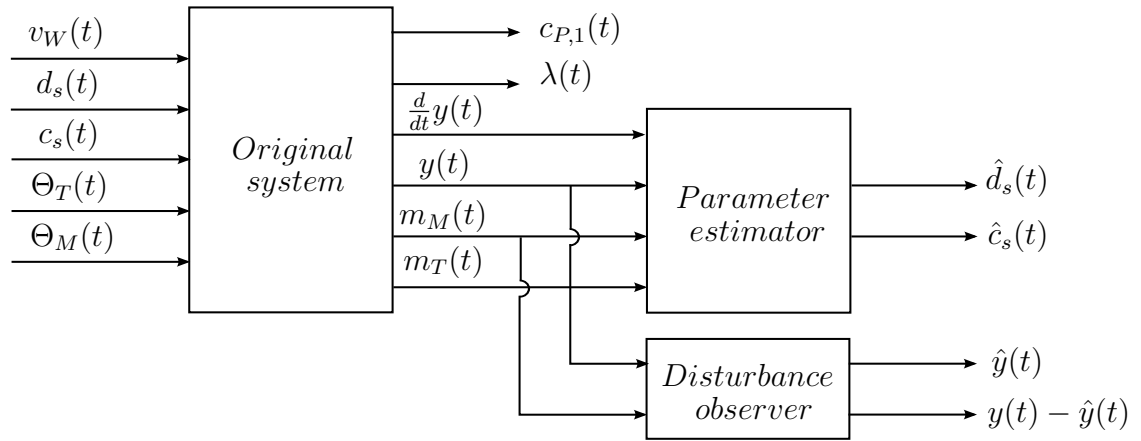
Figure 5.11: *Simulation results for the turbine's torque observer designed by pole placement and LQR method with a stability margin, and the difference between them*

## 5.2 Parameter estimation

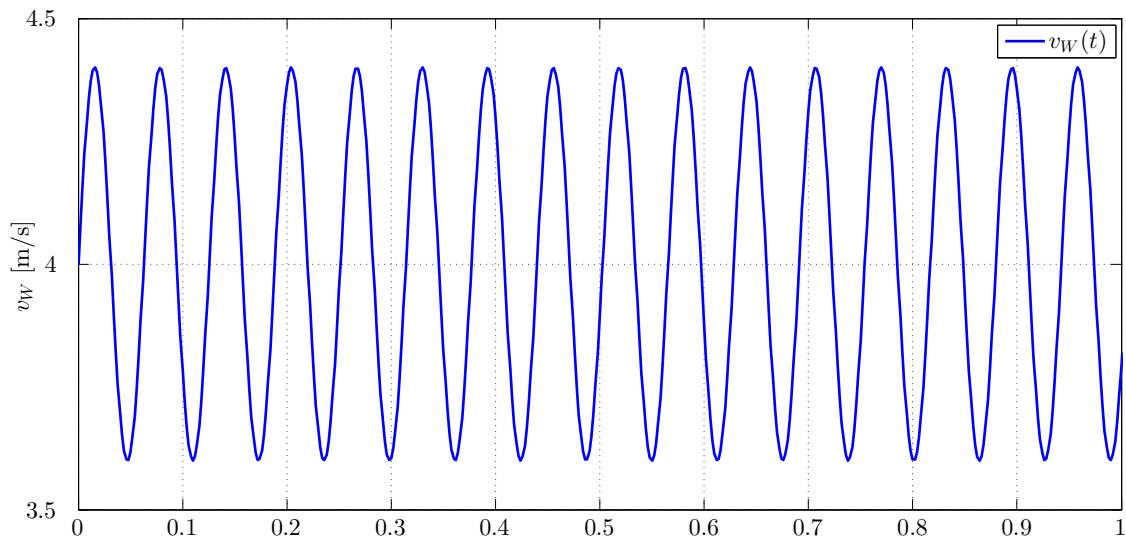
### 5.2.1 Simulation results

After the realization that besides both parameters are not observable in an static point of view, they are dynamically, the simulation is implemented using the equations (4.119), (4.128), (4.129) and (4.130).

The simulation diagram up to this point is shown in Fig. 5.12

Figure 5.12: *Simulation diagram for the parameter estimation*

For the results, there are two different input signals that were tested: a sinusoidal signal as the one shown in Fig. 4.8 and Fig. 5.13, and the wind profile that was used before for previous simulations (see Fig. 5.9).

Figure 5.13: *Sinusoidal input for the parameter estimation of the low-speed shaft damping  $d_s$  using a sinusoidal input*

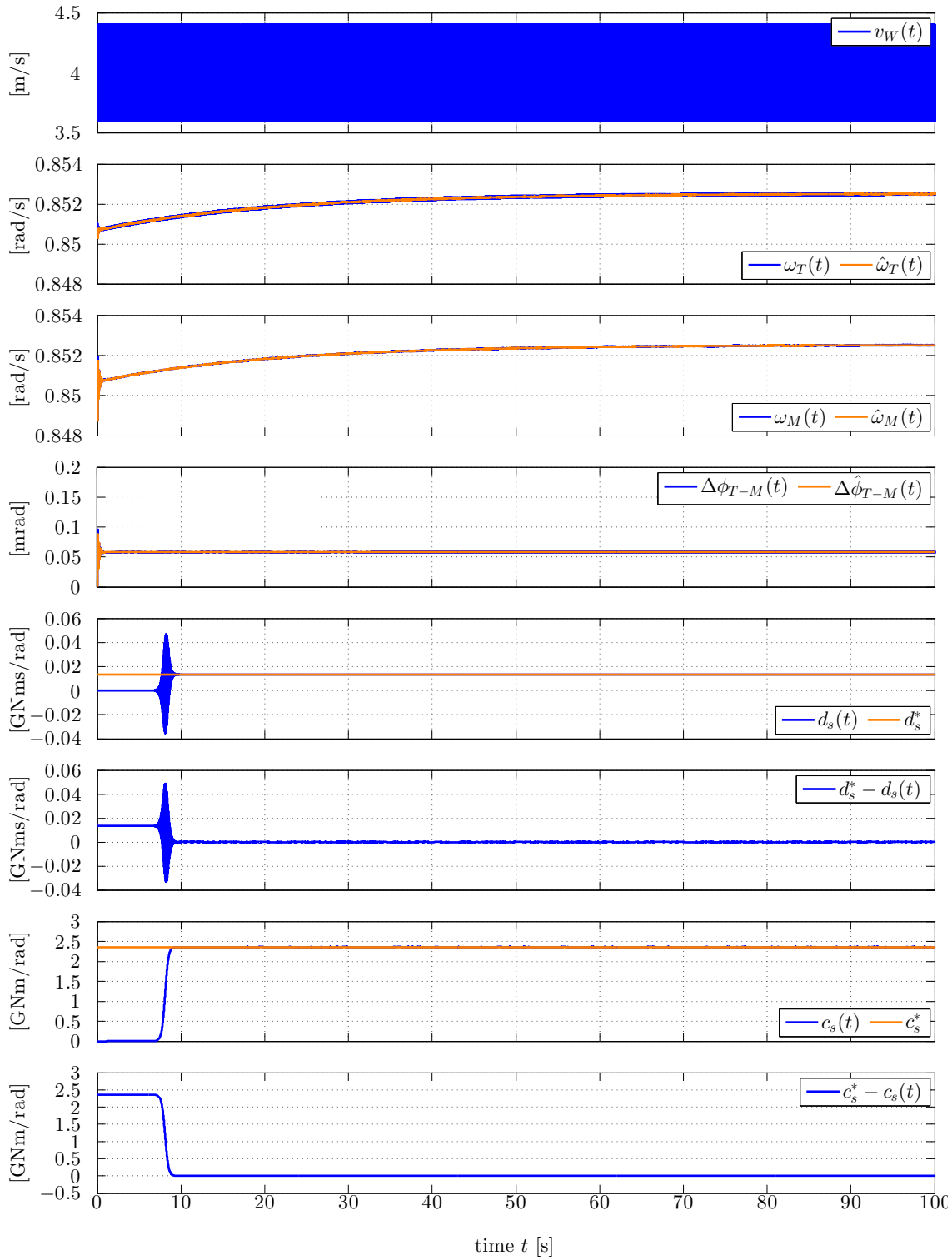


Figure 5.14: *Simulation results of the parameter estimation of the low-speed shaft damping  $d_s$  and the low-speed shaft stiffness  $c_s$  using a sinusoidal input*

## 5.2. PARAMETER ESTIMATION

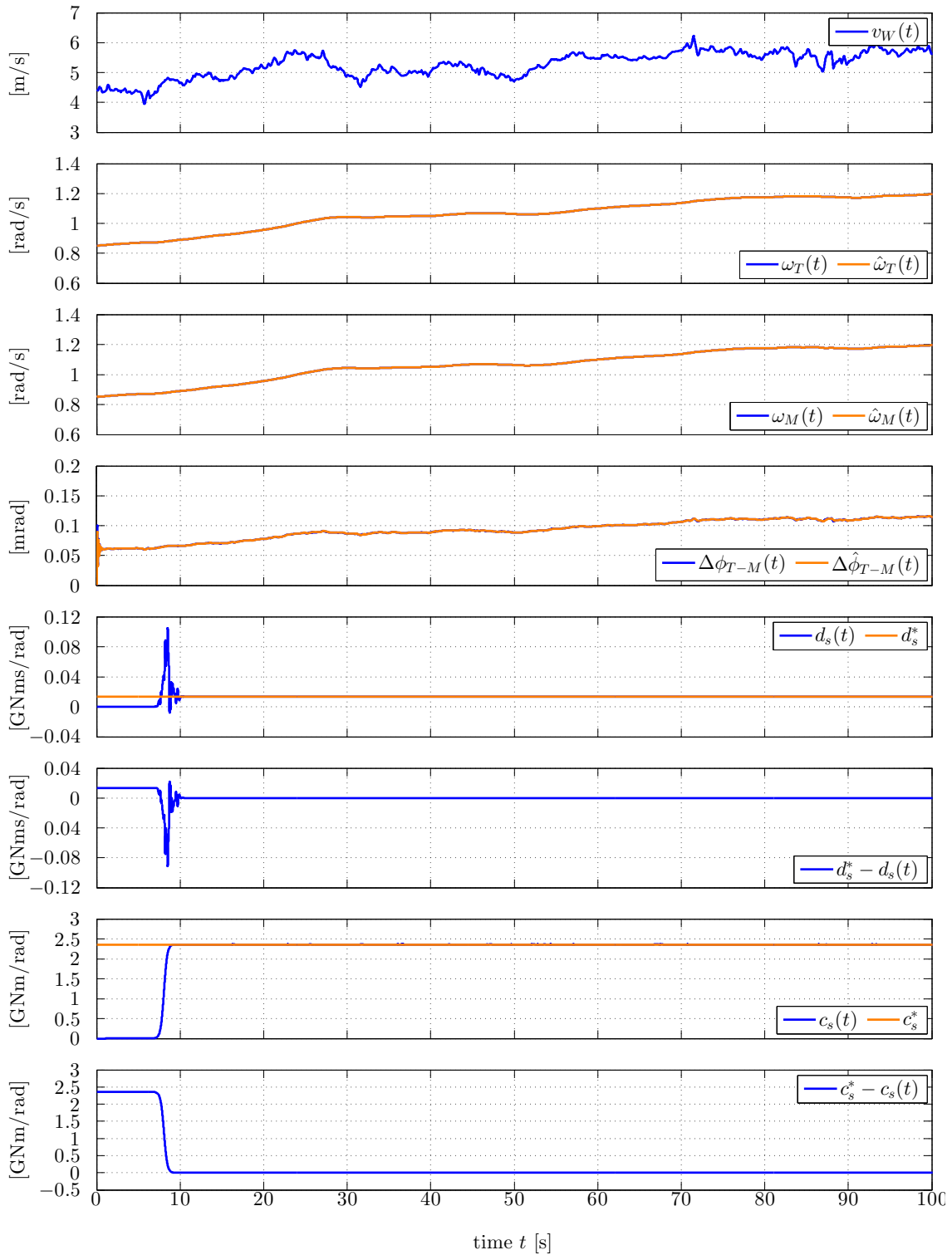


Figure 5.15: *Simulation results of the parameter estimation of the low-speed shaft damping  $d_s$  and the low-speed shaft stiffness  $c_s$  using a wind profile as input*

As for the graphs, in Fig. 5.13 it is shown initially the sinusoidal input in graph 1, followed by the three main states in graphs 2, 3 and 4. The turbine's rotational



speed is shown in graph 2, the machine's rotational speed in graph 3 and the angle displacement between the turbine and the machine in graph 4.

In graphs 5 and 6, the behavior of the low-speed shaft's damping is shown. Graph 5 shows the original low-speed shaft's damping value and the estimated one. There is a big fluctuation at the beginning of the simulation that is attributed to the forgetting factor of the RLS method used. With this method, it is given a specific weight to the previous measurement, lasting a few seconds reaching the expected value.

Graphs 7 and 8 show the behavior of the low-speed shaft's stiffness. In here there is more of a progressive reach to the expected value, also attributed to the forgetting factor.

It is stated that the results are more than satisfactory due to the achievement of the expected value in both cases.

Quite the same happens in Fig. 5.15 where the three main states are shown in graphs 2, 3 and 4. The wind profile is shown in graph 1 and the low-speed shaft's damping and stiffness behaviour is shown in graphs 5, 6, 7 and 8.

The big variation between the different input signals was shown in a reduction of the oscillation before the final value of the parameters were reached, but makes no difference in the final outcome.

There is not a really big difference between the methods, but deciding over the designing method itself. It is chosen to keep on working with the observer that was designed by LQR with a stability margin due to the amount of cancellations made for the pole placement method and because of the smaller error respecting the original system.

## 5.3 Detection of mechanical faults

Finally, after obtaining a system that is able to describe correctly the wind turbine dynamics and estimate the mechanical parameters of the low-speed shaft, it is possible to put the model up to some tests to see if with these two parameters, mechanical faults can be detected.

The tests that are going to be carried on are changes in the turbine and machine's inertia and changes to the values of the low-speed shaft damping and stiffness to see the effect on the overall behavior of the turbine and on the observer.

### 5.3.1 Changes on the turbine's inertia

Since the beginning of the simulations, the turbine inertia has been stated as  $8.6 \times 10^6 \text{ kg m}^2$ , so the simulation results for that inertia value can be checked in Figures: 5.9, 5.10 for the overall turbine's behavior with a wind profile.

The changes made to the turbine's inertia consisted of decreases and increases of the value itself as shown in the second graph of Fig. 5.16. The behavior of the overall turbine with the changes and a wind profile input are shown in Fig. 5.16, the behavior or response of the turbine's torque observer in Fig. 5.17. The parameter estimation of the low-speed shaft's damping and stiffness is also shown in Fig. 5.18.



5.3.1.1 Results

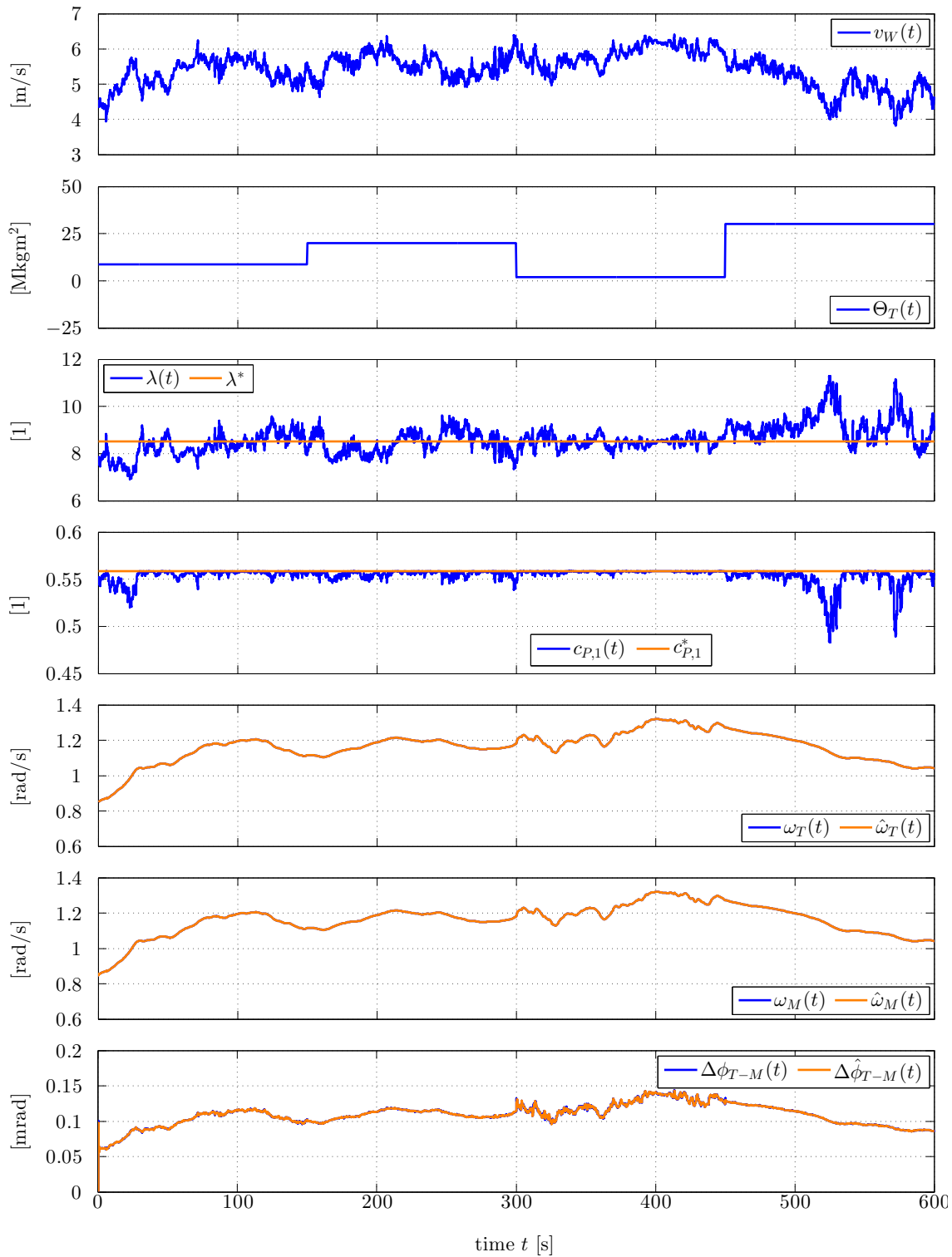


Figure 5.16: *Simulation results of wind speed, changing turbine’s inertia, tip speed ratio, power coefficient, and original system’s and observed system’s response for the rotational speeds and angle displacement in a wind turbine with a two-mass system*

### 5.3. DETECTION OF MECHANICAL FAULTS

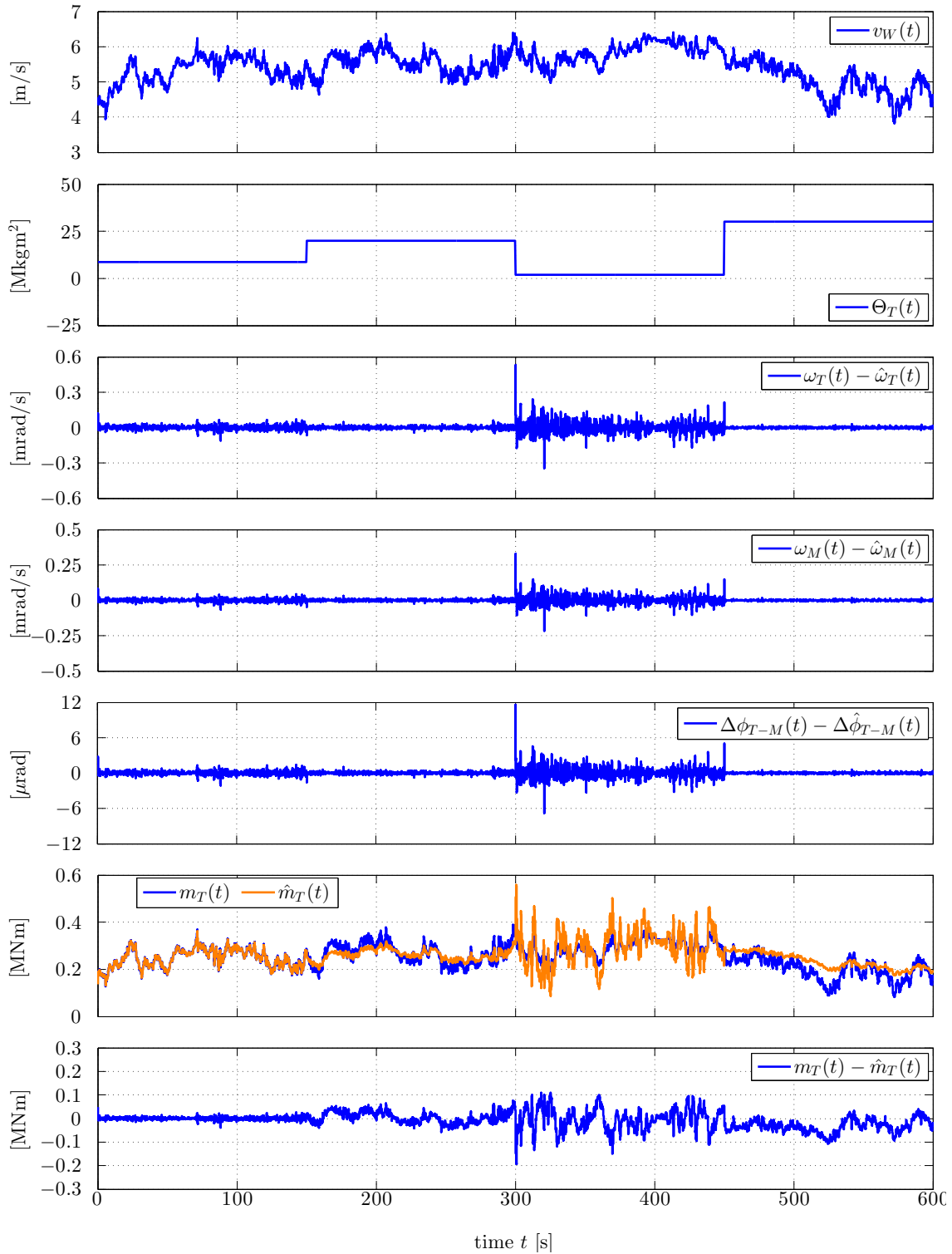


Figure 5.17: *Simulation results of wind speed, changing turbine's inertia, difference between the original system's and observed system's response for the rotational speeds and angle displacement, original and observed turbine's torque and the difference between them in a wind turbine with a two-mass system and changing turbine's inertia*

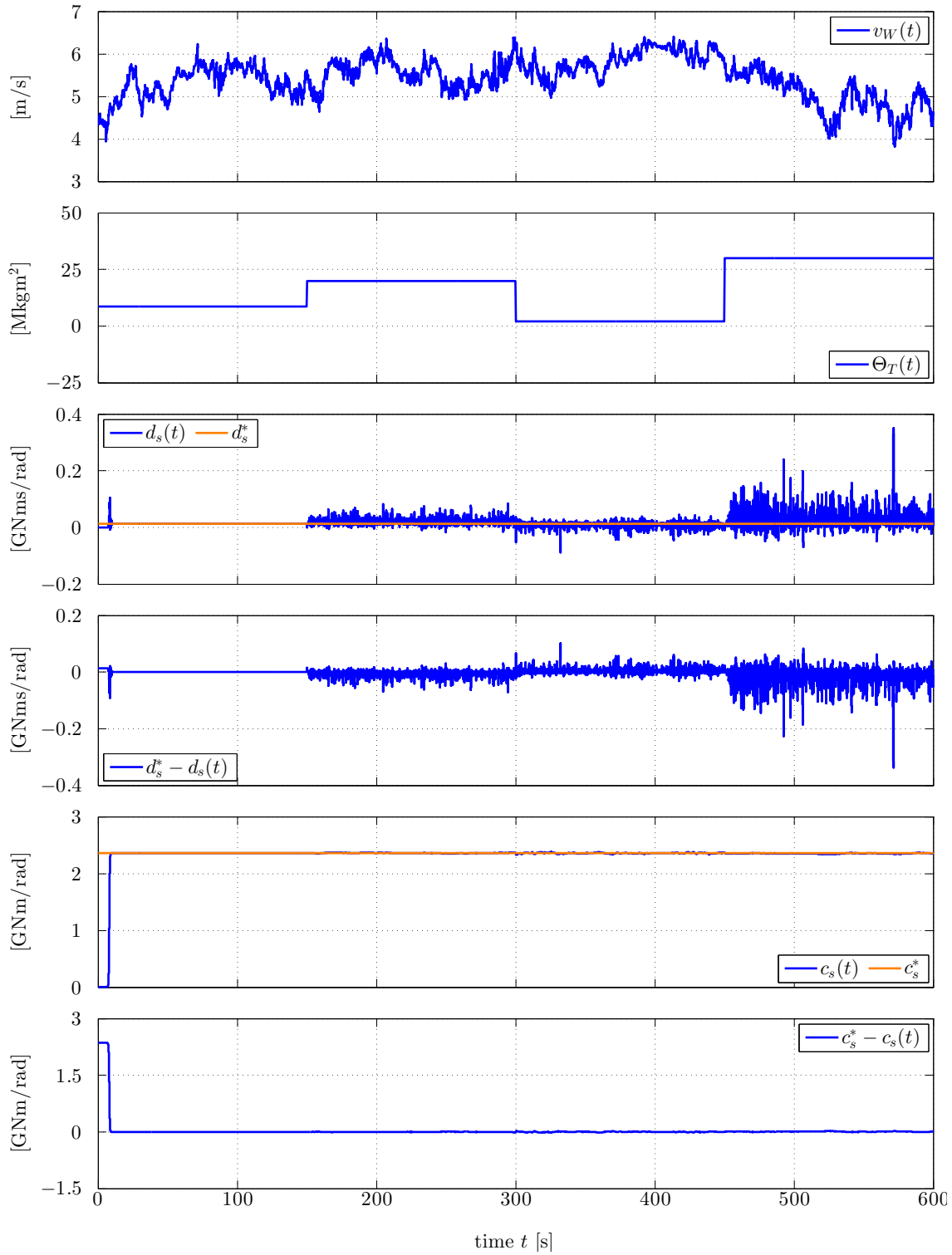


Figure 5.18: *Simulation results of wind speed, changing turbine's inertia and parameter estimation for the low speed shaft's damping and stiffness in a wind turbine with a two-mass system*

### 5.3.1.2 Discussion

From the turbine's inertia increases, it can be noted that with each increase the system becomes slower. This behavior can be noted by some aspects such as the decrease in the tip speed ratio  $\lambda$  of the turbine, as well as the decrease in the power coefficient.

It can also be shown with the progressive decrease of the values that the turbine's rotational speed  $\omega_T$  and machine's rotational speed  $\omega_M$  take. But the same expected behavior happens with the decreases, which can all be attributed to physics.

The turbine's torque observer that was designed seems to follow through even as the changes were made even though it sometimes follows very vaguely. It is noted that with each increase the turbine's torque becomes less fluctuating or more stable. And when the turbine's inertia decreases, even a little bit, it fluctuates much more. This behavior actually gives up a hint for fault detection, showing that with big turbine's torque fluctuations something is not right with the turbine's inertia.

The parameter estimation of the low-speed shaft's stiffness was carried on in a very robust way, where the only fluctuations are shown in the very beginning of the simulation. Showing that the parameter estimation method converges very fast to the expected value.

For the parameter estimation of the low-speed shaft's damping, with every increase in the turbine's inertia, the estimation became more erratic. Even with the small decrease, it starts fluctuating a lot, showing big disturbances in the expected value. This gives up another hint and actually showing how susceptible the low-speed shaft's damping is to changes in the turbine's inertia.

From the results, the traceable hints for the detection of mechanical faults would be the detection of big errors in the estimation of the low speed shaft's damping and the big fluctuations in the turbine's torque measurements.

Nevertheless, in reality the errors are unknown, so errors are not good parameters to look at for detectability of a fault.

## 5.3.2 Changes on the machine's inertia

The machine's inertia has been stated as  $1.3 \times 10^6 \text{ kg m}^2$  since the beginning, so the simulation results for that inertia value can be checked in Figures: 5.9, 5.10 for the overall turbine's behavior with a wind profile.

The changes made to the machine's inertia consisted of increases and decreases of the value itself as shown in the second graph of Fig. 5.19. The behavior of the overall turbine with a wind profile and the changes made are shown in Fig. 5.19 and the behavior or response of the turbine's torque observer in Fig. 5.20. The parameter estimation of the low-speed shaft's damping and stiffness is also shown in Fig. 5.21.



5.3.2.1 Results

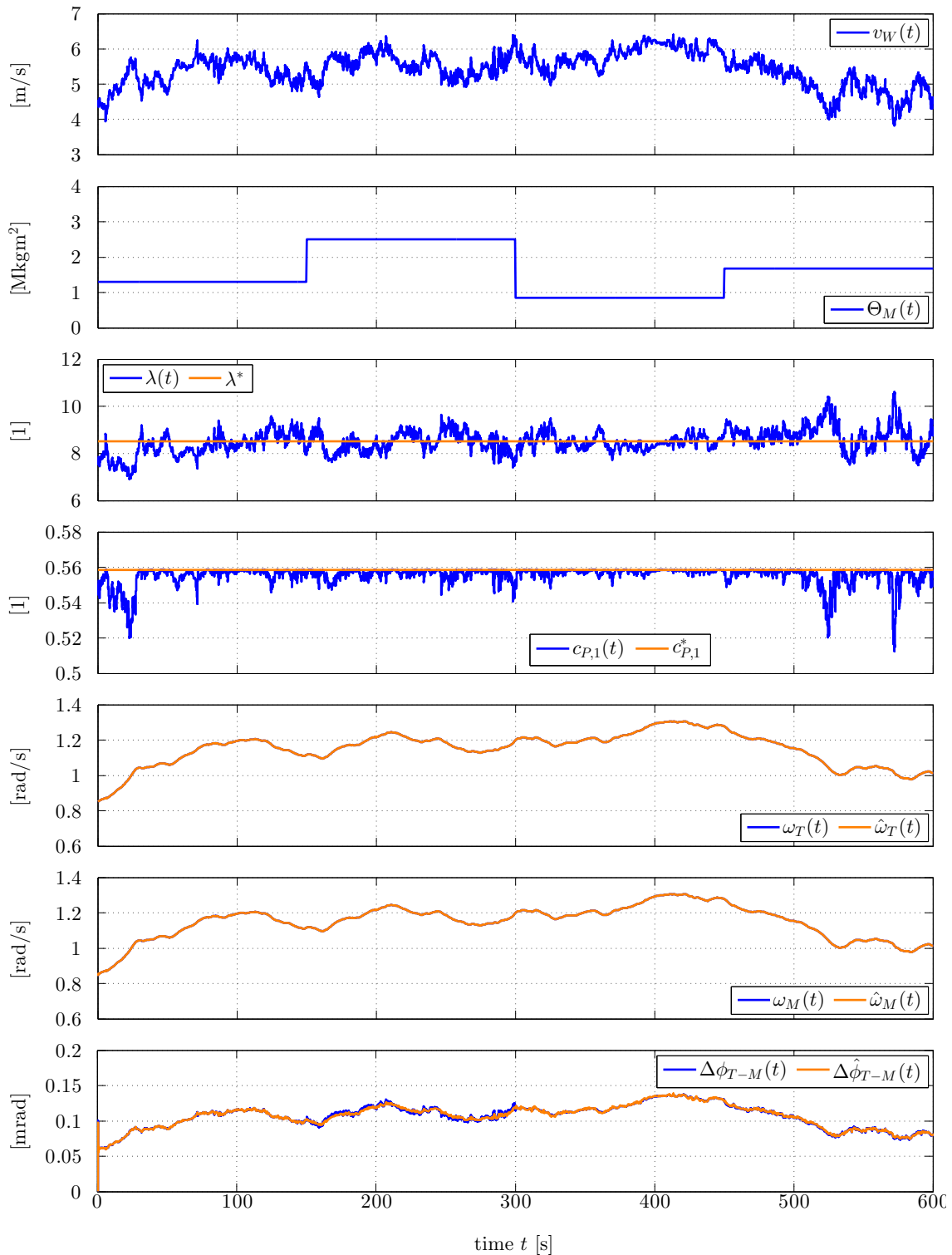


Figure 5.19: *Simulation results of wind speed, changing machine's inertia, tip speed ratio, power coefficient, and original system's and observed system's response for the rotational speeds and angle displacement in a wind turbine with a two-mass system*



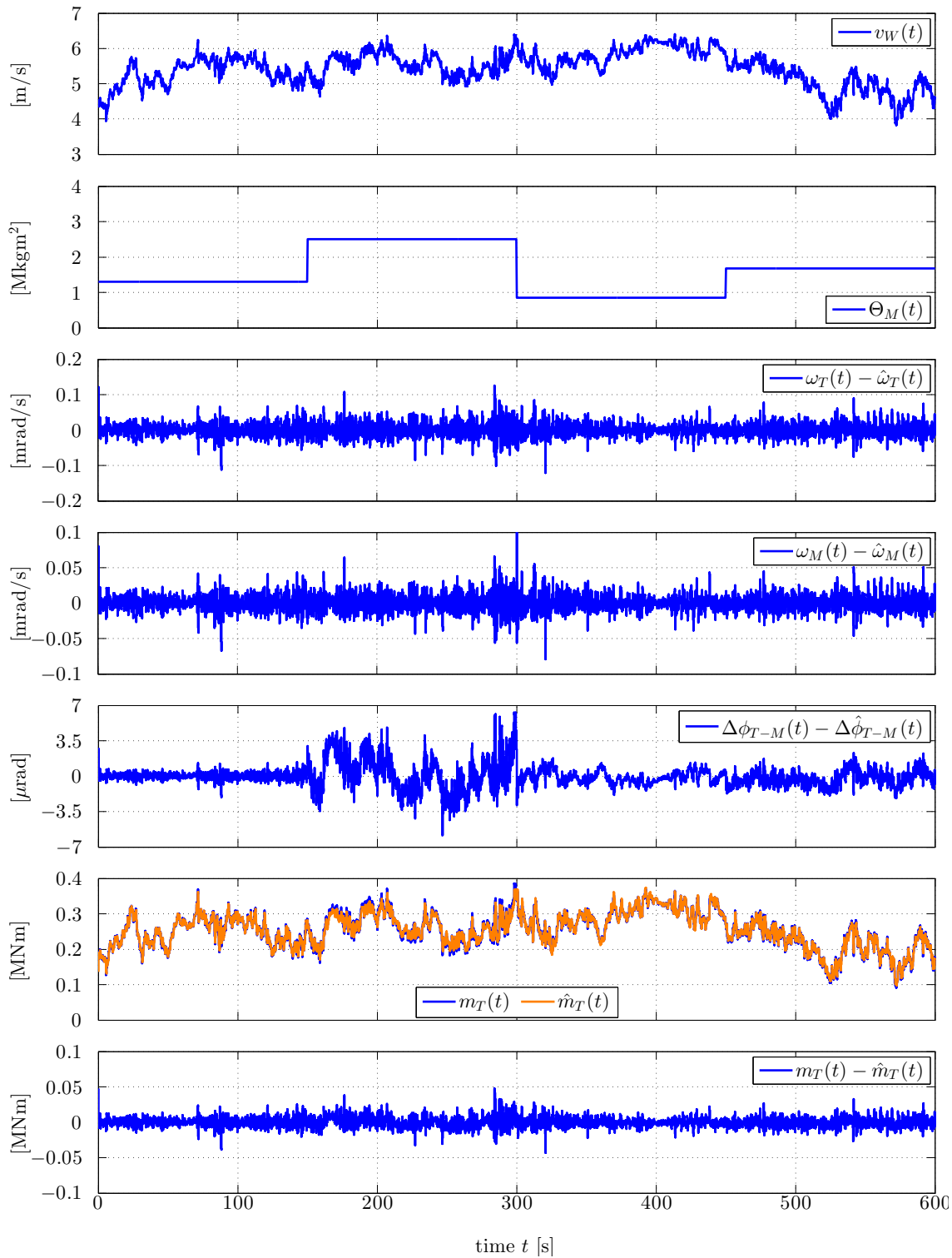


Figure 5.20: *Simulation results of wind speed, changing machine's inertia, difference between the original system's and observed system's response for the rotational speeds and angle displacement, original and observed turbine's torque and the difference between them in a wind turbine with a two-mass system*

### 5.3. DETECTION OF MECHANICAL FAULTS

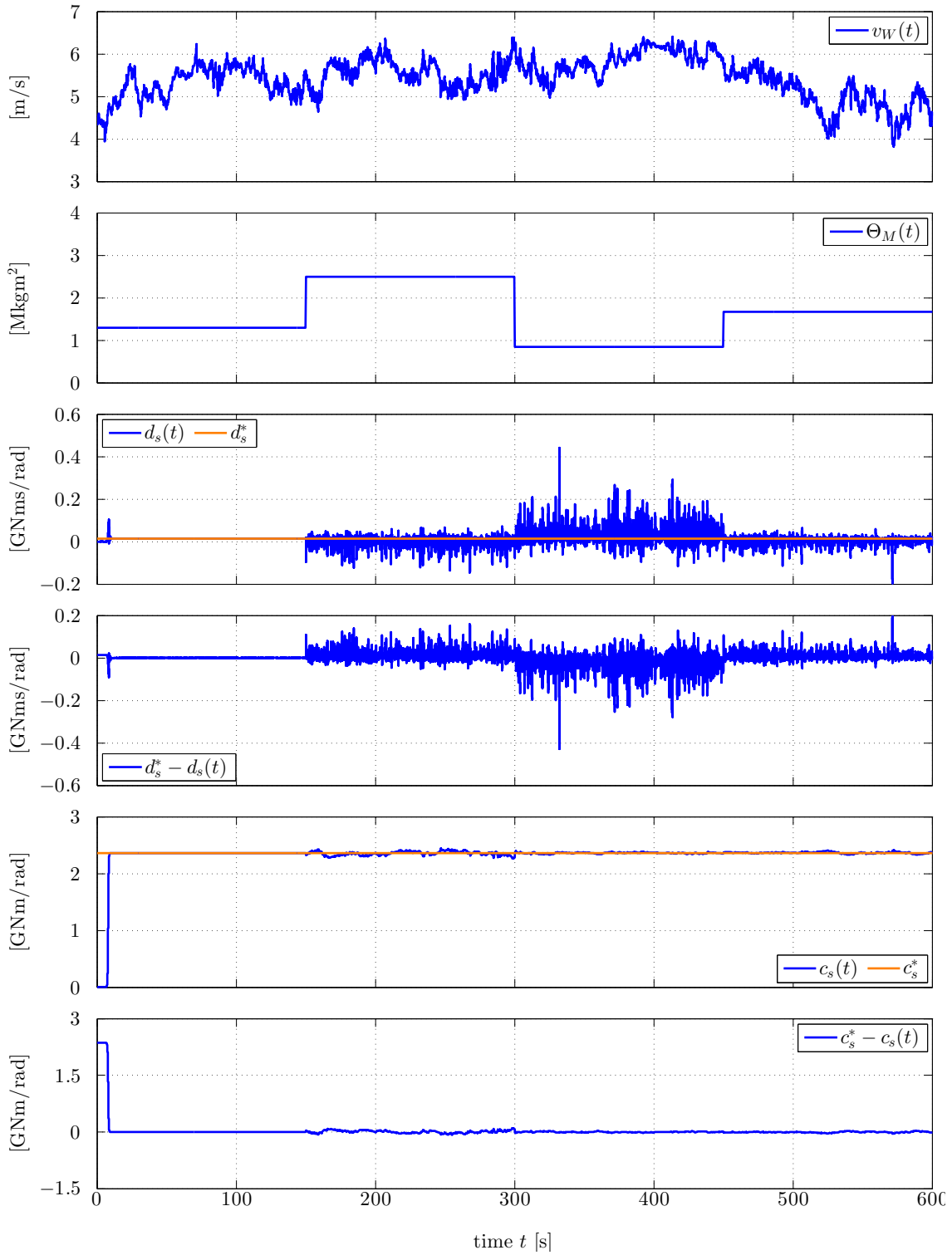


Figure 5.21: *Simulation results of wind speed, changing machine's inertia and parameter estimation for the low speed shaft's damping and stiffness in a wind turbine with a two-mass system*

### 5.3.2.2 Discussion

From the machine's inertia increases, it can be noted that with each increase the system becomes slower and that the angle displacement in between the turbine's rotational speed  $\omega_T$  and machine's rotational speed  $\omega_M$  actually becomes more unstable, fluctuating more than in other cases. But these changes can be given to physics.

The turbine's torque observer that was designed seems to work as if no change was made, showing that the observer actually follows through with the turbine's dynamics still in a stable and robust way.

The parameter estimation of the low-speed shaft's stiffness is also carried on in a very robust way, where some fluctuations are shown with the changes but around the expected value. For the estimation of the low-speed shaft's damping, big fluctuations happen through the increases and even decreases of the value itself.

In this case, it shows that as the machine's inertia increases, so the fluctuation at the beginning of the low-speed shaft's damping estimation does. And a more stable low-speed shaft's stiffness estimation.

From the changes to the machine's inertia the only possible hint on how to detect mechanical faults using the estimation of the low-speed shaft's parameters is alerting over big changes in the low speed shaft's damping estimation. Even though, the machine's inertia is not likely to change in such ways, denoting that there are no useful hints on how to detect mechanical faults with this experiment.

### 5.3.3 Changes on the low-speed shaft's damping

The low-speed shaft's damping has been stated as  $1.35 \times 10^7 \frac{\text{Nms}}{\text{rad}}$  since the beginning, so the simulation results can be checked for the overall turbine behavior with a wind profile in Figures: 5.9, 5.10.

The changes made to the low-speed shaft's damping are increases and decreases on the value, as shown in graph 2 of Fig. 5.22. For one quarter of the simulation the low-speed shaft's damping has its original value, for the next quarter it is increased then decreased and finally, increased again. Each of the changes happened for one quarter of the simulation time. So the behavior of the turbine with a wind profile and the observer is going to be shown in each of the cases, as well as the parameter estimation for those variations.



## 5.3.3.1 Results

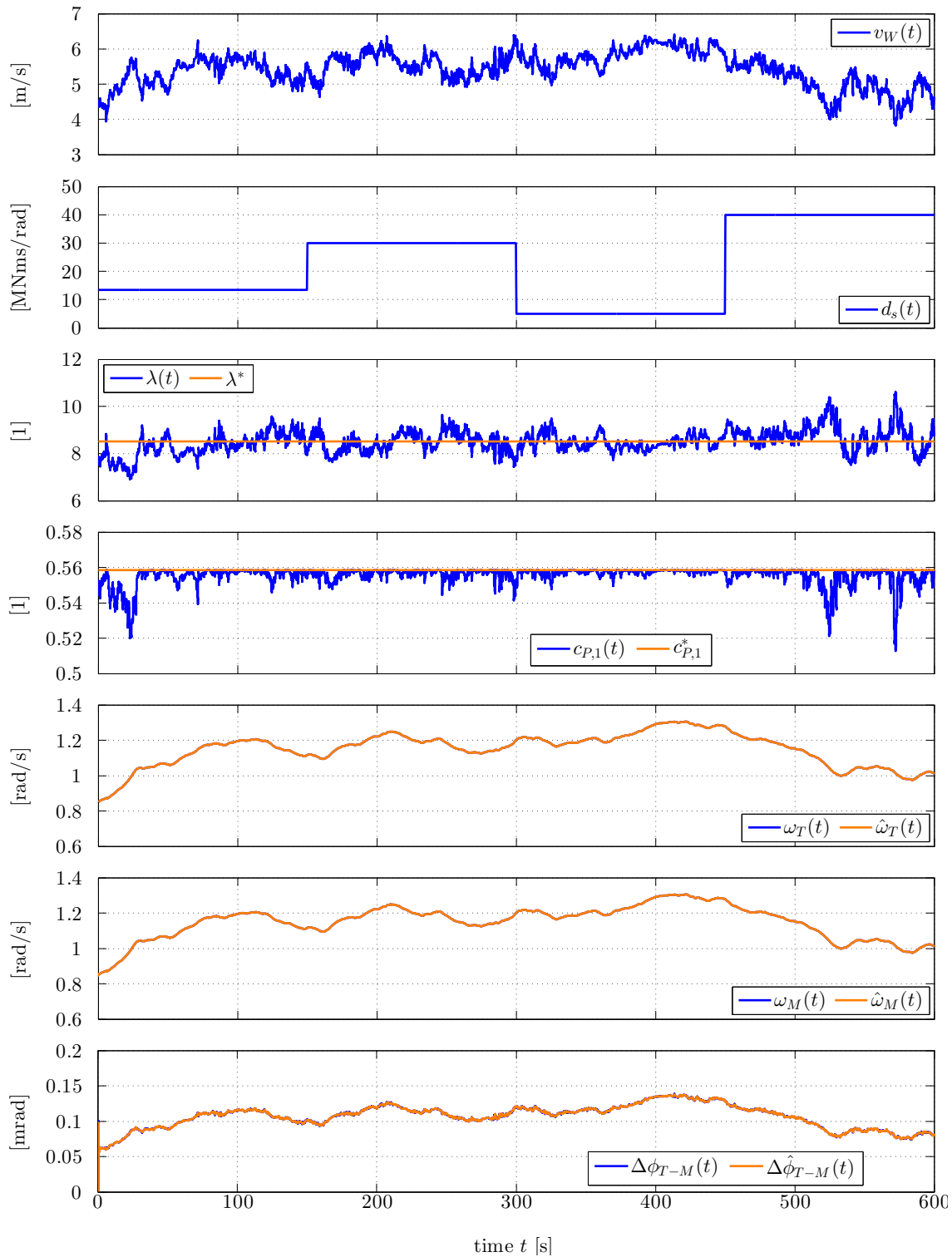


Figure 5.22: Simulation results of wind speed, changing low-speed shaft's damping, tip speed ratio, power coefficient, and original system's and observed system's response for the rotational speeds and angle displacement in a wind turbine with a two-mass system

### 5.3. DETECTION OF MECHANICAL FAULTS

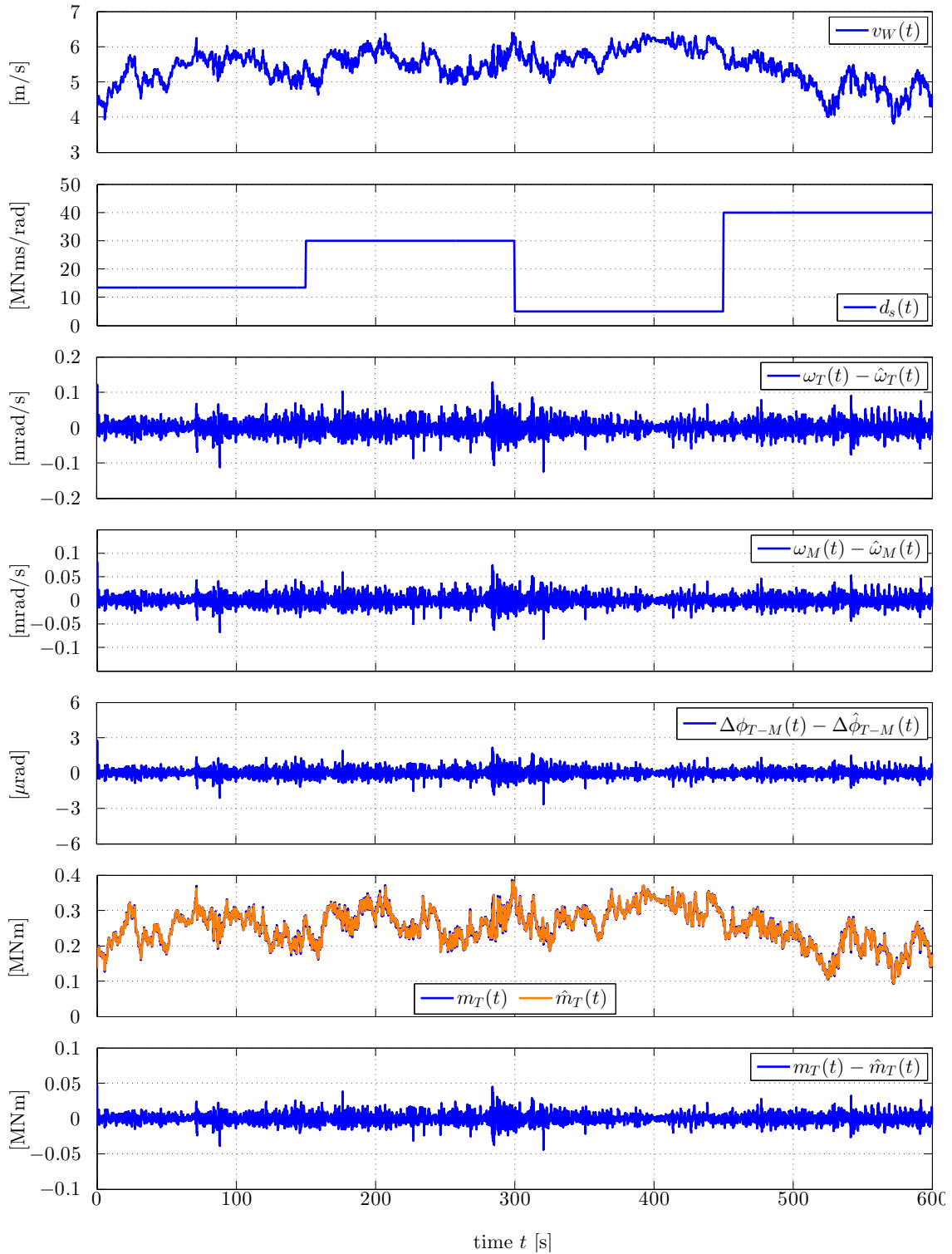


Figure 5.23: *Simulation results of wind speed, changing low-speed shaft's damping, difference between the original system's and observed system's response for the rotational speeds and angle displacement, original and observed turbine's torque and the difference between them in a wind turbine with a two-mass system*

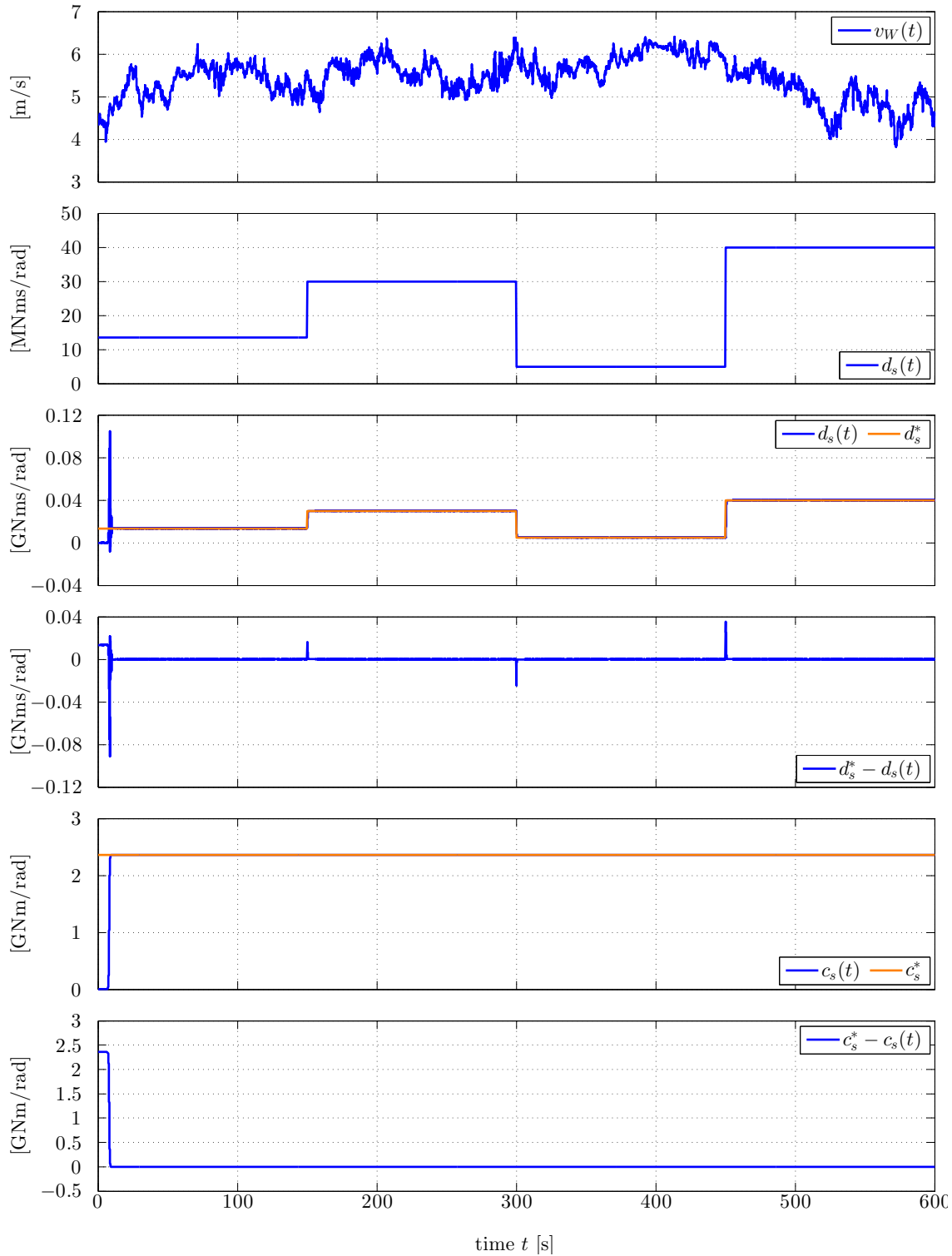


Figure 5.24: *Simulation results of wind speed, changing low-speed shaft's damping and parameter estimation for the low speed shaft's damping and stiffness in a wind turbine with a two-mass system*

### 5.3.3.2 Discussion

From the changes to the low-speed shaft's damping, it can be noted that it has almost no traceable effect on the value of the tip speed ratio and power coefficient. As well as in the turbine's rotational speed, machine's rotational speed nor angle displacement.

But as it is shown in the Fig. 5.23, the increases in the low-speed shaft's damping actually increases the difference in between the original system and the observed one for the machine's rotational speed.

The designed observer for the turbine's torque is able to follow through the changes, even though it is noted a small increase in the error between the original system and the observed one.

The parameter estimation is once more very stable and converges to the expected values. For the low-speed shaft's damping, in Fig. 5.24 is noted a small fluctuating when a change in the low-speed shaft's damping is made and right at the beginning of the simulation when the iterations are being made.

As for the low-speed shaft's stiffness estimation, the value converges to the known value as fast as in the other cases.

In this case, there is an explicit and very precise way of detecting faults in the wind turbine by tracking the changes in the low speed shaft's damping. This due the simulation and estimation actually follows through the changes made as shown in graph 3 of Fig. 5.24.

## 5.4 Changes on the low-speed shaft's stiffness

The low-speed shaft's stiffness, from the beginning, was stated as  $2.36 \times 10^9 \frac{\text{Nm}}{\text{rad}}$  since the beginning, so the simulation results can be checked for the overall turbine behavior with a wind profile in Figures: 5.9, 5.10.

The changes made to the low-speed shaft's stiffness are one increase and one decrease. For two quarters of the simulation the low-speed shaft's stiffness has its original value, at the beginning and at the end. For the in between quarters it is initially increased and then decreased. So the behavior of the turbine with a wind profile and the observer is going to be shown in each of the cases, as well as the parameter estimation for those variations.





5.4.0.1 Results

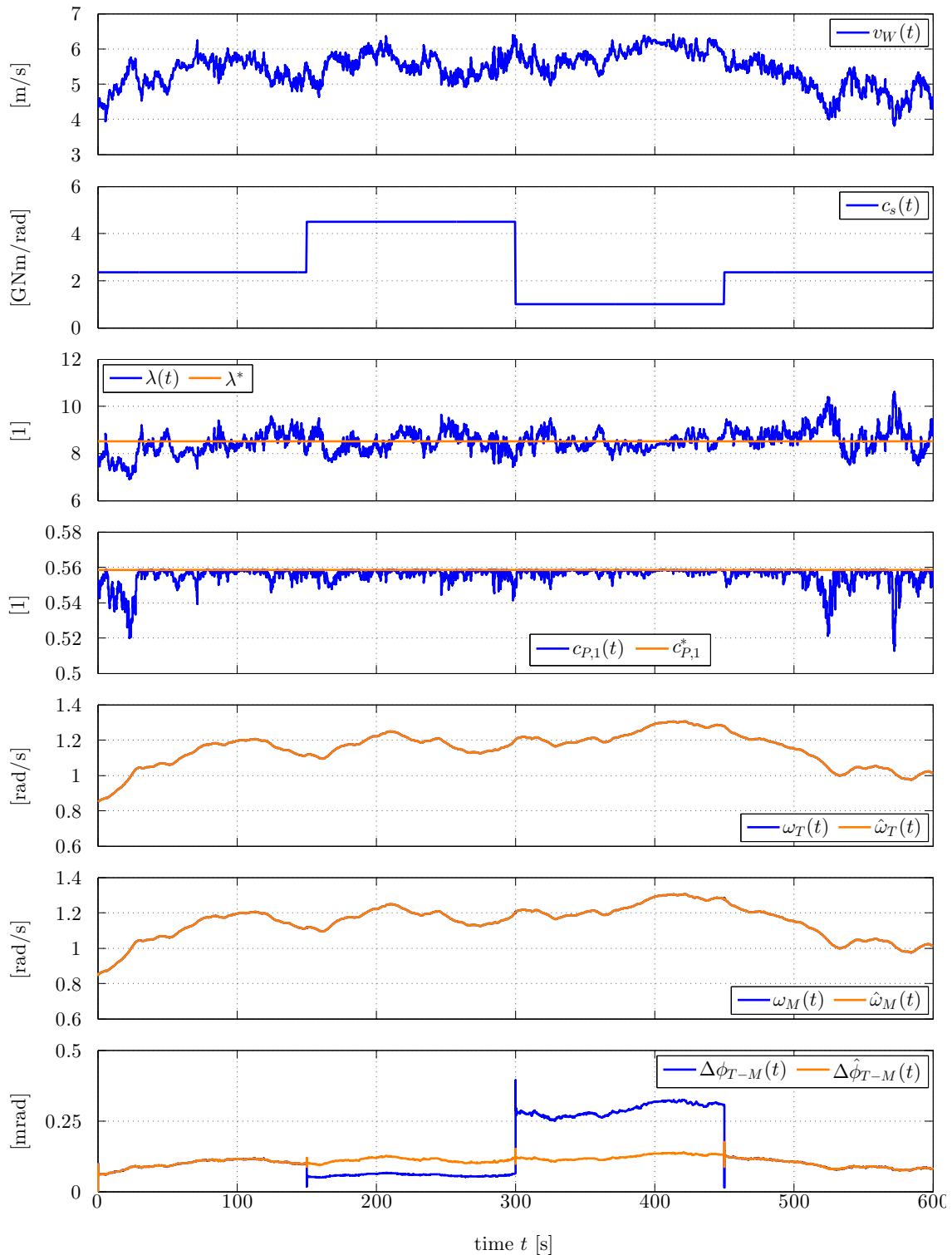


Figure 5.25: Simulation results of wind speed, changing low-speed shaft's stiffness, tip speed ratio, power coefficient, and original system's and observed system's response for the rotational speeds and angle displacement in a wind turbine with a two-mass system

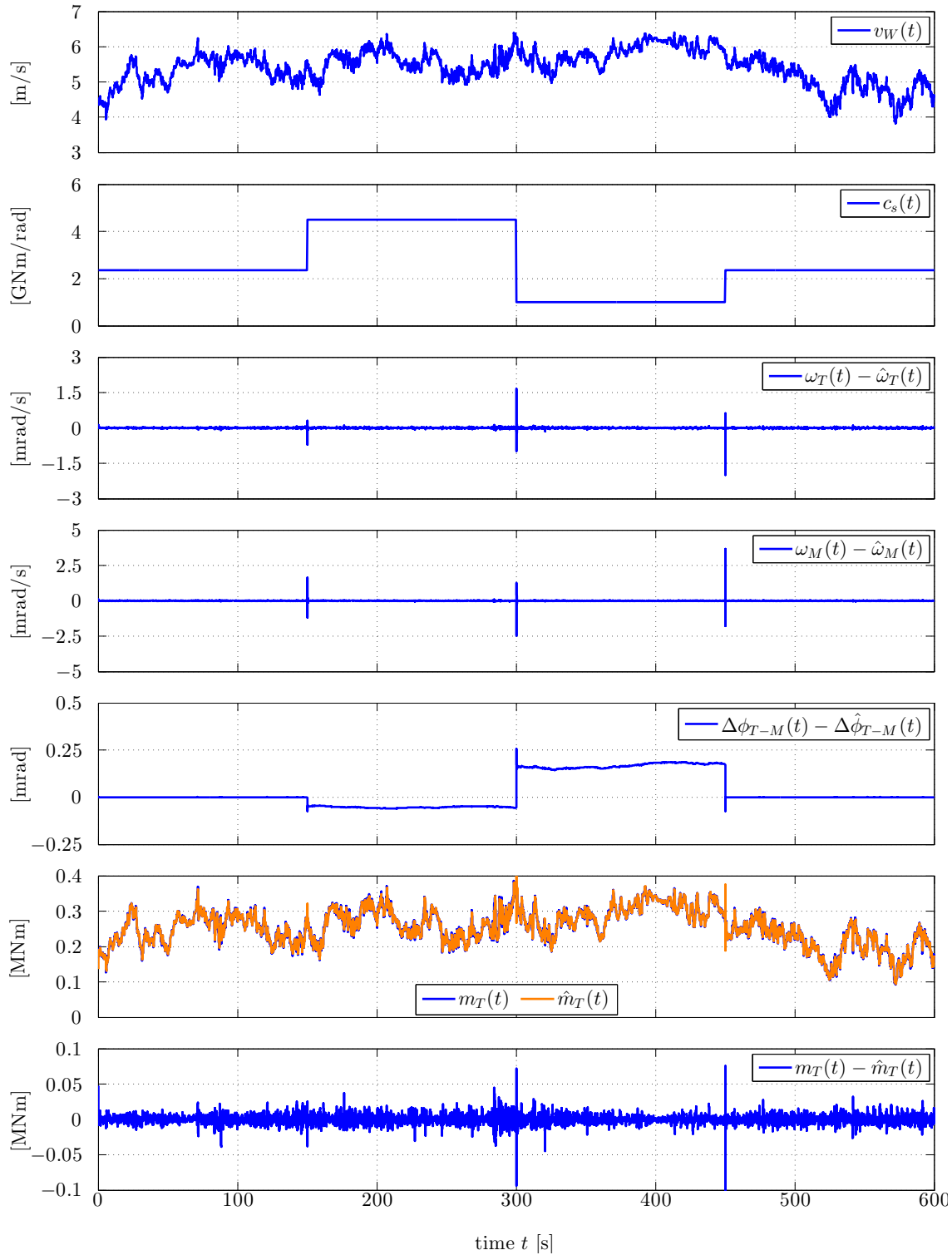


Figure 5.26: Simulation results of wind speed, changing low-speed shaft's stiffness, difference between the original system's and observed system's response for the rotational speeds and angle displacement, original and observed turbine's torque and the difference between them in a wind turbine with a two-mass system

## 5.4. CHANGES ON THE LOW-SPEED SHAFT'S STIFFNESS

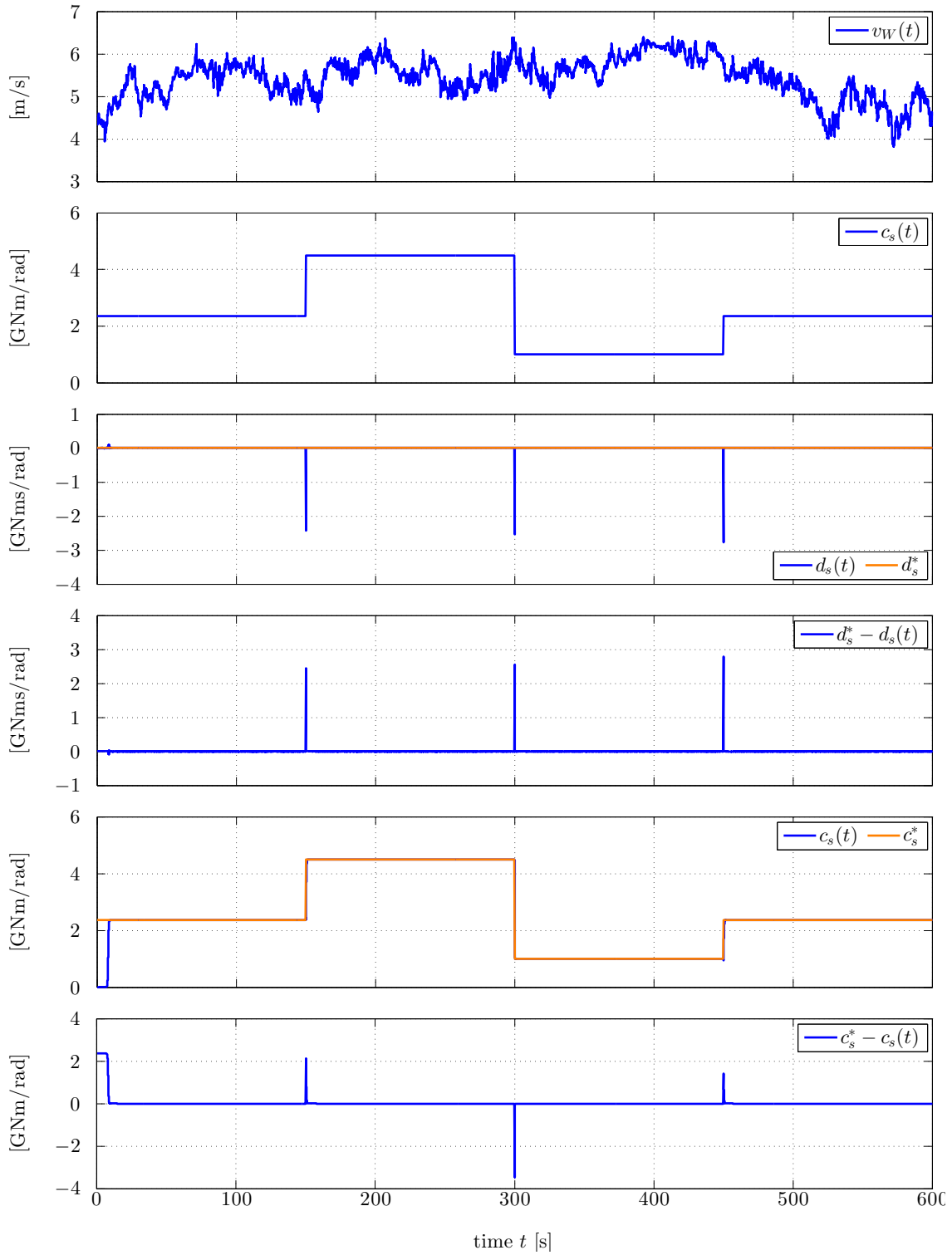


Figure 5.27: *Simulation results of wind speed, changing low-speed shaft's stiffness and parameter estimation for the low speed shaft's damping and stiffness in a wind turbine with a two-mass system*

### 5.4.0.2 Discussion

Analyzing the changes to the low-speed shaft's stiffness, it can be noted that it has almost no traceable effect on the value of the tip speed ratio and power coefficient, as well as in the changes for the low-speed shaft's damping.

In this case, there are no big changes in between the turbine's rotational speed and the machine's rotational speed. Although, it is clearly shown in Fig. 5.25 that every time the low-speed shaft's stiffness is increased, the angle displacement in between rotational speeds is decreased. It could easily be given to the fact that if the shaft is stiffer, it will be harder to bend it since it becomes less flexible.

The designed observer for the turbine's torque is able to follow through the changes as in all the other changes, even though it is noted a small increase in the error between the original system and the observed one just as in the dynamic changes to the low-speed shaft's damping.

The parameter estimation is once more very stable and converges to the expected values. For the low-speed shaft's damping, in Fig. 5.27 is noted a big fluctuation when a change in the low-speed shaft's stiffness happens, but ends up converging to the expected low speed shaft's damping value.

As for the low-speed shaft's stiffness estimation, the value converges to the known value as fast as in the other cases, showing variations every time the low-speed shaft's stiffness is changed, but it actually converges to the expected values.

As well as before, with this experiment there are very explicit and precise hints for the detection of mechanical faults. First of all, there is the explicit effect of increasing and decreasing the low-speed shaft's stiffness in the angle displacement. And the precise way the estimator tracks the changes made to the low-speed shaft's stiffness gives another method of detecting mechanical faults that explicitly affect those parameters.

## 5.4.1 Summary of the experiment results

The table 5.3 shows the summary of the effect that the main experiment has on the three main states, turbine's torque, low speed shaft's damping and low speed shaft's stiffness

#### 5.4. CHANGES ON THE LOW-SPEED SHAFT'S STIFFNESS

---

Table 5.3: *Summary of the experiment results for detection of mechanical faults in wind turbines*

	$\omega_T(t)$	$\omega_M(t)$	$\Delta\phi_{T-M}(t)$	$m_T(t)$	$\hat{d}_s(t)$	$\hat{c}_s(t)$
Turbine's inertia	<b>X</b>	<b>X</b>	<b>X</b>	<b>X</b>	<b>X</b>	-
Machine's inertia	-	-	-	-	<b>X</b>	<b>X</b>
Low speed shaft's damping	-	-	-	-	<b>X</b>	-
Low speed shaft's stiffness	-	-	<b>X</b>	-	-	<b>X</b>



# Chapter 6

## Conclutions and recomendations

### 6.1 Conclutions

- The mathematical modeling of a wind turbine with a one mass system and a two mass system were proposed.
- The speed control implemented for the wind turbine worked as expected for the one mass and two mass system's models.
- The observer designed by the LQR method with an stability margin was chosen due to its confiability towards the original turbine's torque.
- The turbine's torque observer followed through all the changes made to the original turbine's torque with an error smaller than 10 percent.
- The observability issue was solved by the use of the alternative method of the RLS with a sinusoidal input.
- Changes in the turbine's inertia had the most detectable changes on the turbine's torque observer.
- Disturbances in the low speed shaft's mechanical constants are trackable for fault detection.

### 6.2 Recomendations

- A different wind profile, with greater changes, to set the wind turbine model under a more difficult simulation environment could be used to check the effects on the results.
- A turbine's inertia observer should be designed and tried for the same matter of the turbine's torque designed in this thesis.
- A more sensitive method for the sensing of the wind speed and turbine's torque should be found and opens up the research and development chances.



- The observability issue might be solved in an alternative way by implementing a new two mass system model with less assumptions and neglections.

# Bibliography

- [1] SUPPORT FOR THE DEVELOPMENT OF RENEWABLE ENERGY IN VIET NAM: The Structure of a Modern Wind Turbine. An Overview. 2009. – Forschungsbericht
- [2] ABDELRAHEM, M. ; HACKL, C. ; KENNEL, R. : Application of extended Kalman filter to parameter estimation of doubly-fed induction generators in variable-speed wind turbine systems. In: *Clean Electrical Power (ICCEP), 2015 International Conference on IEEE*, 2015, S. 226–233
- [3] AHMED, W. K.: Mechanical Modeling of Wind Turbine Comparative Study. In: *International Journal of Renewable Energy Research (IJRER)* 3 (2013), Nr. 1, S. 94–97
- [4] ASIF, M. ; MUNEER, T. : Energy supply, its demand and security issues for developed and emerging economies. In: *Renewable and Sustainable Energy Reviews* 11 (2007), Nr. 7, S. 1388–1413
- [5] BINDICHEN.CO.UK: *Introduction to Wind Turbine*. <http://www.bindichen.co.uk/post/Wind%20Turbine/Introduction%20to%20Wind%20Turbine.html>. Version: November 2012. – Visited on 14.04.2016
- [6] BOLOGNANI, S. ; TUBIANA, L. ; ZIGLIOTTO, M. : Extended Kalman filter tuning in sensorless PMSM drives. In: *IEEE Transactions on Industry Applications* 39 (2003), Nr. 6, S. 1741–1747
- [7] BOUKHEZZAR, B. ; SIGUERDIDJANE, H. : Nonlinear control of a variable-speed wind turbine using a two-mass model. In: *Energy Conversion, IEEE Transactions on* 26 (2011), Nr. 1, S. 149–162
- [8] BURTON, T. ; SHARPE, D. ; JENKINS, N. ; BOSSANYI, E. : *Wind energy handbook*. John Wiley & Sons, 2001
- [9] CERDAS, R. : *Modelado de Sistemas*. 2013. – System analysis and simulation class material
- [10] DIRSCHERL, C. ; HACKL, C. ; SCHECHNER, K. : Explicit model predictive control with disturbance observer for grid-connected voltage source power converters. In: *Industrial Technology (ICIT), 2015 IEEE International Conference on IEEE*, 2015, S. 999–1006

- [11] DIRSCHERL, C. ; FESSLER, J. ; HACKL, C. M. ; IPACH, H. : State-feedback controller and observer design for grid-connected voltage source power converters with LCL-filter. In: *2015 IEEE Conference on Control Applications (CCA)* IEEE, 2015, S. 215–222
- [12] DIRSCHERL, C. ; HACKL, C. : Dynamic power flow in wind turbine systems with doubly-fed induction generator, 2016
- [13] *Kapitel Modellierung und Regelung von modernen Windkraftanlagen: Eine Einführung.* In: DIRSCHERL, C. ; HACKL, C. ; SCHECHNER, K. : *Elektrische Antriebe – Regelung von Antriebssystemen.* Springer-Verlag, 2014 (to be published in the 4. edition)
- [14] DORF, R. C. ; BISHOP, R. H.: *Modern control systems.* 12. Pearson (Addison-Wesley), 2011
- [15] ENERGY, A. : *Wind energy as Renewable Energy, pros and cons of Wind Energy.* <http://www.altenergy.org/renewables/wind/>. – Visited on 20.09.2016
- [16] ENERGY EFFICIENCY & RENEWABLE ENERGY, O. of: *How do wind turbines work?* <http://energy.gov/eere/wind/how-do-wind-turbines-work>. Version: 2014. – Visited on 2016.04.28
- [17] ENGINEERING, M.-H. C. E.: *Sensitivity.* <http://encyclopedia2.thefreedictionary.com/Sensitivity>. Version: 2006. – Visited on 20.10.2016
- [18] ENGINEERING, M. S.: *Research group "Control of Renewable Energy Systems" (CRES).* <http://www.cres.mse.tum.de/index.php?id=team>. – Visited on 15.02.2016
- [19] ENGINEERING, M. S.: *TUM.Energy Valley Bavaria.* <http://www.evb.mse.tum.de/index.php?id=5>. – Visited on 15.02.2016
- [20] HACKL, C. M.: *Contributions to High-gain Adaptive Control in Mechatronics.* München, Lehrstuhl für Elektrische Antriebssysteme und Leistungselektronik – Technische Universität München, Diss., 2012. <http://mediatum.ub.tum.de/download/1084562/1084562.pdf>
- [21] INTERIANO, E. : *Modelos en Tiempo Discreto.* <http://www.ie.itcr.ac.cr/einteriano/control/clase/Clase2ModelosenTiempoDiscreto.pdf>. Version: 03 2016. – Visited on 23.05.2016
- [22] ISERMANN, R. ; MÜNCHHOF, M. : *Identification of Dynamic Systems.* Springer, 2011
- [23] J.R. RAOL, G. G. ; SINGH, J. : *Modelling and Parameter Estimation of Dynamic Systems.* The Institution of Engineering and Technology, 2004

- [24] LAYTON, J. : *How Wind Power Works*. <http://science.howstuffworks.com/environmental/green-science/wind-power2.htm>. Version: 2014. – Visited on 2016.04.28
- [25] LEITHEAD, W. ; ROGERS, M. : Drive-train characteristics of constant speed HAWT's: part I - representation by simple dynamic models. In: *Wind Engineering* 20 (1996), 1, Nr. 3, S. 149–174
- [26] LIU, Q. ; HAMEYER, K. : A fast online full parameter estimation of a PMSM with sinusoidal signal injection. In: *2015 IEEE Energy Conversion Congress and Exposition (ECCE)* IEEE, 2015, S. 4091–4096
- [27] LUDYK, G. : *Theoretische Regelungstechnik 2: Zustandsrekonstruktion, optimale und nichtlineare Regelungssysteme*. Springer Berlin Heidelberg, 1995 (Springer-Lehrbuch)
- [28] MATHWORKS: *Basic Principles of Modeling Physical Networks*. <http://www.mathworks.com/help/physmod/simscape/ug/basic-principles-of-modeling-physical-networks.html>. Version: 2016. – Visited on 17.08.2016
- [29] RUGH, W. : *Linear System Theory*. 2nd. Upper Saddle River, New Jersey : Prentice Hall International Inc., 1996
- [30] SENTÉ, P. : *Mechatronics (MCTR)*. <https://www.uclouvain.be/en-mctr.html>. Version: December 2015. – Visited on 21.08.2016
- [31] SHAFIEE, S. ; TOPAL, E. : When will fossil fuel reserves be diminished? In: *Energy policy* 37 (2009), Nr. 1, S. 181–189
- [32] TAVNER, P. ; XIANG, J. ; SPINATO, F. : Reliability analysis for wind turbines. In: *Wind Energy* 10 (2007), Nr. 1, S. 1–18
- [33] WEBSITE, T. R. E.: *Wind Turbine Tip Speed Ratio*. <http://www.reuk.co.uk/Wind-Turbine-Tip-Speed-Ratio.htm>. Version: 2014. – Visited on 2016.05.03
- [34] WELCH, G. : Kalman Filter. In: *Computer vision*. Springer, 2014, S. 435–437



# Appendix A

## Context of the project

The thesis in study was carried on in a research project called "Control of Renewable Energy Systems" from the Technische Universitaet Muenchen (TUM) in Germany. The research project is one of four projects that form part of an energy project called "TUM.Energy Valley Bavaria".

### A.1 TUM.Energy Valley Bavaria

The energy project comes under the justification that future energy's needs in various regions of the world are determined primarily by analysis of time series such as increased integration of renewable energies and new challenges to conventional power plants.

Then, there are various power plant concepts and possible locations that are being evaluated by a large number and variety of simulation calculations and optimization systems, where the focus stays in Germany and Europe.

The current base of power, nuclear power, will no longer be available in 2022. Therefore, activities for production of energy from renewable sources are inevitable. In the development there is a commitment, increasingly visible among the progressive reduction of nuclear energy, reducing emissions of greenhouse gases and economically acceptable cost of electricity. [19]

The program has four research projects, managing to cover a variety of related topics.

The first research project called "Organic Photovoltaics" and has to do with the peculiarities associated with the generation of electricity from solar energy.

The next project is called "Flexible Power Plants", where different technical possibilities are explored to replace the missing capabilities in systems of renewable energy generation by optimizing the technologies and the development of new existing technologies.

An important part of total energy consumption is caused by buildings and transport, this aspect is analyzed in the third research project "Energy Efficiency and Smart Cities". This project aims to develop measures to reduce the energy consumption.

Finally, the fourth research project called "Control of Renewable Energy Systems", which focuses on improving the reliability of wind turbine systems at an early stage. Each research project has been developed as a research center with a highly specialized for each team areas.

## A.2 Control of Renewable Energy Systems (CRES)

The research group "Control of Renewable Energy Systems" (CRES) was established in 2014 as a part of the "TUM.Energy Valley Bavaria" project of the Munich School of Engineering (MSE). The group is led by Dr. Ing. Christoph Hackl and has other engineers from different related areas as part.

The research group focuses on energy efficiency, robust and optimized renewable energy systems control. The special expertise of the interdisciplinary research group lies in the combination of engineering disciplines such as electrical drive technology, power electronics, mechatronics, control disciplines of mathematics and system theory. [18]

Currently, the research focuses on modeling and control of electrical components for wind turbines. [18]